INFORMATION TO USERS

This material was produced from a microfilm copy of the original document. While the most advanced technological means to photograph and reproduce this document have been used, the quality is heavily dependent upon the quality of the original submitted.

The following explanation of techniques is provided to help you understand markings or patterns which may appear on this reproduction.

1. The sign or "target" for pages apparently lacking from the document photographed is "Missing Page(s)". If it was possible to obtain the missing page(s) or section, they are spliced into the film along with adjacent pages. This may have necessitated cutting thru an image and duplicating adjacent pages to insure you complete continuity.

2. When an image on the film is obliterated with a large round black mark, it is an indication that the photographer suspected that the copy may have moved during exposure and thus cause a blurred image. You will find a good image of the page in the adjacent frame.

3. When a map, drawing or chart, etc., was part of the material being photographed the photographer followed a definite method in "sectioning" the material. It is customary to begin photoing at the upper left hand corner of a large sheet and to continue photoing from left to right in equal sections with a small overlap. If necessary, sectioning is continued again — beginning below the first row and continuing on until complete.

4. The majority of users indicate that the textual content is of greatest value, however, a somewhat higher quality reproduction could be made from "photographs" if essential to the understanding of the dissertation. Silver prints of "photographs" may be ordered at additional charge by writing the Order Department, giving the catalog number, title, author and specific pages you wish reproduced.

5. PLEASE NOTE: Some pages may have indistinct print. Filmed as received.

University Microfilms International
300 North Zeeb Road
Ann Arbor, Michigan 48106 USA
St. John's Road, Tyler's Green
High Wycombe, Bucks, England HP10 8HR

An Analysis of the New York City Aerosol For Trace Element Constituents Using Proton Induced X-Ray Emission Spectroscopy

by

Sene E. Bauman

A dissertation submitted to the Graduate Faculty in Chemistry in partial fulfillment of the requirements for the degree of Doctor of Philosophy, The City University of New York.

1978

This manuscript has been read and accepted for the Graduate Faculty in Chemistry in satisfaction of the dissertation requirement for the degree of Doctor of Philosophy.

April 21, 1978
date

Evan T Williams
Chairman of Examining Committee

April 21, 1978
date

Leonard H. Schwartz
Executive Officer

David C. Lohr

Harmon L. Finston

Supervisory Committee

The City University of New York

Acknowledgements

I wish to express my sincerest appreciation to the members of my thesis committee for their advice and encouragement during the preparation of this dissertation, to the college machinists, Sol Coltun and Marty Berman, for their cooperation and expert workmanship, and to my friends, fellow graduate students and faculty members, who helped ease many a trying moment. A special thanks must go to Prof. E.T. Williams and Prof. H.L Finston for their encouragement and sometimes forceful shoves in the right direction.

To Bob L., Tony, Bob R., Lucia, Al, Ottmar, Armand, and Prof. T.I. Ishida a special special thanks for their friendship and generosity and also Prof. Richard Pizer for proving you don't have to be good at basketball to enjoy it.

But most of all, I would like to thank and dedicate this manuscript to my wife and friend, Susan, who had to endure it all from a distance.

Table of Contents

List of Tables

List of Figures

Introduction

When monitoring pollutants in cities, it is not always possible to locate a collector to give a representative sample and therefore, it is necessary to consider the effect of sampling location on collected samples. Frequently samplers are situated at roof-top levels or in locations which do not best represent the area in question, and, in addition, 24 hour sample averaging often disguises the severe conditions existing during the workday hours. High concentrations of certain pollutants may occur during short time intervals and exceed threshold tolerences, which may be as deleterious to general health as long time exposure to lower concentration levels.

A series of experiments was performed to examine two different and distinct types of sampling locations in the city, and many different sampling situations at these locations, to determine how to best interpret data taken at various locations. There are certain advantages in sampling at roof-top level, for example, security and vandalism are not serious problems, but is a roof-top sample representative of street-level exposure or can the 2 types of samples be related? Samples were taken at both street level and at an elevated level for comparison of the effects of street-level circumstances and meteorological conditions, etc. This thesis describes an investigation performed from April to August 1977, the results of which, it is hoped, will help

provide a basis for establishing criteria from which sampling locations can be chosen on a more rational basis. The sites chosen for this investigation were provided by the N.Y.C. Department of Environmental Protection (D.E.P.), the local agency whose primary responsibility is to monitor ambient pollutant levels throughout the city on a year-round basis.

Samples were collected using cascade impactors (Del-Ron model DCI-6) whose 50% stage collection efficiency diameters were 16, 8, 4, 2, 1, and 0.5 μm and whose stages were modified by using Mylar instead of glass as the impaction surface. Chemical analysis was performed by Proton Induced X-Ray Emission Spectroscopy (PIXE), using the Brooklyn College Dynamitron linear accelerator to generate the 3.0 MeV protons used in this method. The thesis also describes in detail the PIXE system which was developed in the course of this work.

Section I.

A. Aerosol Formation

An aerosol is a dispersion of solid or liquid material in a gaseous medium which may be a consequence of gas-to-particle conversions or the break up of solids or liquids. Atmospheric aerosols, which generally have many modes of input, may also result from the suspension or resuspension of wind-blown materials. Material introduced into the atmosphere as particulate matter is called primary, whereas that which results from gas-to-particle conversion is termed secondary[1]. The size distribution (relative mass of particulate material in a given particle size range) of atmospheric aerosols is almost always multimodal, as shown by Whitby, Husar and Liu[2], Willeke and Whitby[3], and Whitby, et al.[4], and may sometimes be trimodal near sources of combustion. The different aerosol formation mechanisms may or may not increase the number of particles, but they can change the size distribution. Aerosol systems are generally dynamic, i.e. small particles (<1 μm) will collide as a result of their Brownian motion and coagulate to form larger particles. The rate of collisions will depend upon the number concentration of particles, and growth by coagulation is usually considered significant only for particles between .01 and 1.0 μm.[5] Other methods of particle accretion from the gas phase are condensation on already existing nuclei, and homogeneous nucleation of gaseous material through a

complex process of molecular clustering followed by coagulation. Examples of gaseous materials which can react to form aerosols through one of the above pathways are SO_2, NO_2, organics (olefins,etc), and NH_3. Condensation can result, for example, when hot stack gases are expelled into the much cooler ambient air and the cooling which occurs upon mixing can cause saturation of the air mass followed by condensation. Dilution of these stack gases will oppose this process since it will prevent saturation. Determination of whether condensation will occur thus depends on such factors as wind velocity (this will affect dilution time), the ambient temperature and pressure (affects saturation curve), and the number concentration of existing particles which will encourage surface absorption and chemical reaction.

Nucleation sites upon which condensation can normally take place are dust particles, smoke, and ionized species usually present in the atmosphere. Historically, particles of this type, which encourage condensation and are <0.1 μm in diameter, are called Aitken nuclei. In the absence of such sites, molecular clusters play an important role in the formation of particles from the gas phase. Gas phase chemical reactions may also generate condensable species, and since such reactions are often photochemical their kinetic rate often depends on the availability of sunlight. Also, chemical reactions of gases may be catalyzed on particle surfaces or in a liquid drop. Both "self-nucleation" and

condensation on existing nuclei will change the mass distribution of the aerosol, whereas only the former will change the number of particles. Usually an urban aerosol will contain up to 10^5 nuclei/cm^3 in the size range of 0.01 to 0.1 μm. If the surface-area concentrations (i.e. total surface area of particles/cm^3 air) of existing nuclei is < 500 $\mu m^2/cm^3$ then new nuclei will be formed in the .01 to .02 μm size range.(6) At surface area concentrations above a few thousand $\mu m^2/cm^3$ condensation of chemically and photochemically produced material will take place on existing particles in the 0.1 to 0.5 μm range.(7)

The size range of suspended particulate material is from ca. 0.01 μm to ca. 50 μm with most of the particles in the region from .01 to 0.1 μm. Particles less than 1.0 μm generally result from nucleation, condensation, chemical or photochemical reactions, or emissions from combustion processes. These particles are called fine particles. The coarse particle mode represents particles greater than ca. 2 μm which are usually introduced as primary particulate material from erosion, sea salt spray, fly ash particles, ablation due to mechanical processes, volcanic activity, etc. According to Whitby(8) there seems to be very little exchange between coarse and fine particles and the ratio of the two varies from region to region.

Figure I-A-1(8) is a simplified description of aerosol dynamics. The relative importance of any one input mechanism

Fig I-A-1 General Atmospheric Aerosol Dynamics

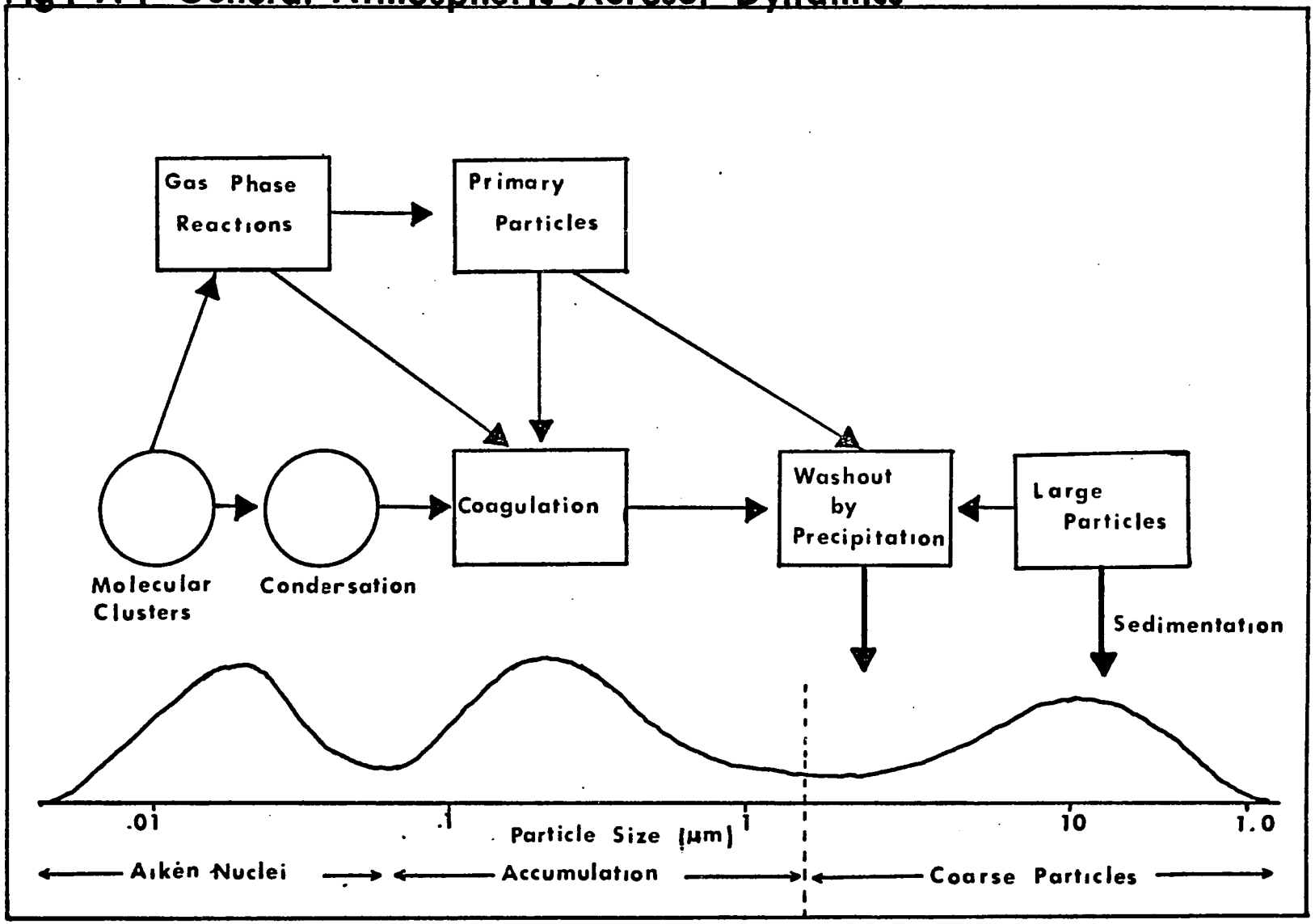

will depend upon the aerosol characteristics and location. As elevation increases, the size distribution will consist mainly of small particles and become unimodal[9], and the accumulation mode will account for essentially all particles.[10]

Recent investigations[11],[12] have shown that aerosols can be transported over long distances in predictable fashion and can account for major portions of atmospheric particles in cities hundreds of miles away. The loss of particulate material from atmospheric aerosols occurs through either sedimentation of gravitationally affected particles (>ca. 2-3 μm) or by washout from precipitation. Table I-A-1[13] gives the settling rate (cm/sec) for some different sized particles.

A fine and coarse (bimodal) distribution of particles seems to be a characteristic of most analyzed aerosols and there seems to be no significant exchange of material between the fine and the coarse fractions although encapsulation[14], and agglomeration of 5-10 μm particles into particles ranging from 20-74 μm can occur in fly ash and similar high-temperature particle-forming mechanisms. Encapsulation and agglomeration can account for 20-30% of all fly ash particles less than 5-10 μm produced under power plant conditions.[15]

Table I-A-1 Particle Settling Velocities

d_p (μm.)	settling velocity(cm/sec) (ρ_p= 1 g/cm^3)
0.1	8.62×10^{-5}
0.2	2.26×10^{-4}
0.5	1.00×10^{-3}
1.0	3.52×10^{-3}
2.0	1.31×10^{-2}
5.0	7.80×10^{-2}
10.0	3.07×10^{-1}
20.0	1.22
50.0	7.58
100.0	30.3

Bibliography

1. S.K. Friedlander, Smoke Dust and Haze-Fundamentals of Aerosol Behavior , John Wiley and Sons, Inc.(1977).
2. K.T. Whitby, R.B. Husar, and B.Y.H. Liu, "The Aerosol Size Distribution of Los Angeles Smog", J. Colloid Interface Sci., 39, p. 211 (1972).
3. K. Willeke, K.T. Whitby, "Physical Characteristics of Denver Area Aerosols", J. Air Pollution Control Assoc., 25 ,p 529 (1975).
4. K.T. Whitby, W.E. Clarke, V.A. Marple, G.M. Sverdrup, G.M. Sem, K. Willeke, B.Y.H. Liu, and D.Y.H. Pui, "Characterization of California Aerosols I. Size Distribution of Freeway Aerosol", Atmospheric Environment, 9 ,p. 463 (1975).
5. S.K. Friedlander, op. cit. p. 177.
6. W.E. Clarke, K.T. Whitby, "Movement of Aerosols Produced by the Photochemical Oxidation of SO_2 in Air", J. Colloid

and Interface Science, 51 ,p. 477 (1975).

7. K.T. Whitby, B. Cantrell, "Atmospheric Aerosols- Characteristics and Measurement", published report, Mechanical Engineering Dept., Univ. Of Minn, Minn.

8. K.T. Whitby, ibid. , p 3.

9. R.D. Cadle, The Measurement of Airborne Particles , J. Wiley and Sons (1975).

10. K.T. Whitby, B. Cantrell, op. cit. , p 3.

11. J.W. Winchester, "Atmospheric Aerosol Chemistry of Sulfur: Nuclear Accelerator Methods in Energy-Related Research", Third Internl. Confer. Nuclear Methods in Environmental and Energy Research, Univ. of Mo., in press, Oct., 1977.

12. K.T. Whitby, B. Cantrell, op. cit. , p2.

13. R.D. Cadle, op. cit.

14. J. Baker, C.F. Bauer, C.A. Evans, A. Loh, D.F.S. Natusch, "Small Particle Encapsulation: A Natural Control Phenomenon?", submitted for publication- referenced from "Characterization of Trace Metals in Fly Ash", Institute for Environ. Studies, Univ. of Ill. at Urbana, Report #3.

15. ibid, p 10.

B. New York City Aerosol

The aerosol of the New York Metropolitan area is a consequence of the contributions from local point sources (industries, power plants, and incinerators), vehicular traffic (cars, busses, trucks), planes, trains, space heating, natural background (land and ocean), and wind-blown particles from other geographic locations. It is generally estimated that the regional natural background is on the average about 35 $\mu g/m^3$[1]. The background, of course, will be determined by the prevailing winds (winds which have blown over land generally bring a greater concentration of particulate material than winds which have blown off the ocean). Since general air-flow patterns are seasonal, the aerosol will show seasonal variation. In addition, atmospheric stability (i.e., comparing the adiabatic lapse rate with the actual lapse rate determined by measuring the temperature difference between ground level and the height at which the barometric pressure is 350 mbar), a parameter closely associated with the mixing depth and therefore particulate concentrations, shows both diurnal and seasonal variations.[2] The chief sources of particulate material by classification are:

1. space heating
    a) schools, colleges, hospitals, and city housing
    b) private housing
    c) private and governmental office buildings

Fig I-B-1 Seasonal Variability of Pb and V

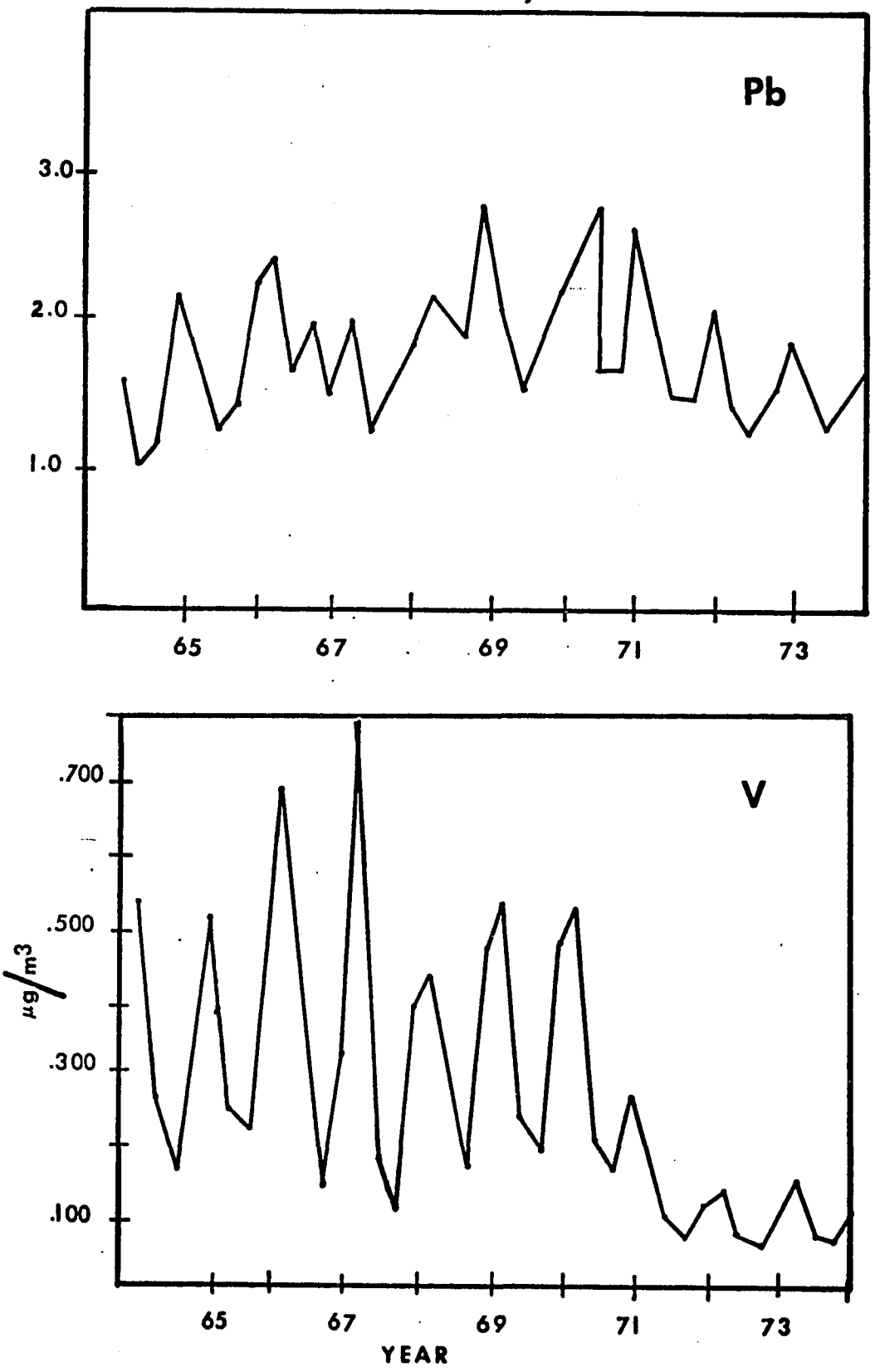

d) commercial and industrial businesses

2. incineration
3. power generation-electric and steam
4. industry
5. mobile sources
    a) vehicular traffic
    b) planes (commercial and passenger)
    c) trains
6. transported aerosol

Table I-B-1 gives the estimated source inventory for some of the principal contributors in the city for the year 1972.(3) These estimates are based upon calculation of fuel consumption, refuse tonnage, electrical consumption, etc. Seasonal variability of local sources also complicates accurate assessment of the emission of particulate material. Space heating increases in the winter months whereas electric power consumption (due to air conditioning) increases during the summer. The National Air Surveillance Network (NASN) has been monitoring 92 urban centers for Total Suspended Particulates (TSP) since 1965. Fig. I-B-1, taken from the NASN data, demonstrates the highly seasonal variations that are often encountered. These data are taken from the 29 stations in the Northeast sector. The general decline in V levels are indirectly related to the stricter standards (1% S to 0.3% S from 1968-69 to 1973) placed on residual fuel oils imported into the Northeast. A research group at

Table I-B-1 Estimated Source Inventory of Particulate Material for City and Boroughs.(1972) (tons/yr)

Source	Bronx	Brooklyn	Manh.	Queens	St.Is.	City	%
Sp.Ht.	176.2	330.9	349.4	92.3	373.4	1332.	7.3
Incin.	0.	6676.	1786.	1356.	0.	9818.	54.8
Power	342.	493.	1356.	2404.	467.	5062.	28.2
Indust.	270.	826.7	37.5	403.2	184.2	1722.	9.6
Total	788.8	8327.	3529.	4456.	1025.	17925.	100.
%	4.4	46.5	19.5	23.5	5.7	100.	

Estimates for 1975 and 1976 Power usage (Con Ed and LILCO)

1975	5751
1976	5690

Table I-B-3 A Comparison of TSP for the Calendar Years 1969-1976($\mu g/m^3$)

Borough/	1969	1970	1971	1972	1973	1974	1975	1976
Bronx	101	105	105	91	80	76	75	68
B'klyn	89	104	110	78	78	77	77	69
Manh.	124	124	113	89	91	89	83	73
Queens	83	97	98	75	74	71	66	66
St.Is.	94	102	97	77	85	81	77	71
City	98	104	105	82	82	79	75	69

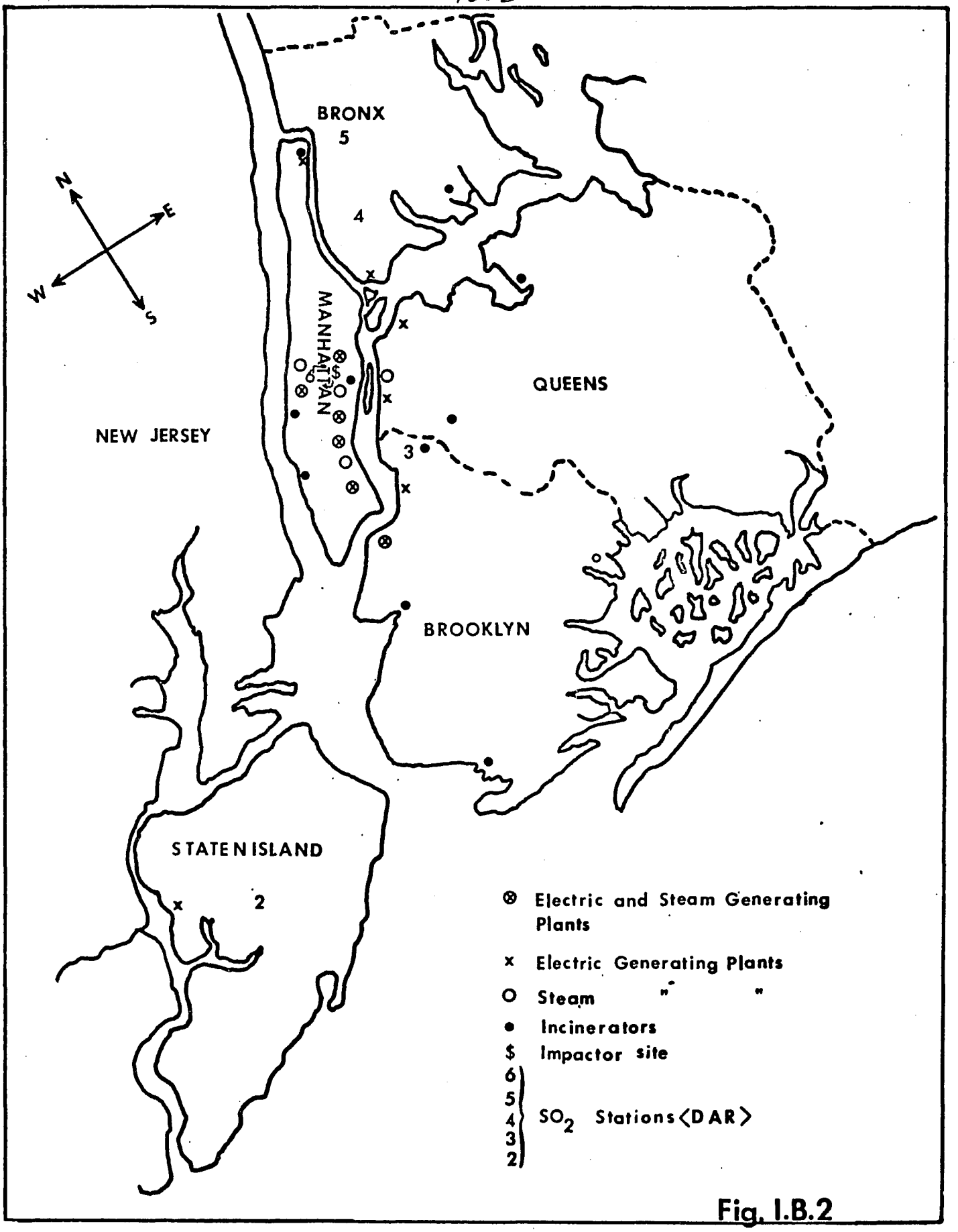
BRONX
5
4
N
E
W
S
MANHATTAN
QUEENS
NEW JERSEY
3
BROOKLYN
STATEN ISLAND
2
⊗ Electric and Steam Generating Plants
x Electric Generating Plants
O Steam " "
• Incinerators
$ Impactor site
6
5
4
3
2
SO2 Stations (DAR)

Fig. I.B.2

N.Y.U. under the direction of T.J. Kneip and Merrill Eisenbud have been examining the N.Y.C. aerosol for many years and on the basis of collected data have tried to assign the relative contributions of some of the major sources. They selected for each source an element which was, to a good approximation, almost exclusively associated with it and thus could serve as a tracer. That is, copper is assumed to be almost exclusively associated with incineration, vanadium from fossil fuel, lead and bromine from autos, etc. By employing such a technique one can theoretically assign the relative contribution of a particular source to the entire aerosol. Based upon such a procedure Kneip, et al., established the various aerosol contributors according to Table I-B-2 for the years 1969,1972-1974.(4)

Table I-B-2 Percent of TSP Contributed by Sources
Kneip and Eisenbud.(1975)

Source	1969	1972	1973	1974
auto	14	32	32	28
fuel oil	22	9	9	14
incin.	30	6	5	4
natural	11	15	19	17
other	24	39	35	37

Since any composite picture of the N.Y.C. particulate distribution will show variations due to season, weather conditions and local point sources, any attempt to characterize the aerosol will involve many years of simultaneous sampling at many locations throughout the city. Figure I-B-2 shows some of the local sources for the city and the surrounding area. The success of any technique to establish a

source inventory depends on its ability to incorporate meteorological as well as other parameters to normalize data. If the inventory is based on experimental data, it is critical to obtain accurate and representative samples for the area in question. The D.E.P. has 36 sampling stations located throughout the greater New York City area taking 24 hr. total suspended particulate samples with high-volume air samplers.(5) Table I-B-3 is a compilation of data gathered by the D.E.P. for the calendar years 1969-1976.

The overall picture presented in Table I-B-3 seems to indicate that the average concentration of particulate material in the N.Y.C. aerosol has shown a general decrease since '69. The general trend shows a yearly decline to about 69 $\mu g/m^3$, a decline of almost 34% since the years of '70-'71. It is important to compare these results with those of N.Y.U. as shown in Table I-B-4.(6) The N.Y.U. data were normalized by first correcting each sample using a "dispersion factor" derived by taking the product of the wind speed and the mixing depth. Thus the data were corrected for changes in the rate of atmospheric mixing, and then normalized to the mean dispersion factor obtained by taking the average of annual dispersion factors from 1967-1975.

Looking to the normalized data for the individual elements, we see that even though the total mass of the aerosol shows no clear pattern, the Pb, Cr, and V concentrations

Table I-B-4 Average Trace Metal Concentration in N.Y.C. Air(ng/m^3).
A=ambient
N=normalized

	1967	1968	1969	1972	1973	1974
	A	A	A	A	A	A
TSP($\mu g/m^3$)	106	114	118	76	69	76
Pb	2400	3600	2400	1500	1300	1000
Cd	13	19	10	5	5	3
Zn	203	2200	670	315	280	250
Fe	-	-	-	1000	1400	1200
Mn	17	62	63	25	29	33
Cu	44	196	240	51	51	39
Cr	104	54	33	10	5	13
Ni	110	129	420	110	130	66
V	1040	1040	810	61	78	122
	N	N	N	N	N	N
TSP($\mu g/m^3$)	99	88	104	66	76	110
Pb	2200	2800	2100	1300	1400	1500
Cd	12	15	9	4	6	4
Zn	190	1700	592	270	310	280
Fe	-	-	-	1400	1500	1500
Mn	16	48	55	22	32	50
Cu	41	150	210	44	56	53
Cr	97	42	29	9	6	16
Ni	102	100	310	95	140	126
V	920	800	710	53	86	218

show a steady decline over the period 1967-1974. The decrease in Pb and V concentrations have been attributed to federal and city requirements for lower Pb in gasoline and lower S in fuel oil. The N.Y.U. group seems to have been very sucessful in demonstrating seasonal and meteorological variations in the data and it appears that they have been able to correct for these variations in their normalization procedures. Their sampling procedure consisted of taking air samples for one week, filtering almost 6,000 m^3. In addition, a particle-size classifier, also sampling for one week duration, segregated particles in 3.5, 2.5, 1.5, 0.5 μm size ranges. The major focus of their report was "... the development of an alternative approach to apportioning the pollution levels amoung sources so that attempts to regulate these levels by legislated emission standards will have a more rational basis than at present.".(7) The aerosol was measured from four roof-top sampling locations in the metropolitan area.

One other effect which I have chosen to pursue is the "canyon" effect that is a result of the tall skyscrapers which line the streets of Manhattan. These tall buildings create corridors through which the prevailing winds may get funnelled, often producing air-flow patterns very different from those experienced at rooftop levels. In addition, mixing factors may be very different at street level than at rooftop owing to these different air flows.

It seems that if one wishes to establish criteria from which "legislative emission standards" could be established, then a sampling of the aerosol at the location of most significant impact, (i.e. street level), is required. Goldstein, et al.,[8],[9] using data obtained by the D.E.P. showed that very poor correlation was obtained when trying to match SO_2 and smokeshade levels between pairs of D.E.P. monitoring stations. The conclusions drawn from these papers were that variability of local sources and/or poor atmospheric mixing can distort data that would otherwise have been thought valid. Goldstein's data indicated that variations in the SO_2 concentrations and smokeshade at any one station in the D.E.P. monitoring system gave poor correlation with any other station. There was also no consistency in the findings from one season to the next and between the same seasons in different years.

Bernstein, et al.[10], have indicated that the lead particle size distribution in the aerosol at rooftop levels is bimodal with a small, but significant fraction associated with particles >3.5 μm. He also reported that 70-90% of all Pb is associated with particles < 1.5 μm and of this 70-90%, 40-50% is associated with particles < 0.5 μm. This is somewhat consistent with our ground-level measurements made at Rockefeller Center. Habibi[11] determined that as much as 50-60% of all lead emitted from exhaust of automobiles could be associated with particles > 5 μm., and at-

tributed this effect to entrapment of the lead in the exhaust system and subsequent release at a later time through some mechanical process such as blow out due to sudden acceleration. Habibi also pointed out that these large particles should settle out of the aerosol rather quickly, within the first several meters of the exhaust system. This would imply that much lead could enter the aerosol through a resuspension process where these settled particles are thrown back into the aerosol after an indeterminate lifetime on the streets. In addition, the nature and size of particles that are resuspended will not be predictable. Fragmentation of large particles through abrasion could result in new particles of completely different nature and composition, while dissolution of settled particlulate material followed by evaporation and subsequent resuspension could also alter the size distribution for some elements.

The kind of particulate distribution that one can expect from a given urban area varies. For New York City, the aerosol background is:

1) Caused by man's activities in other areas, e.g
   SO_2 to Sulfate
2) Natural Background
   a) dust from land erosion
   b) Condensation and nucleation of natural gases,
      i.e. SO_2 to Sulfate
   c) Sea salt

Suspended particles resulting from the introduction of soil or sea salt into the atmosphere tend to be > 2μm in diameter. The composition of aerosols containing no man-made particles should correspond to the natural abundance pattern for the area in question.

Condensation and accumulation particles can be transported over long distances because of their very small settling velocities (see table I-A-1). Gaseous pollutants with long residence times in the atmosphere can be converted during transport to condensed species which serve as further nucleation sites for particle growth. Such is the case for gaseous SO_2 to particulate $SO_4^=$ conversion as shown by Sheih.[12] Time constants of 3 to 30 hours were reported for 1/e conversion of gas to particle. With average wind speeds of 5 m/sec, the corresponding distances travelled are from 50 to 500 km. This implies that $SO_4^=$ particles are, except under extreme conditions of stagnant air masses, almost always the result of long-range transport. Sulfates are of particular importance because of the belief that they are mostly associated with the acid, H_2SO_4, making them especially hazardous. Sheih has pointed out that the tall stacks originally designed to carry SO_2 away from local sources are chiefly responsible for the greater photochemical conversion of SO_2 to sulfate due to the increased residence time of SO_2 in the atmosphere. and also that the

most efficient mechanism for the removal of SO_2 from the atmosphere is dry deposition on ground contours, a process reduced by tall stacks.

Bibliography

1. Environmental Impact Report on Proposed St. Louis Airport.
2. T.J. Kneip, M. Eisenbud, "Trace Metals in Urban Aerosols", Research Report #117, Final Report, Electric Power and Research Institute, Oct. 1975
3. Data Report- Aerometric Network - N.Y.C.D.E.P. 1972
4. T.J. Kneip, loc cit.
5. Data Report- Aerometric Network - N.Y.C.D.E.P. 1977
6. T.J. Kneip, loc cit.
7. T.J. Kneip, loc cit.
8. I.F. Goldstein, L. Landovitz, "Analysis of Air Pollution Patterns in New York City- I. Can One Station Represent the Large Metropolitan Area?", Atmospheric Environ., 11, p 47-52.
9. I.F. Goldstein, L. Landovitz, "Analysis of Air Pollution Patterns in New York City- II Can One Aerometric Station Represent the Area Surrounding It?", Atmospheric Environ., 11, p 53-57
10. D.M. Berstein, M.T. Kleiman, T.J. Kneip, T.L. Chan, M.L. Lippmann, "Development of a High Volume Air Sampler for the Determination of Particle Size Distributions in Ambient Air", Proceedings of the 68th Annual Meeting of the Air Pollution Control Assoc., Boston, 1975.
11. K. Habibi, "Characterization of Particulate Matter in Vehicle Exhaust", Environ. Sci. and Tech., 7, #3, p223-

234, Mar. 1973.

12. C.M. Sheih, "Application of a Statistical Trajectory Model to the Simulation of Sulfur Pollution Over Northeastern U.S.", Atmospheric Environ., 11, p 173-178, 1977.

C. Problems Associated With Aerosol Sampling in N.Y.C.

Inhomogeneity is a major problem which must be circumvented in order to characterize the N.Y.C. aerosol. A criticism leveled at studies of atmospheric aerosol is that the errors encountered in sampling significantly affect the interpretation of the data.[1] Some studies have shown[2],[3],[4],[5],[6] variations in concentrations of materials collected at different locations and elevations located in the same general area. These differences, attributable to local point sources, and nonuniform mixing of the atmosphere (lateral and vertical turbulence) caused by factors such as uneven heating of the air mass, ground-level contour variations, local inversions, etc., make the study of local aerosols a very complex task. A solution usually adopted by monitoring agencies in cities such as New York, Boston, Chicago, St. Louis, Denver, and Los Angeles is to construct a network of sampling stations throughout the city and to establish long term trends. However, this approach still ignores many significant sources of error, principally, the problem of sampling station location. For a well-mixed air mass containing particulate material from distant sources, the concentration at ground level is the same at higher elevation, but, for street-level emissions, this work and others have shown a dilution effect with height. Mainwaring and Harsha[7] have shown a decrease in TSP concentration with height up to 30% on the average for a series

of samples collected at heights from 11 to 66 m. from a building in Melbourne, Australia. Furthermore, they saw no difference in the mass distributions for the particles less than ca. 2μm, indicating that air turbulence is sufficient to provide for circulation of material to all levels sampled. A second type of effect, which further enhances the dilution effect just discussed, is associated with the "canyon" type situations prevalent in most large cities. The lack of mixing to upper levels is due to 2 basic conditions. First, since the sun cannot penetrate to street-level till late morning (10-11 a.m.) because of the tall buildings, local inversions can take place trapping the stagnant air mass and will prevent the normal vertical mixing, causing accumulation of pollutants with concentrations at street level much higher than the concentrations being monitored at roof top. This is particularly significant when wind speeds are low. On the other hand when the sun does begin to heat the air mass at street-level (usually ca. noon) this local inversion will cease and the air will undergo normal vertical mixing. Second, because of these corridors, the funneling of winds through the city is nonuniform, often resulting in air flows for uptown-downtown streets being very different from crosstown streets. This implies that samplers located around the corner from each other could provide different results. The questions to be asked at this point are:

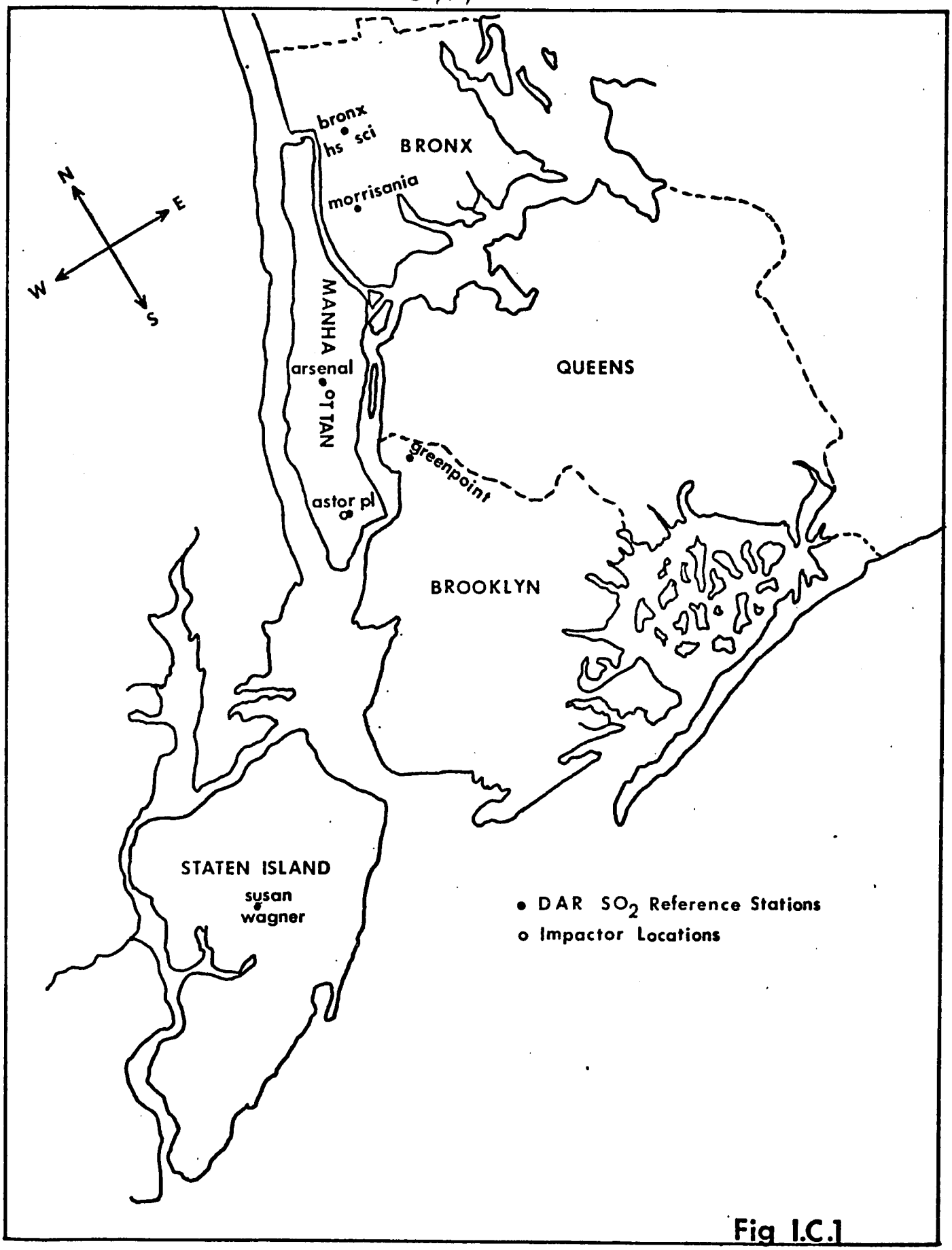
N
E
W
S
bronx hs sci
BRONX
morrisania
MANHA
arsenal
9TTAN
QUEENS
greenpoint
astor pl
BROOKLYN
STATEN ISLAND
susan wagner
• DAR SO_2 Reference Stations
o Impactor Locations

Fig I.C.1

a) Can representative samples be obtained?

b) If a) is not possible under the limited scope of a sampling network then what criteria should be used to obtain the best possible samples?

Assuming the first is not possible then the monitoring stations should be placed at elevations where the general population is maximally exposed (i.e street-level) and in locations which "best" monitor urban pollution patterns (i.e. most severe rush-hour conditions). Of course there is no a priori way of knowing these conditions. Such knowledge must be determined experimentally. To establish such criteria, knowledge of the magnitude of these errors just described is necessary. The following experiments were performed to add to the data base from which these guidelines will be established.

Sampling Stations

Two separate projects were undertaken during the spring and summer of 1977. During the period 4/29-5/2 a series of samples were collected at a downtown Manhattan location, the Cooper Union School of Engineering, situated between 3rd Ave. and Broadway and E. 8th St. This is the present location of the Air Resources Div. of the New York City Dept. of Environmental Proctection. The second series of samples were collected from 7/19 to 7/29 at Rockefeller Center in midtown Manhattan. Fig. I-C-1 shows both of these locations. The purpose of both experiments was to determine the degree

of variance one could expect when simultaneously sampling with 3 cascade impactors located at various degrees of proximity to one another. The Cooper Union sampling configuration was the 1st, 3rd, and 6th floors on the north side of the building. The Rockefeller Center project used the 3 impactors to determine variance of 2 street-level locations, situated around the corner from each other, and a third, which was located 16 floors above street-level over one of the ground-based impactors.

The general topography and source characteristics for these locations are very different. In addition, samples taken in April at one location cannot be meaningfully compared to samples taken somewhere else in July. Thus the results from the two sample periods will be considered independently.

Cooper Union is a six story building situated in an essentially low profile area. There are no "canyon" environments in the immediate vicinity of the building, although there is a 20 story apartment house across the street. Traffic patterns for the uptown-downtown streets indicate a definite rush-hour pattern. The samplers were located on the 1st, 3rd, and 6th floors of the building overlooking W. 5th St., a cross-town street. Traffic flow on this street is relatively light compared to 3rd Ave. The 3 impactors were situated in vertical alignment on the window ledges of each floor. Sampling probes, 6" diameter polyvi-

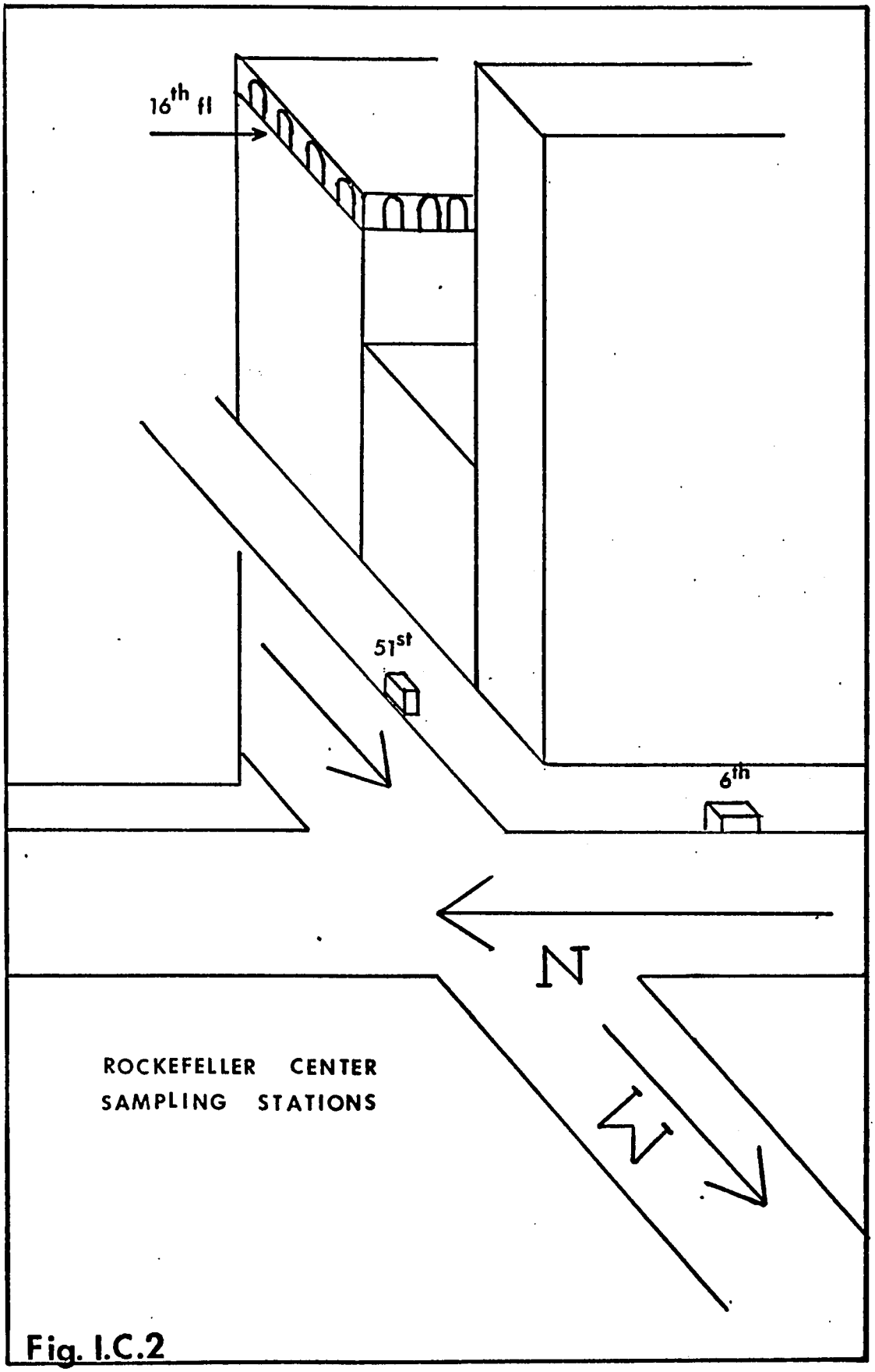

Fig. I.C.2

nylchloride pipe, were attached to each impactor and extended out the window. All probes hung with the opening downward to prevent settleable particulates or rain from entering. On 4/29 samples were collected for two consecutive 2 hr. intervals from ca. 6:00 p.m. to 8:00 p.m. and 8:00 p.m. to 10:00 p.m. On 5/2 samples were collected for 3 two hr. intervals from 6:00-8:00, 8:00-10:00, and 10:00-12:00 p.m. During these sampling periods there were no unusual weather conditions, such as heavy rains, although winds were slightly higher on 5/2 than on 4/29.

In the second project, we decided that a three-point profile with respect to height and location would provide interesting information on the characteristics of the aerosol at Rockefeller Center, located in the center of Manhattan and typical of the midtown area. The sampling locations were chosen to explore both the effects of height and N-S vs. E-W streets (see fig. I-C-2.). The first sampler was located in a wooden shed approximately mid-block between 50th and 51st streets on 6th Ave. The impactor was about 1-2 feet from the curb and about 3 feet above street level. The surrounding area contains tall skyscrapers lining both sides of the street for many blocks in either direction. Traffic on 6th Ave. (3000-4000 vehicles/hr. during the day) rarely exceeds 20 mph and considerable time is spent idling at traffic lights. We estimated that 50% of all vehicular traffic in this area (and probably true of mid-town general-

ly) is composed of taxi cabs, another 10% is due to busses except during rush-hour when the number of express busses entering and leaving the area increases. In addition, the 6th Ave. subway is located below street level with ventilating grids on both sides of the street. The traffic density increases from 7:00 a.m. to 8:30 a.m. and then levels off until around 4:00 p.m., when the commuter busses begin arriving. This rush-hour mode continues until around 6:30 p.m. after which traffic again becomes very light. The pattern is similar for 51st St., except that there are no busses.

The impactor on 51st St. was also housed in a shed as on 6th Ave. The "canyon" environment is also prevalent on 51st St. with many tall buildings lining each side of the street; traffic flow is about 1/4 that of 6th Ave. Also, there was less idling near the sampling shed because cross-town blocks are longer than avenue blocks and stopped traffic did not often back up to the sampling site. The elevated sampling location was an open ledge on the 51st St. side of the top floor of 50 Rockefeller Plaza about 100 feet east and 16 floors above the ground-level site. Meteorological conditions on the 16th floor were somewhat different from ground level; temperatures were generally somewhat cooler (about 2 degrees on the average) than ground level and winds tended to be stronger. During the period July 19 to July 29, 1977, samples were collected on seven weekdays for 3 con-

secutive 2-hour intervals (pre, mid, and post-rush hour) either morning or afternoon, simultaneously at each location.

The above sampling configuration at Rockefeller Center enabled determination of the extent of atmospheric mixing from ground level to the 16th floor. The two ground-level stations allowed the extent of ground-level mixing to be determined. This information is, of course, important in answering the question of whether a sample at a particular elevated location is representative.

Bibliography

1. J. Forrest, L. Newman, "Ambient Air Monitoring for Sulfur Compounds.", J. of Air Poll. Control Assoc., 23, #9, p761-768, Sept. 1973
2. I. Goldstein, "Analysis of Air Pollution Patterns in New York City-I. Can One Station Represent the Large Metropolitan Area?", Atmospheric Environ., 11, p47-52, (1977).
3. I. Goldstein, "Analysis of Air Pollution Patterns in New York City-II. Can One Aerometric Station Represent the Area Surrounding It?", Atmos. Environ., 11, p53-57, (1977)
4. M.T. Kleinman, T.J. Kneip, M. Eisenbud, "Seasonal Patterns of Airborne Particulate Concentrations in New York City", Atmos. Environ., 10, p9-11, (1976).
5. S.E. Bauman, E.T. Williams, H.L. Finston, "Suspended Particulate Matter in New York City: Element Concentrations as a Function of Particle Size and Elevation above Street", Third Intern. Confer. on Nuclear Methods in Environ. and Energy Research, Univ. of Mo., 1978
6. S.J. Mainwaring, S. Harsha, "Size Distribution of Aerosols in Melbourne City Air", Atmos. Environ., 10, p57-60, (1976).
7. ibid., p57-60.

Section II.

A. Historical Development of Impaction Techniques

Although public attention has recently prompted extensive investigation into the nature of air pollution problems, the instrumentation necessary for these studies was developed many years earlier. Historically, particle sampling instrumentation was used for industrial hygiene and safety or laboratory experimentation. Particle collection has been performed for study of radioactive fallout, asbestos, dust collection, etc.

The cascade impactor was first described as an analytical tool in 1945 by K.P. May[1]. This first impactor consisted of 4 stages plus the after filter. The size range collected was from 50 to 1.5 microns at a sampling rate of 17.5 liters/min. Modifications of May's impactor were carried out by Laskin[2] and later by Sonkin[3] to extend measurements into the submicron range.

During the 1950's there was extensive work done on the experimental and theoretical aspects of the cascade impactor. In 1952 Ranz and Wong[4],[5] did an in-depth analysis of the theoretical foundations for impaction, while in 1955 Gillespie and Johnstone[6] investigated the effects of various particle growth parameters such as humidity, nucleation, time, and concentration on the mass distribution of generated aerosols. In 1957, Mitchell and Pilcher[7] developed an improved design for an impactor consisting of six stages

with cutoffs (particle size for which a particular stage has a 50% efficiency for collection, i.e. stage 1 collects 16 μm. particles with 50% efficiency) at 16, 8, 4, 2, 1, and 0.5 microns. This new design is the model from which the impactor we are now using was taken. In 1958 J.A. Brink Jr.,[12] then working for Monsanto Chemical Co., presented a new design for an impactor with a collection cup as the impaction surface. The range of this 5 stage impactor was from 3.0 to 0.3 microns.

During the 1960's modification for specific applications of impactors were made by Junge[8] and Manson, Andersen[9], Lundgren[10], Casella[11], and many others. Andersen developed a multi-jet impactor consisting of over four hundred jets which impinge on a collection surface of glass or stainless steel. There are 6 stages and a sampling rate of approx. 1 cfm. Lundgren designed an impactor employing rotating collection surfaces so that particle build-up and re-entrainment are kept at a minimum. However, due to the curvature of the surface of the rotating drums, bounce-off losses seemed a significant problem. Casella produced a modified version of May's original impactor under the name "Mark I".

A partial list of the impactors available today follows.

A)Casella Impactor-(200-0.5 microns) 4 stage

17.5 lit/min

B) Unico Environmental Instruments- 4 stage

C) Hi-Vol Sierra Instruments-(10-1.3 microns)
5,4,3,1 stages, 20-60 cfm

D) Andersen Impactor- 6 stages 1 cfm

E) Tag Impactor- Environmental Research Corp.
9 stages (9-0.6 microns) 0.5 cfm

F) Lundgren Impactor- 4 stage 3.0 cfm

G) Battelle, Scientific Advances Inc., now Delron
(16.0-0.5 microns) 6 stages 12.5 l/min
5 stages 1.05 l/min

The basic theory of impaction for all of the above is similar and will be described below for the general case of a circular jet (theories for circular or rectangular jets are available).

B. Theory of Impaction:

Nomenclature:

C = an empirical correction factor for the resistence of gas to the movement of small particles as defined by eqs. 3,4,5

D_c = diameter of impactor jet, cm.

D_p = diameter of aerosol particle, microns

D_{pc} = characteristic diameter of aerosol particle for impactor stage, microns

g_c = $1 g/(atm.)(cm.)(sec)^2$

L = mean free path of gas molecules, cm, $L = 2\frac{\mu}{\rho\bar{v}}$

P_0 = absolute pressure at inlet to impactor, atm

P_2 = pressure after jet, atm

ΔP = pressure drop across impactor, in. Hg

T_2 = temperature after jet, ^oK

V_o = gas flow at inlet to impactor, cc/second

$V_o = 24.5(\Delta P)^{0.440}$

for air at 25°C and 14.7 p.s.i.a.

v_2 = average linear velocity of a gas through a jet at P_2 and T_2, cm/sec

$\bar{v}$ = average molecular velocity of gas, cm/sec

$$\bar{v} = (10)^3 \sqrt{\frac{8 g_c P_2 (1.013)}{\pi \rho}}$$

ϕ = dimensionless inertial parameter

$$\phi = \frac{C \rho_p v_2 D_p^2}{18 \mu D_c 10^8}$$

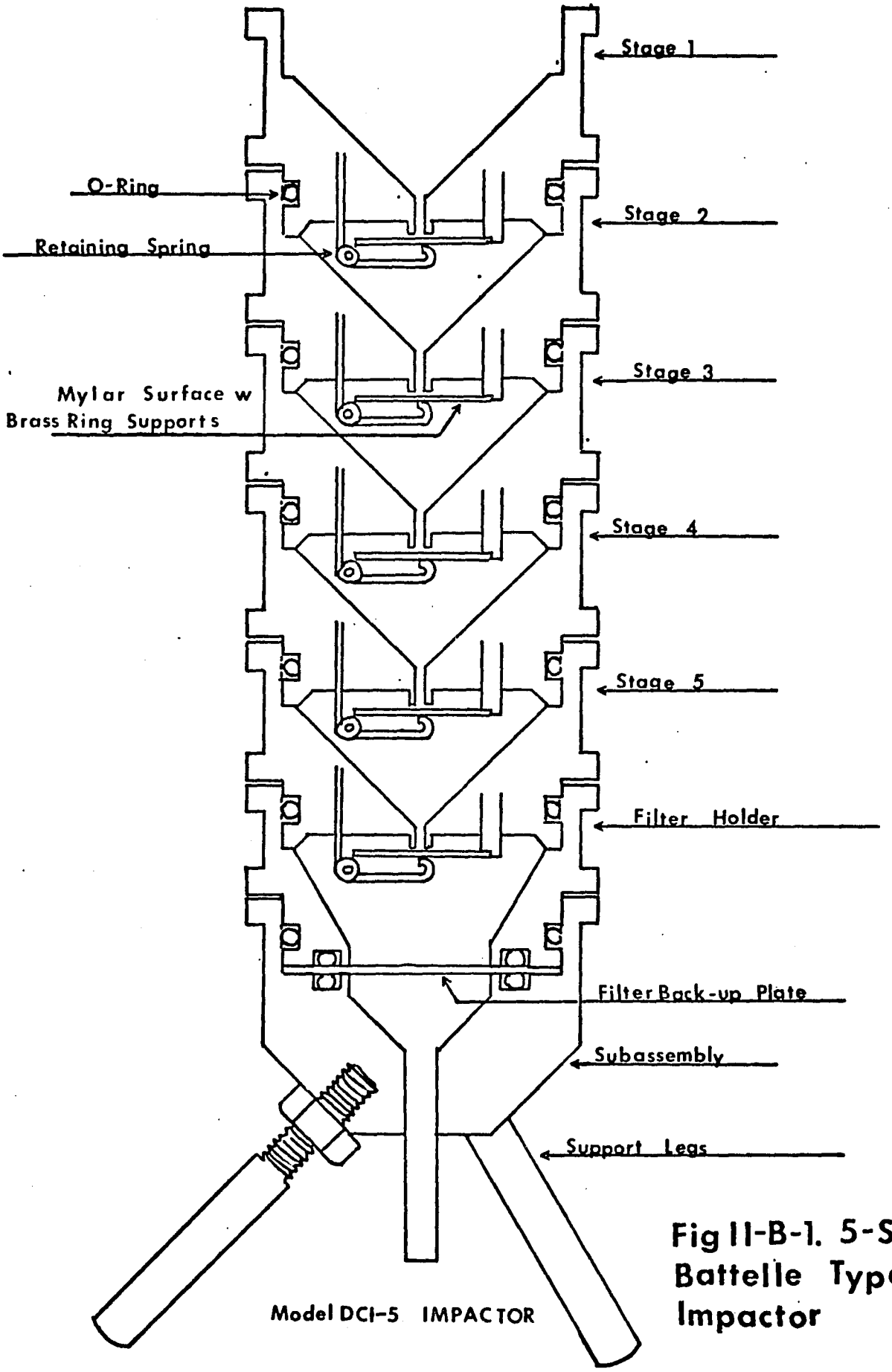

Fig II-B-1. 5-Stage Battelle Type Impactor

ϕ_{50} = inertial parameter for 50% impaction efficiency

ρ = gas density after jet at T_2 and P_2, gram/cc

ρ_p = density of aerosol particle, gram/cc

μ = viscosity of gas after jet at T_2 and P_2, g/(cm)(sec)

For a complete discussion of impactor theory as well as a detailed derivation of the mathematics involved in describing such systems the reader is referred to references (4) and (5). Only a brief discussion of the general mechanism followed by the necessary equations to develop a statement for impaction efficiency will be discussed here.

Multistage impaction systems designed to sample aerosol and to separate the collected particles into designated size fractions are based upon the particles developing a momentum proportional to their "aerodynamic size". Fig II-B-1 is a schematic diagram for the Battelle type impactor developed by Mitchell and Pilcher and is presently being used in our study. This is a six stage impactor with 50% cut-off diameters of 16, 8, 4, 2, 1, .05 microns. To obtain these cutoff parameters the ratio of the jet diameter to impaction plate distance must be fixed for a given flow rate and pressure drop across the system. Consider an aerosol being isokinetically drawn through the above impactor by a vacuum of about 20 in. Hg. The aerosol will be accelerated as it funnels

Figll-B-2 Effective Cut-Off Diameters for 6 Stage Impactor

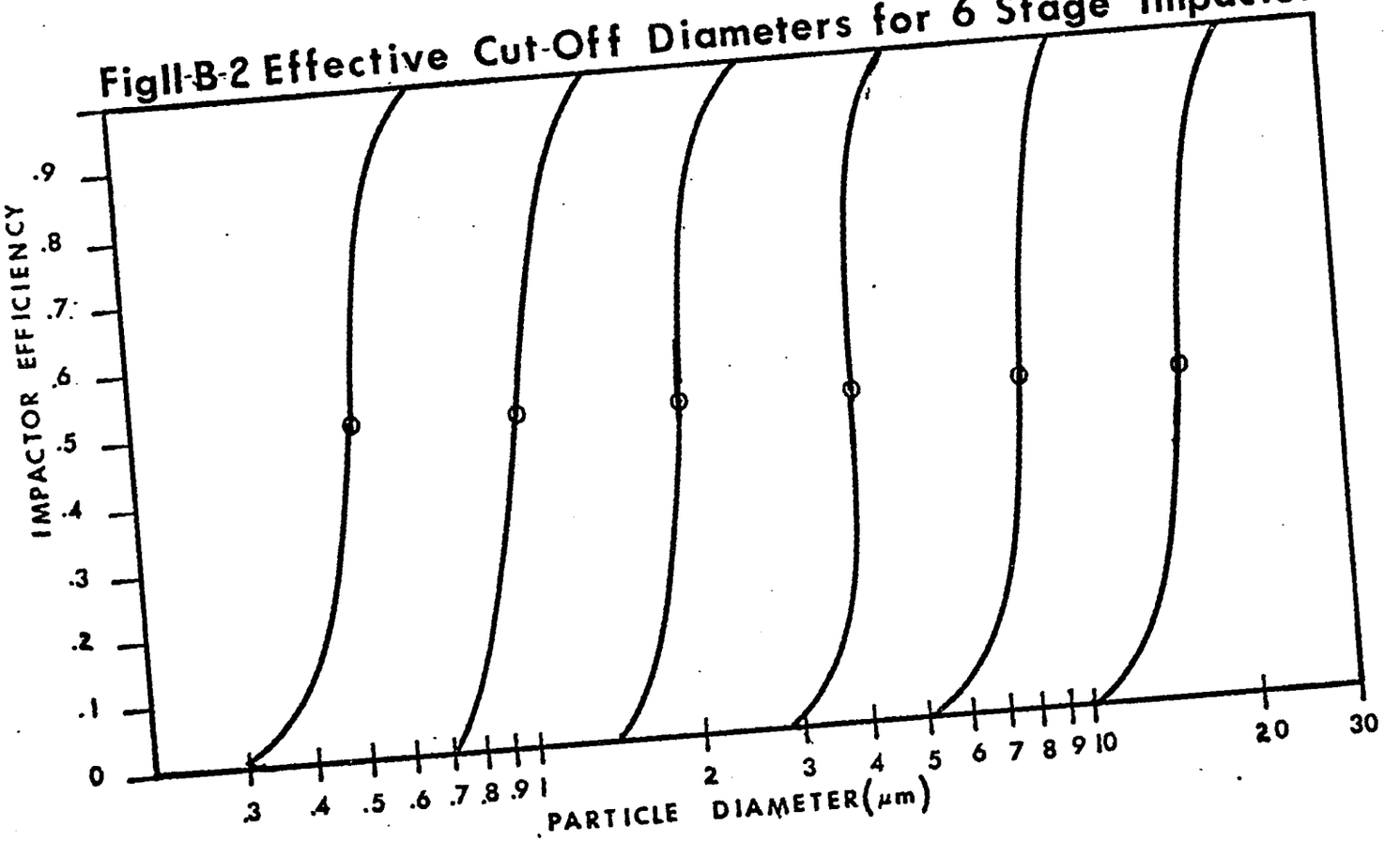

down through the first jet opening. Particles with sufficient momentum will not be able to follow the air stream around the first stage and will impact onto the surface. The airstream will then be further accelerated through the slightly smaller jet of the second stage. The distance of the second plate to the jet opening will be less than the previous stage, allowing for impaction of the smaller size particles. This process will continue until the aerosol reaches the final filter located after the 6th impaction stage. Fig II-B-2 is a plot of the effective cut-off diameter for each stage plotted against the percent impaction efficiency for each size particle assuming the particles to have unit density.

The efficiency of an impactor for collecting particles from an aerosol was shown by Ranz and Wong[4] to depend upon a separation number, ϕ, which they define as:

$$\phi = \sqrt{\frac{C\ D_{pc}^2\ v_2\ \rho_p}{18\ \mu_g\ D_c\ 10^8}} \qquad \text{(II.B.1)}$$

ϕ represents the ratio of the force required to stop a particle, whose size is D_{pc}, moving with a velocity v_2, in a distance $\frac{D_c}{2}$ to the aerodynamic drag defined for the gas by its viscosity, μ_g. The separation number, ϕ, will vary from 0 to 1 and a plot of ϕ vs. collection efficiency will yield an s-shaped curve. To determine a characteristic cu-

toff diameter for a given stage of the impactor, it is a common practice to use the value of .375 for ø which corresponds to 50% collection efficiency. Solving for D_{pc}, we get:

$$D_{pc} = \phi_{50}\ 10^4 \sqrt{\frac{18\ \mu_g\ D_c}{C\ \rho_p\ v_2}} \qquad \text{(II.B.2)}$$

where:

$$C = 1 + \frac{2 \times 10^4\ L}{D_p}\left[1.23 + 0.41e^{\frac{-0.44 D_p 10^{-4}}{L}}\right] \qquad \text{(II.B.3)}$$

for

$$0.1 < \left[\frac{2 \times 10^4\ L}{D_p}\right] < 134 \qquad \text{(II.B.4)}$$

C, also called the Cunningham correction factor, can be simplified when

$$\frac{D_p\ 10^{-4}}{L} > 2.7 \qquad \text{(II.B.5)}$$

Under these conditions the exponential term in equation 3 may be neglected and

$$C = 1 + \frac{2 \times 10^4\ L}{D_p}\ 1.23 \qquad \text{(II.B.6)}$$

If one considers running the impactor at room temperature and normal pressures (1 atm) then the correction factor

reduces to

$$C = 1 + \frac{0.165}{D_p} \qquad \text{(II.B.7)}$$

The velocity of the gas at the jet opening will depend on the pressure drop across the jet, the surface area of the jet opening, and the initial velocity of the gas flow into the impactor. To a good approximation the velocity can be given by

$$v_2 = \frac{v_o}{\pi \left(\frac{D_c}{2}\right)^2} \frac{P_o}{P_2} = \frac{4\ v_o}{\pi D_c^2} \frac{P_o}{P_2} \qquad \text{(II.B.8)}$$

If one now sets $D_p = D_{pc}$, equations 2,7,8 can be combined to give

$$D_{pc} = \frac{-15.3\mu}{\sqrt{g_c p P_2}} + \sqrt{\frac{234\mu^2}{g_c p P_2} + \frac{2.05 \times 10^8\ \mu\ D_c^3\ P_2}{\rho_p\ v_o\ P_o}} \qquad \text{(II.B.9)}$$

Equation 9 can be used to determine the characteristic particle diameter for each impactor stage.

Table II-B-1 gives the jet width and the plate distance as well as the cutoff diameters for three types of impactors. Another parameter critical to the construction of a reliable impactor is the wall to slide distance. Referring back to fig. II-B-1 one can see that if the radius of curvature for the trajectory of the particles passing around a given stage is wide enough, then the possibility for it hit-

Table II-B-1 Jet Diameter, Plate Spacing, and Cut-Off Diameters for Some Impactors.

	Battelle			Brink			Gillespie		
	dia. (cm.)	space (cm.)	cut (μ)	dia. (cm.)	space (cm.)	cut (μ)	dia. (cm.)	space (cm.)	cut (μ)
st1	1.364	.5115	16.0	0.249	0.747	3.14	0.251		2.95
st2	0.859	.3221	8.0	0.178	0.533	1.63	0.181		1.72
st3	0.541	.2029	4.0	0.140	0.419	1.10	0.138		1.09
st4	0.341	.1279	2.0	0.095	0.282	0.57	0.095		0.60
st5	0.216	.0810	1.0	0.073	0.220	0.33	0.077		0.38
st6	0.141	.0529	0.5						

Table II-B-2: Wall losses as Determined by Radiotracer Technique

			Percent Wall Loss				
Test	Temp(^{o}C)	%Rel Hum.	Wall 2	Wall 3	Wall 4	Wall 5	Wall 6
1	25	25	1.43	0.38	0.09	0.36	0.22
2	26	46	3.09	0.71	0.23	0.22	0.14
3	28	30	3.18	0.78	0.18	0.30	2.63[c]

a) % wall loss=100% x wt of material on wall/wt on wall + wt on sucessive stages
b) walls were not treated in run #3
c) believed to be erroneous result.

ting the wall increases. This effect, called aerodynamic wall loss, becomes significant as the wall to plate distance, d_{ws} , becomes smaller. Mitchell and Pilcher[7] empirically determined that the impaction plate should be about 3.8 cm in diameter and the d_{ws} , should be greater than 1.27 cm. This means a plate width to d_{ws} ratio of at least 3:1. To test the wall loss of the final design impactor a radiotracer, phosphorus-32, was used in the generated aerosol. The slides of the impactor were coated with a sticky solution of gelatin-water and for two of the three trials the walls were also coated with a similar solution. Table II-B-2 shows the result of the test.

Also to be considered in impactor sampling techniques is the problem of "bounce-off", a phenomenon which results from either the aerosol being too dry and collisions being very elastic or impaction surfaces becoming loaded due to lengthy sampling periods. The solution to the latter cause is to restrict sampling times to avoid overloading the collection surfaces. Another technique frequently employed is to apply a sticky film to the impaction surface to trap the particles. The major concern with bounce-off is the error that results in the mass distribution, since particles which bounce will appear on one of the succeeding stages.

Another interesting problem associated with bounce-off was proposed by Weslowski, et al.[13], who pointed out that relative humidity will affect the elasticity of the impact,

thus bounce-off problems should depend on both the sampling location and the weather conditions. For example, particles generated in a dry, dusty environment will bounce more than particles generated in a humid or coastal environment (where sea spray is responsible for a large percentage of the large particles.). This implies that sampling errors associated with bounce-off may not be uniform for all elements, even for the same sampling location. Consider for example that particles generated in a coastal area can arise from soil erosion, sea salt, urban, industrial, etc. sources. Particles generated by soil erosion will be more sensitive to bounce-off on dry days than sea salt particles and hence the elemental distribution can be shifted considerably according to the contribution of the soil particles to the total aerosol, wind direction and velocity (wind velocity will increase erosion). Large particles seem much more susceptible to bounce-off than small particles. This, in a sense, is preferable since most aerosol studies deal with combustion source particles generated by urban centers and of course these particles tend to be small (< 2.0 microns).

Bibliography

1. May, J.R., "The Cascade Impactor: An Instrument for Sampling Coarse Aerosols", J. Sci. Instr., 22:187(1945).
2. Laskin, S., "Pharmacology and Toxicology of Uranium Compounds", ed. by C. Voegtlin and H.C. Hodge,McGraw-Hill, New York,(1949).
3. Sonkin, L.S., J. Ind. Hyg. Toxicol., 28 ,269(1946).
4. Ranz, W.E., Wong, J.B., AMA Arch. Ind. Hyg. Occupational Med., 5 ,464-77 (1952).
5. Ranz, W.E., Wong, J.B., Ind. Eng. Chem., 44 ,1371 (1952).
6. Gillespie, G.R., Johnstone, H.F., "Particle Size Distribution in Some Hygroscopic Aerosols", Chem. Eng. Prog., 51 ,no.2, 74-80 (1955).
7. Mitchell, R.I., Pilcher, J.M., "Improved Cascade Impactor for Measuring Aerosol Particle Sizes in ....", Air Cleaning Symposium,U.S.A.E.C., Boston,Mass (1957).
8. Junge, C.E., Manson, J.E., J. Geophys. Res., 66, 2163 (1961).
9. Andersen, A.A., Am. Ind. Hyg. Assoc. J., 27, 160 (1966).
10. Lundgren, D.A., J. Air Poll. Cont. Assoc., 17 ,225 (1967).
11. Casella, C.F., Ltd.
12. Brink, J.A. Jr., "Cascade Impactor for Adiabatic Measurements", I.&E.C., 50, no. 4, 645-648, Apr. (1958).
13. Wesolowski, J.J., Appel, B.P., Alcocer, A., "Prelim-

inary Report on the Use of the Lundgren Impactor for Particle Size Measurements", Air and Industrial Hygiene Laboratory Report #138, AIHL Program, State of Calif. Dept of Health, 2151 Berkeley Way, Berkeley, Calif. 94704, Feb. 1973.

C. Impactor Calibration

As has been previously mentioned, the impactor inherently suffers from two disadvantages, wall loss and bounce-off, which can be minimized but not eliminated. The effects of wall loss are that the sample will contain less material than if there were no loss. Bounce-off effects, however, are not so obvious and can result in material loss to some suceeding stage(s), irretrievable loss to the walls, or if bounce is not extreme, dispersion of the sample from the center of the sampling stage. In the case where analysis requires confinement of the sample to some designated area, as in PIXE analysis, this latter case is tantamount to wall loss.

Modifications were made to the impactor design (see section on experimental set-up) to allow for the method of analysis, i.e. Mylar impaction surfaces instead of glass, making it necessary to calibrate the impactor to determine whether the modification had affected the operation of the instrument. Arrangements were made with the Health and Safety Division of E.R.D.A. which permitted use of their aerosol laboratory for calibration.

The calibration of the impactor involved, 1) measuring the flow rate, 2) determining under specified operating conditions, whether wall loss and/or bounce-off were significant problems and 3)if they were, to see if we could minimize these effects by applying a sticky medium to the collec-

tion surfaces.

Flow calibration was checked by connecting the 6-stage impactor, loaded with uncoated Mylar on all six stages and Gelman glass fiber filter paper as the after filter, downstream from an American Meter Company dry gas meter. The meter was calibrated with a standard volume source and found to be accurate. A mercury manometer was connected in parallel downstream of the impactor to measure the pressure drop applied by the vacuum pump. Manufacturers specifications require a vacuum of >17" Hg for a flowrate of 12.5 liters/min. Under these conditions, the flow rate is controlled by a critical orifice located at the last stage of the impactor. Two separate 2 min. runs were performed at vacuums corresponding 19" Hg and 17" Hg respectively. The results shown in table II-C-1 indicate a flow rate 4.0% higher than specified, a result probably due to an oversized diameter at the critical orifice.

Table II-C-1. Flow rate Calibration

Run Time (min.)	Vacuum ("Hg)	Volume (liters)	Flow Rate (l/min.)
2	19	26.08	13.04
2	17	26.00	13.00

A spinning-disk generator was used to produce monodisperse 8.5 μm methylene blue spheres for the second and third parts of the experiment. The impactor was placed into a clean positive pressure box connected via conduit to the

spinning disk generator. The impactor was wrapped in plastic so that all external surfaces were covered except for the inlet. This was done to guard against external contamination by the methylene blue spheres. According to the efficiency curves for collection by stage, the 8.5 μm particles should have been collected with 50% efficiency by stage 2.

After approximately half an hour the impactor was removed from the chamber and disassembled stage by stage and the Mylar rings removed. Each stage section was soaked in alcohol to remove the methylene blue spheres adhering to the walls. The Mylar rings were first separately analyzed visually and with a microscope. To ascertain the extent of wall loss and to determine the mass distribution of the spheres each ring was separately washed with alcohol to recover all the methylene blue deposited. These solutions together with the solutions prepared by washing the stage walls were measured using a spectrophotometer to determine the absorption of each solution. The absorbtivities were compared to absolute standards to determine the amount of material collected by each section. The results, summarized in table II-C-2, clearly show both of the inherent problems with the impactor. Almost 37% of the material entering the impactor is lost to the walls. The 6.28% and 9.32% losses associated with stage sections 1 and 2 are unavoidable because the particles have not yet reached critical velocity

for impaction. However, the losses associated with the suceeding stages, 19.17%, and the wall losses on subsequent stages, 21.04%, should be, at least in part, avoidable.

Table II-C-2. Wall Loss and Bounce-off for Modified Impactor (slides were uncoated.)

Stage	vol. Alcohol ml.	Spect. Reading 0-100	Conc. (g/ml) $x10^{-5}$	Total Weight $x10^{-5}$g.	% Total
1	12.	98	.145	1.74	2.88
2	20.	77	1.25	25.00	41.32
3	10.	84	.840	8.40	13.88
4	10.	97	.175	1.75	2.89
5+6	10.	98	.145	1.45	2.40
				38.34	63.36
Stage section Wall Losses					
1	19.	96	.200	3.80	6.28
2	24.5	95	.230	5.64	9.32
3	32.0	97	.175	5.60	9.25
4	25.	98	.145	3.63	6.00
5	13.5	98	.145	1.96	3.24
6	12.5	99	.123	1.54	2.55
				22.17	36.64

Dow Corning Antifoam Silicone spray was used as a coating material for the slides in a second run to minimize the losses already discussed. The impactor was again run for half an hour under the same conditions. The results are summarized in Table II-C-3. Of note is the lack of material both on the walls and on the stages following stage 3. The losses associated with pre-impaction surfaces (all impactor surfaces available to the particles before they reach critical velocity for impaction) are essentially the same, but we have recovered 16% of the total mass which would otherwise have been lost. Also to be noted is that the 50% collection efficiency associated with the second stage is almost real-

ized. Increasing the coating thickness to attempt to retrieve more material was not possible since we had to maintain a thin target for analysis. It was decided that a 20% error in collection effiicency would be tolerated.

We would have liked to repeat this procedure using different size spheres to monitor the trends on the higher order stages but unfortunately neither time nor available manpower permitted this. However, it is, known that large particles do tend to bounce more than small particles and so we at least set an upper limit on the relative loss for each size fraction.

Table II-C-3. Wall Loss and Bounce-off for Modified Impactor (stages were coated with Dow Corning silicone spray)

Stage	vol. alcohol ml	Spect. Reading 0-100	Conc. (g/ml) $x10^{-5}$	Total Weight $x10^{-5}$g	% Total
1	10.	96	.2	2.00	2.9
2	27.	77	1.2	3.24	46.8
3	11.	67	1.76	1.94	27.9
4	8.	97	.175	1.4	2.0
5+6	-	-	-	-	-
				55.24	79.63
Stage section Wall Losses					
1	27.	96	.2	5.4	7.8
2	27.	95	.23	6.21	8.9
3	20.	99	.123	2.46	3.6
4	-	-	-	-	-
5	-	-	-	-	-
6	-	-	-	-	-
				14.10	20.30

D. Sampling Methods and Requirements

All samples were collected with a Batelle type cascade impactor manufactured by Delron Reasearch Inc., the DCI-6, which samples 1.5 m^3 in approximately 2 hours at a flow rate of 13.0 liters/min. and has 50% cut-off diameters of 16, 8, 4, 2, 1, and 0.5 μm. It is machined of 303 stainless steel, weighs 31 lbs., is 20 inches tall and is 4 inches in diameter. This final choice of impactor was made because it provided us with a well defined sample (< 0.5 cm diameter for largest particles), fractionated the particles into appropriate ranges and showed excellent collection ability with a reasonable amount of bounce and wall-loss when impaction surfaces were properly prepared (see section II-C). In addition, it could sample the required volume of air (1 m^3) in slightly less than two hours which made it possible to collect more than one sample per day.

Analytical requirements necessitated the use of thin films for the impaction surface so that 0.1 mil Mylar, obtained from Chemplex Industries, was used. Support for the Mylar was achieved by stretching the film between two concentric brass rings machined to a tolerence of 0.25 mil. The Mylar had to be prewashed to remove a surface coating of zinc, which was accomplished in a bath specially constructed for the purpose. The unwashed Mylar could be rolled through the bath manually and wound on a take-up reel. The bath solution was prepared using doubly-distilled deionized water

to make a 0.1 M solution of HNO_3 and the Mylar was usually run through the acid bath at least twice, at a rate no faster than 6 in./min. Since the bath had spools on either side, once started, the Mylar never had to be touched again which minimized the possibility for contamination. The Mylar was then rinsed in a bath containing only the doubly-distilled deionized water to remove any adherent acid which might weaken the Mylar if allowed to remain for any length of time. After the water wash, while the Mylar was still on the spools, a glass plate could be inserted over the top of the bath as a support, and the Mylar then directly mounted onto the brass rings. To prevent bounce-off of particles (see section II-C) a thin coating of Vaseline was sprayed on the Mylar surface prior to sampling. The coating was applied by dissolving ca. .5 gram of Vaseline in ca. 100 ml. of benzene and spraying the solution onto the rings and allowing the solvent to evaporate. The rings were then substituted for the glass slides that are normally used. To prevent distortion of the Mylar surface by the impinging jet stream during sampling, support backings machined from a pure grade of nylon stock were used.

The rings were removed after sampling and stored in a sample holder for transport back to the clean work area for slide mounting. The samples were mounted in 2 x 2 Kodak slide holders with the use of a die-cut, self adhesive, acetate backing which exactly fits the 2 x 2 mounts. Once in

place the acetates were heat sealed inside the mounts which were labeled and the samples were again stored in containers until they were ready to be analysed. Figures II-D-1 and II-D-2 show the various steps in sample preparation.

II-2-1

FIG. III-C SLIDE MOUNTING TECHNIQUE

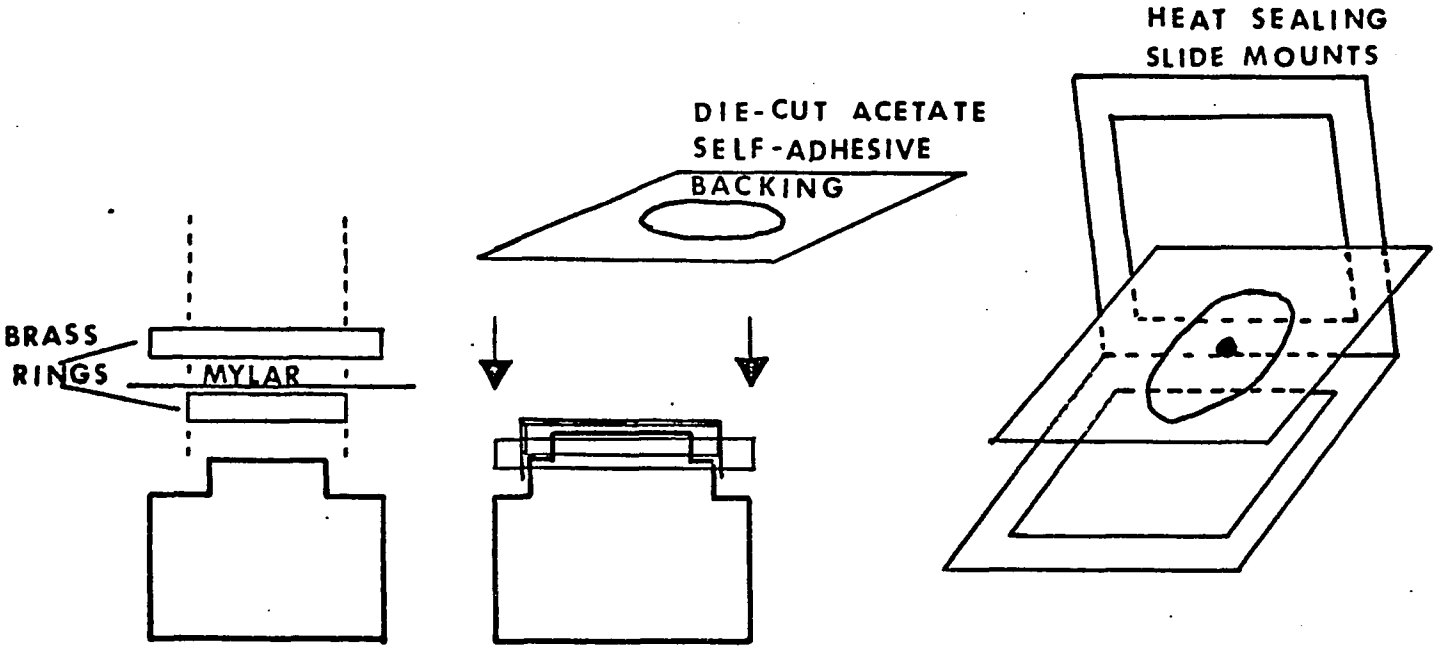

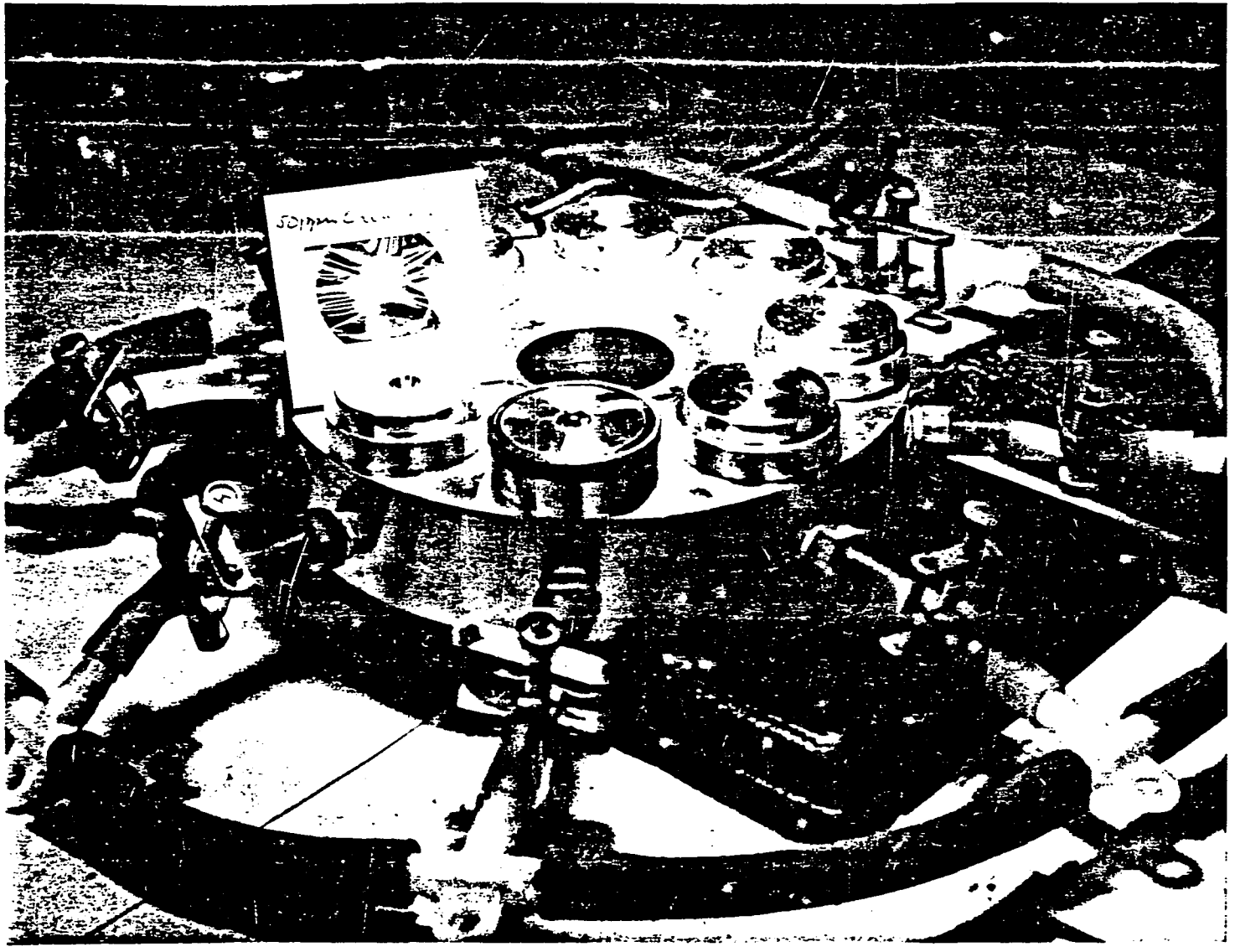

Section III.

A. Introduction to Proton-Induced X-Ray Fluorescence

The production of characteristic x-rays by proton excitation has been extensively studied for many years and the theoretical foundations are also well understood.(1),(2) It is only recently, however, that such an exotic technique has been employed for routine elemental analysis. The increasing need for rapid, multielement, ultrasensitive techniques to analyze for environmental contaminants has presented the challenge to find new tools capable of handling the increased burdens of analysis. The technique of x-ray fluorescence affords the opportunity to perform multielement determinations regardless of the chemical environment of samples and with little, or more often, no sample pretreatment. In addition, the method is essentially nondestructive.

There are three methods by which x-rays may be generated from a target material. The most conventional and therefore most often used method is photon excitation. In this method of excitation a continuum of photons, generated by bombarding a primary target with electrons, is allowed to impinge on the specimen target causing removal of electrons followed by emission of the characteristic x-rays. Only that portion of the continuum above the absorption edge of the target material will be effective in producing x-rays. The other two methods of excitation involve charged parti-

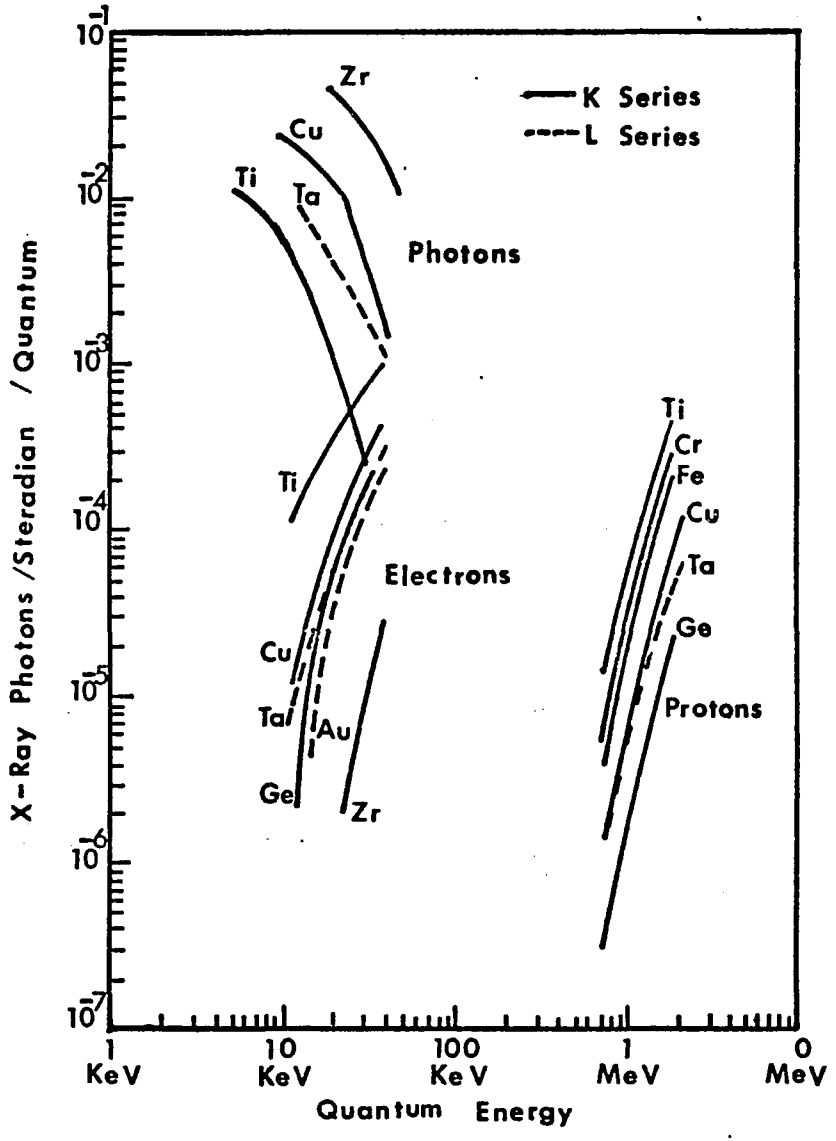

Fig III-A-1. Efficiency of X-Ray Production Techniques

cles. Electron beam excitation is probably the next most often used technique followed by positive ion (H^+,He^{++}, etc.) beam excitation. Since radioactive sources do not provide sufficient intensity for analysis of small amounts of material, most charged particle excitation requires the use of an accelerator. The choice of excitation source depends on many criteria, including target thickness, beam intensity, sensitivity of analysis desired and efficiency for x-ray production. The efficiency for x-ray production of fluorescent radiation is often expressed as total yield, the product of the probability for ionization (σ) and the fluorescent yield (ω). As can be seen from Fig. III-A-1[3] the most efficient method for producing x-rays/quantum of incident radiation is by photon production. However, for electron and proton production (heavier ions follow the same trends) the efficiency increases with increasing energy while for photon production just the opposite is observed. This aspect of photon production creates many practical problems. In order to perform multielement analysis it becomes necessary to increase the quantum energy of the incident flux to excite the high-Z elements. This however, will decrease the sensitivity for the lighter elements. To compensate for this it is often necessary to perform multiple excitations at different photon energies for each sample.

The bremsstrahlung produced by elastic scattering events make electrons very undesirable as an excitation

source. This is because the continuum in general will be so intense that the detectable limits will be only about 20 to 100 ppm for Z=19 to 30. In contrast, the bremsstrahlung continuum for proton excitation is much less intense and thus allows for greater sensitivity. As an example consider that the maximum energy that can be imparted to an electron from a proton in an elastic collision is given by:

$$E_e = 4 \frac{M_e}{M_p} E_p \qquad \text{(III-A-1)}$$

This means that for a 3.0 MeV proton the maximum energy that can be imparted is only 6.5 keV. This corresponds to an x-ray for element no. 26. The intensity of the secondary-electron bremsstrahlung produced by a beam of protons is less than that produced by a beam of electrons of the same energy by a factor of $(\frac{M_p}{M_e})^2$, = 4×10^6, because of the smaller accelerations experienced by the protons due to their greater mass.[4] Since, however, proton energies usually are 10^2 times higher than most electron energies for this microanalytical technique, proton produced bremsstrahlung will only be ca. 10^4 less than electron produced bremsstrahlung. This is still a significant reduction in background and allows for much greater sensitivity and lower limits of detection than do electron induced methods. Another source of background associated with proton excitation is the proton bremsstrahlung produced as a result of

the proton undergoing scattering events which result in energy loss. This background is approximately a linear continuum extending out to the energy of the proton. Thus, for proton excitation the background associated with the actual scattering event is composed of two sources:

a) electron bremsstrahlung

b) proton bremsstrahlung

To eliminate these as a source of background one tries to minimize the proton energy losses by adhering to the requirements of a thin target.

Thin targets of <100 micrograms/cm^2 will attenuate the proton energy by only a few percent and produce virtually no background. This of course, will not only lower detectable limits because of improved signal to noise ratio for low Z elements, but it will also require smaller sample sizes so that counting time and therefore analysis time will be increased. This however, is not a serious problem as all elements are essentially counted simultaneously so that overall the method will still require less time/element than any other technique available for trace-element applications.

B. Production of Fluorescent X-Rays Using 1-4 MeV Protons

The production of fluorescent x-rays for a target specimen can be expressed by the following eq.

$$A = N \phi \sigma_k \omega \rho \left[\frac{\theta}{4\pi} \eta\right] \qquad \text{(III-B-1)}$$

where;

N = number of atoms of a particular element

ϕ = flux of protons (protons/sq.cm.) hitting the target

σ_k = ionization cross section for a specific K shell

ω = fluorescence yield

ρ = relative transition probability

and the term in brackets is the overall efficiency of the detector. The term $\frac{\theta}{4\pi}$ relates the geometric efficiency of the detector while η is the detector efficiency for the given x-rays.

The cross section ,σ_k , varies directly with the energy of the impinging proton as seen in Fig. III-B-1. Thick targets will result in both energy loss and decreased flux as the beam traverses the target, and will also cause attenuation of the emitted fluorescent x-rays; therefore, thin targets of approximately 40-1000 μgrams/cm^2 are used. Returning to eq. III-B-1 the product term $\sigma \omega \rho$ can be combined to a reduced cross section called σ_k', the elemental x-ray production cross section for a given shell. Figure III-B-2 shows both the magnitude of the cross section and its dependence on the atomic number for some middle Z ele-

FIGURE
III-B-1

K X-RAY PRODUCTION CROSS SECTIONS VS. PROTON ENERGY

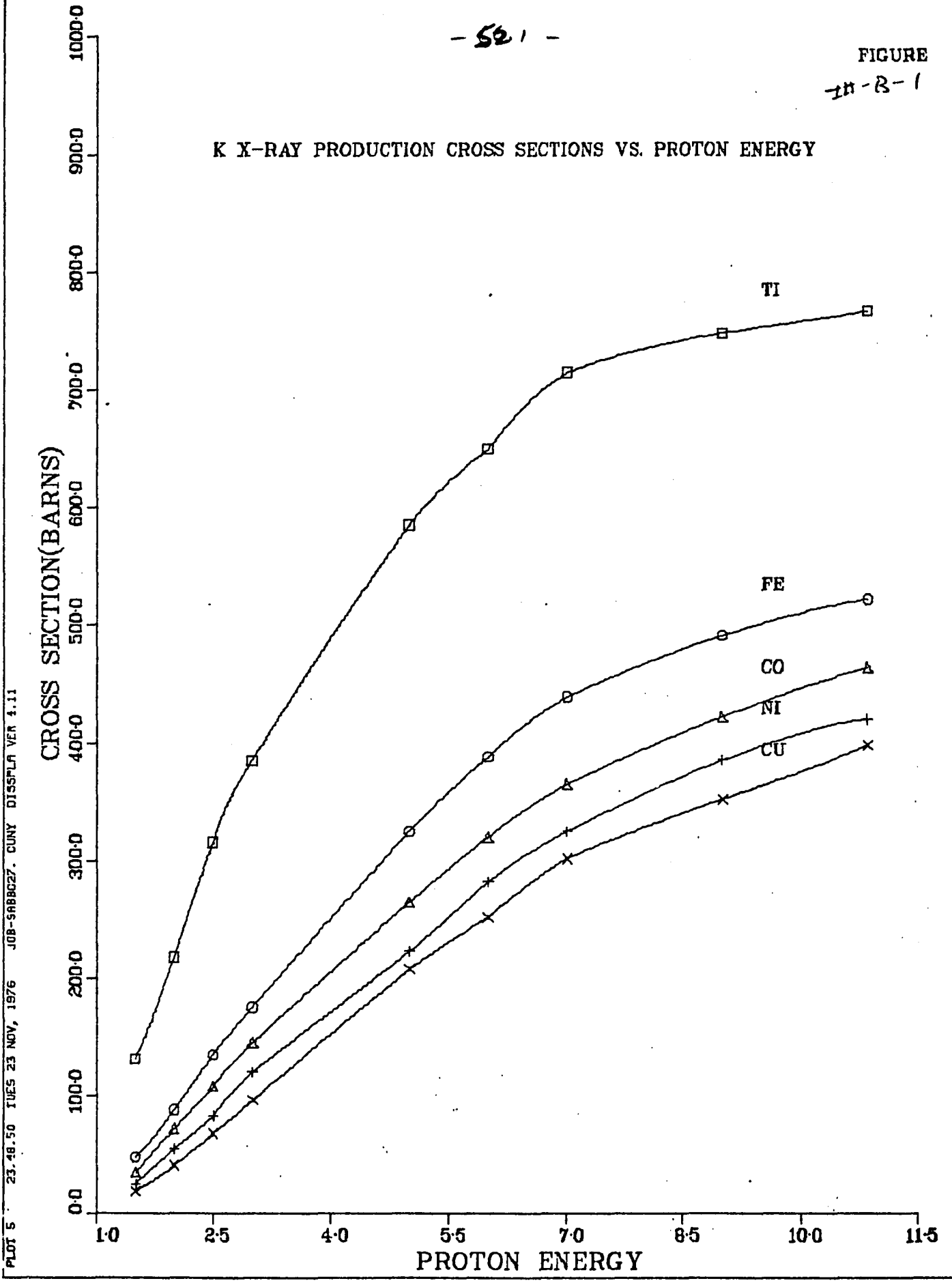

Fig III-B-2. Fluorescent Yield and Ionization Cross Section* vs. Z for 3 MeV Protons

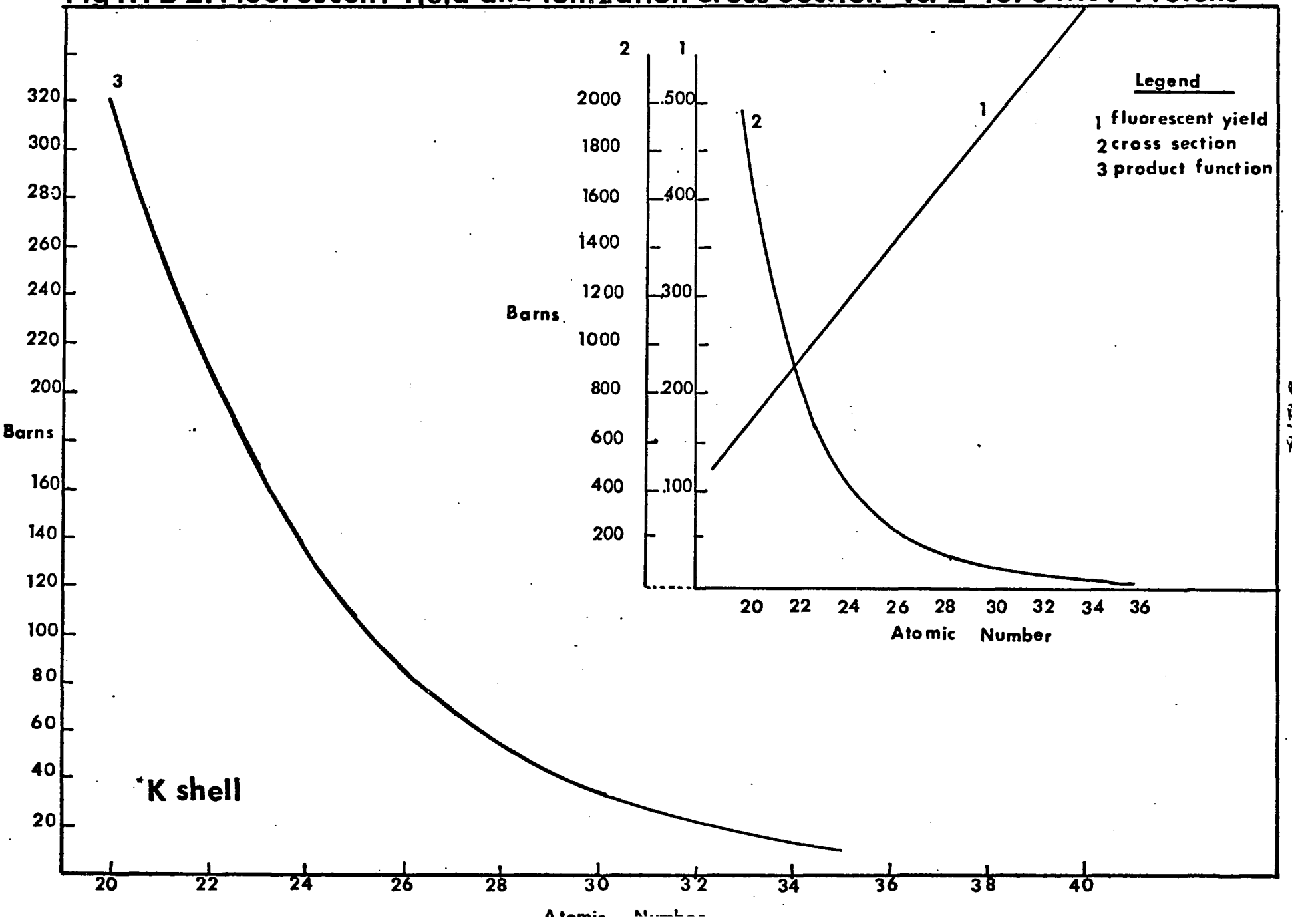

Fig III-B-3. Cross Section vs. Atomic Number for 1 to 4 MeV Protons

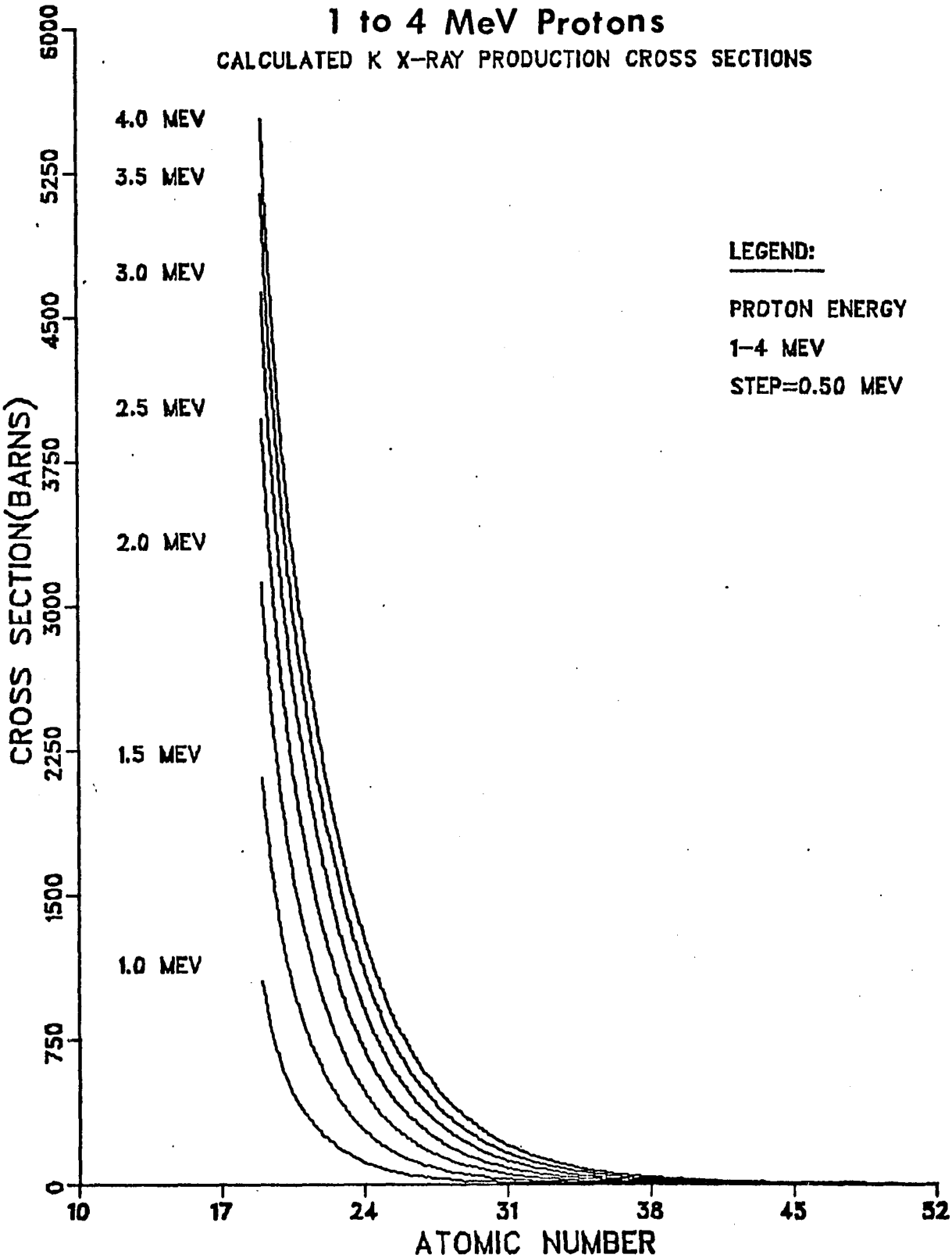

ments using 3.0 MeV protons for excitation. Figure III-B-3 shows how the proton energy affects the cross section from 1.5 MeV to 4.0 MeV. In addition Table III-B-1 presents the calculated K ionization cross-sections for Z=19-50. These cross-sections are obtained using the Binary Encounter Approximation (BEA) given by eq. III-B-2.[5]

$$\phi_i = \frac{1}{I_k^2} \left| \exp \sum_{i=0}^{i=5} b_i \, X^i \right| \qquad \text{(III.B.2)}$$

where:

$$X = \ln \frac{10^{-3} E_p}{I_k}$$

$b_0 = 1.8451$

$b_1 = 0.60365$

$b_2 = 0.44481$

$b_3 = 0.17481$

$b_4 = 0.11142$

$b_5 = 0.09141$

E_p = proton energy (eV)

I_k = ionization energy (eV)

At proton energies above 4.0 MeV the errors associated

Table III-B-1 Calculated K Ionization Cross-sections for Protons (1-4 MeV) {Barns}

At.No.	K(eV)	1.0MeV	1.5MeV	2.0MeV	2.5MeV	3.0MeV	3.5MeV	4.0MeV
19	3507	1052	2111	3120	3965	4630	5139	5535
20	4038	602	1273	1965	2587	3107	3527	3859
21	4496	389	854	1362	1841	2260	2612	2899
22	4965	258	585	960	1329	1665	1957	2204
23	5465	172	403	678	960	1226	1466	1674
24	5989	116	280	482	697	907	1101	1275
25	6540	79.2	196	345	509	673	829	973
26	7112	54.7	139	249	374	502	628	746
27	7709	38.1	99	181	276	377	477	574
28	8333	26.8	71.2	133	205	284	364	442
29	8979	19.0	51.7	97.7	153	215	278	342
30	9659	13.5	37.7	72.3	115	163	213	265
31	10368	9.7	27.6	53.7	86.4	123	164	205
32	11104	6.98	20.3	40.2	65.4	94.6	128	160
33	11868	5.0	15.1	30.2	49.7	72.6	97.9	137
34	12658	3.70	11.2	22.8	38.0	55.9	76.1	97.8
35	13474	2.69	8.45	17.4	29.2	43.4	59.5	76.9
36	14322	1.97	6.36	13.3	22.5	33.7	46.6	60.6
37	15201	1.44	4.81	10.2	17.4	26.3	36.6	47.9
38	16105	1.06	3.65	7.84	13.5	20.6	28.8	38.0
39	17037	.78	2.78	6.06	10.6	16.2	22.8	30.3
40	17998	.58	2.13	4.71	8.29	12.8	18.2	24.2
41	18986	.43	1.63	3.68	6.53	10.2	14.5	19.4
42	20002	.32	1.26	2.88	5.16	8.09	11.6	15.6
43	21054		.97	2.25	4.09	6.45	9.30	12.6
44	22118		.75	1.78	3.26	5.18	7.51	10.22
45	23224		.58	1.41	2.60	4.16	6.07	8.29
46	24350		.45	1.11	2.09	3.36	4.92	6.76
47	25515		.35	.88	1.67	2.72	4.00	5.52
48	26711		.27	.70	1.35	2.20	3.26	4.52
49	27940		.21	.56	1.08	1.79	2.66	3.70
50	29200		.17	.45	.87	1.45	2.18	3.05

with the BEA are about 10% too high; between 4.0 MeV and 1.0 MeV, agreement with experimental values[6] is good. Proton cross sections for K x-ray production are maximum at about 15 MeV. As both of the previous figures indicate, the cross section dependence on both atomic number and proton energy follow smooth curves. This is significant for quantitative analysis since only a few reference standards need be used to monitor changes in proton energies and to readily normalize the results. Therefore, by imposing the requirement of a thin target, eq. 1. is now rewritten as :

$$A = N \sigma_k \phi \left[\frac{\Theta}{4\pi} \eta\right] \qquad \text{(III.B.2)}$$

and can be used for quantitative determination of elements present in specimen targets. In addition, for a given detector with a fixed geometry, the geometry and counting efficiency terms will drop out since standards are counted under the same conditions. Therefore eq. III.B.2 can be even further simplified to:

$$A = N \sigma_k \phi \qquad \text{(III.B.3)}$$

This simplified equation can be used for quantitative analysis as long as the following experimental conditions are met. Since N, the number of atoms that the proton beam irradiates depends on the positioning of the sample with respect to the beam, a method of precise target positioning must be maintained from sample change to sample change, thus

ensuring that the full sample lies in the beam. In addition, any loss of material either through flake-off or volatilization will result in experimental error. Volatilization losses can occur in vacuum systems where beam currents will raise the temperature of the target material. The nature of the loss of course depends on the elements in question and the temperature increase (which is beam current density dependant). Campell, et al.[7] have shown that for beam currents of less than 50 nanoamps in vacuum system, there is no serious loss of even the most volatile materials over many hours. Also, since the cross-section is energy dependent, samples must be thin and matrix effects for standards should be similar to samples. Finally, a precise, although not necessarily accurate measure of the integrated beam flux must be made to ensure that samples are counted for a known standard measure.

Bibliography

1. W. Bambynek, B. Crasemann, R. Fink, H. Freund, H. Mark, C. Swift, R. Price, P. Rao, "X-ray Fluorescent Yields, Auger, and Coster-Kronig Transition Probabilities", Rev. of Mod. Phys., 44, #4, Oct(1972).
2. N.A. Dyson, "The Production of Characteristic X Rays by Proton Bombardment, and the Ratio of Characteristic to Continuous Radiation", J. Phys. B: Atom. Mole. Phys., 6, pp. 562-572, March 1973.
3. Rolf Waldseth, X-ray Energy Spectrometry, Kevex Corp., p. 4.5, Burlingame, Calif. (1973).
4. Ibid., p 2.8
5. K. Akselsson, T.B. Johansson, "X-Ray Production by 1.5-11 MeV Protons", Z Physik, 266, p. 245-255, (1974).
6. N.A. Dyson, op. cit. p. 571
7. J.L. Campell, B.H. Orr, A.W. Herman, L.A. McNelles, J.A. Thomas, W.B. Cook, "Trace Element Analysis of Fluids by Proton Induced X-Ray Fluorescence", Anal. Chem., 47, #9, August, 1975.

C. PIXE System

The PIXE system is composed of five major features;

a] a source of protons,

b] a defocusing and collimating section,

c] a vacuum aperture,

d] a sample chamber.

e] a detector

Protons are generated with a 3.75 MeV modified Cockroft-Walton type linear accelerator called a Dynamitron (RDI Inc.). This accelerator is capable of accelerating heavy ions up to nickel and has current capabilities of up to 2 milliamps for protons (proportionately less for heavier ions). For the PIXE work proton currents from 2 to 5 microamps are taken out of the machine at energies of 3.0 Mev $\pm$0.1%.

To ensure that the cross-sectional profile of the proton beam is uniform, the protons are defocused and recollimated before emerging from the transport system. Defocusing is accomplished by allowing the beam to scatter through a thin metal foil (either gold, nickel,or tungsten). The scattered beam is collimated by three 1 cm diameter graphite apertures located downstream of the scattering foil separated by graphite spacers 5-7 cm long(Fig. III-C-1).

This "homogenizing" system is contained in an aluminum pipe and snugly fits inside the 4" stainless steel transport tube which acts as the heat sink. Proton energy loss for

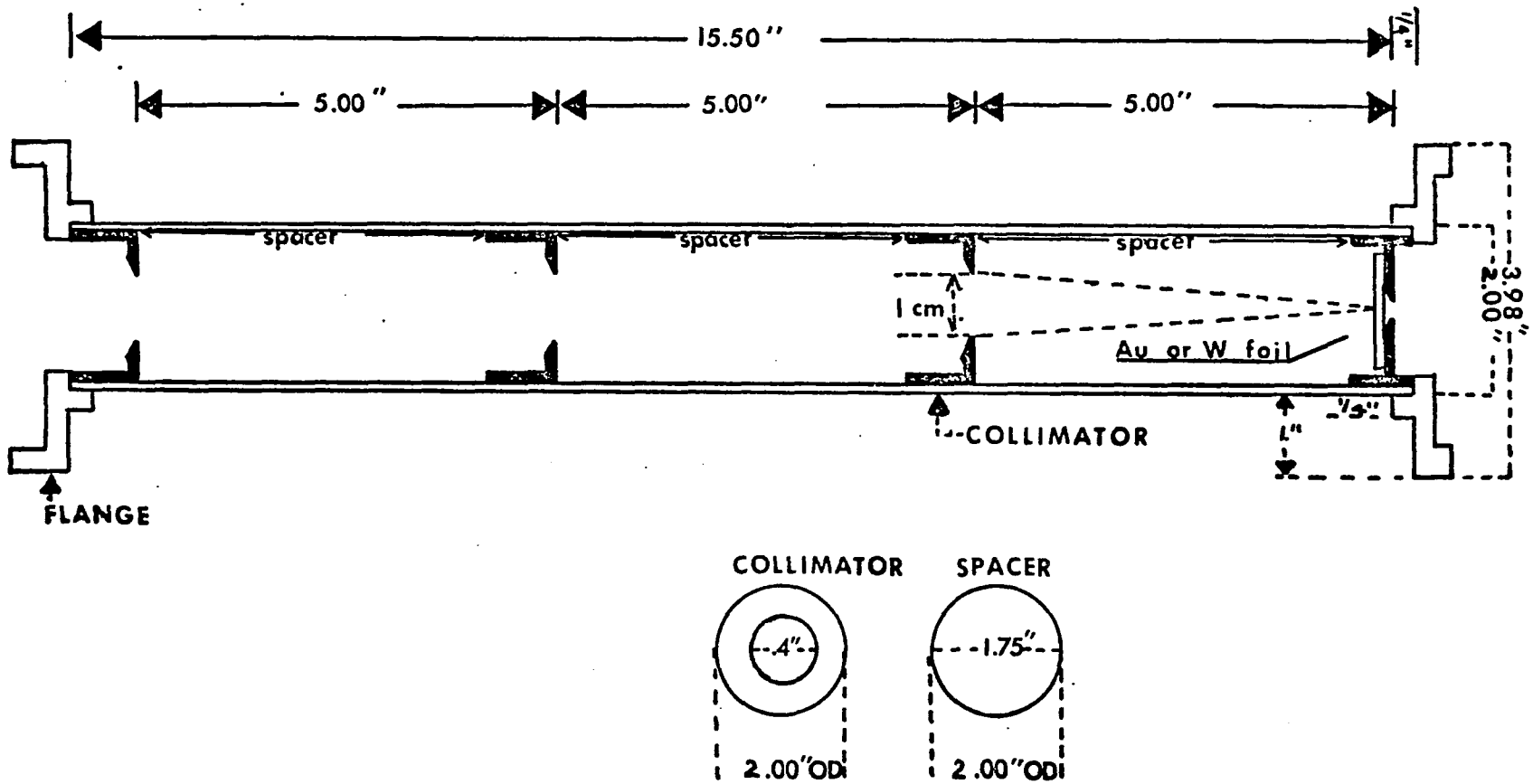

FIG. III-C-1 PROTON BEAM HOMOGENIZER

this process is approximately from 400-600 kev depending on the foil material and thickness. Although not experimentally verified, calculations indicate that the beam should be uniform in cross-sectional density to better than 0.1%. The exact theory for multiple scattering was first presented in 1940 by Goudsmit, et al.[1] it was later approximated by Moliere in 1947[2], and a further approximation appeared in 1959 by B.P. Nigam, et al.[3] In 1966, Marion and Zimmerman[4] presented a method for calculating the distribution function and the value of the scattering angle for charged particles. For the exact theory of multiple scattering the reader is referred to any of the papers cited above, only the method for obtaining the approximately gaussian distribution function and the scattering angle as determined by Marion and Zimmerman wil be presented here.

The angular distribution function for protons scattered by a foil whose atomic number is Z, and whose thickness is t is approximately given by

$$F(x) \alpha \exp-(x_2/x_w^2) \qquad \text{(III-C-1)}$$

where

$$x = \frac{\theta}{x_c B^{1/2}}$$

$$x_c^2 = 0.1569\ Z(Z+1)z^2 \frac{t}{A(pv)^2}$$

$$B - \ln B = b$$

$$b = \ln \frac{2730\ (Z+1)Z^{1/3}z^2 t}{A\beta^2} - 0.1544$$

Fig. III-C-2

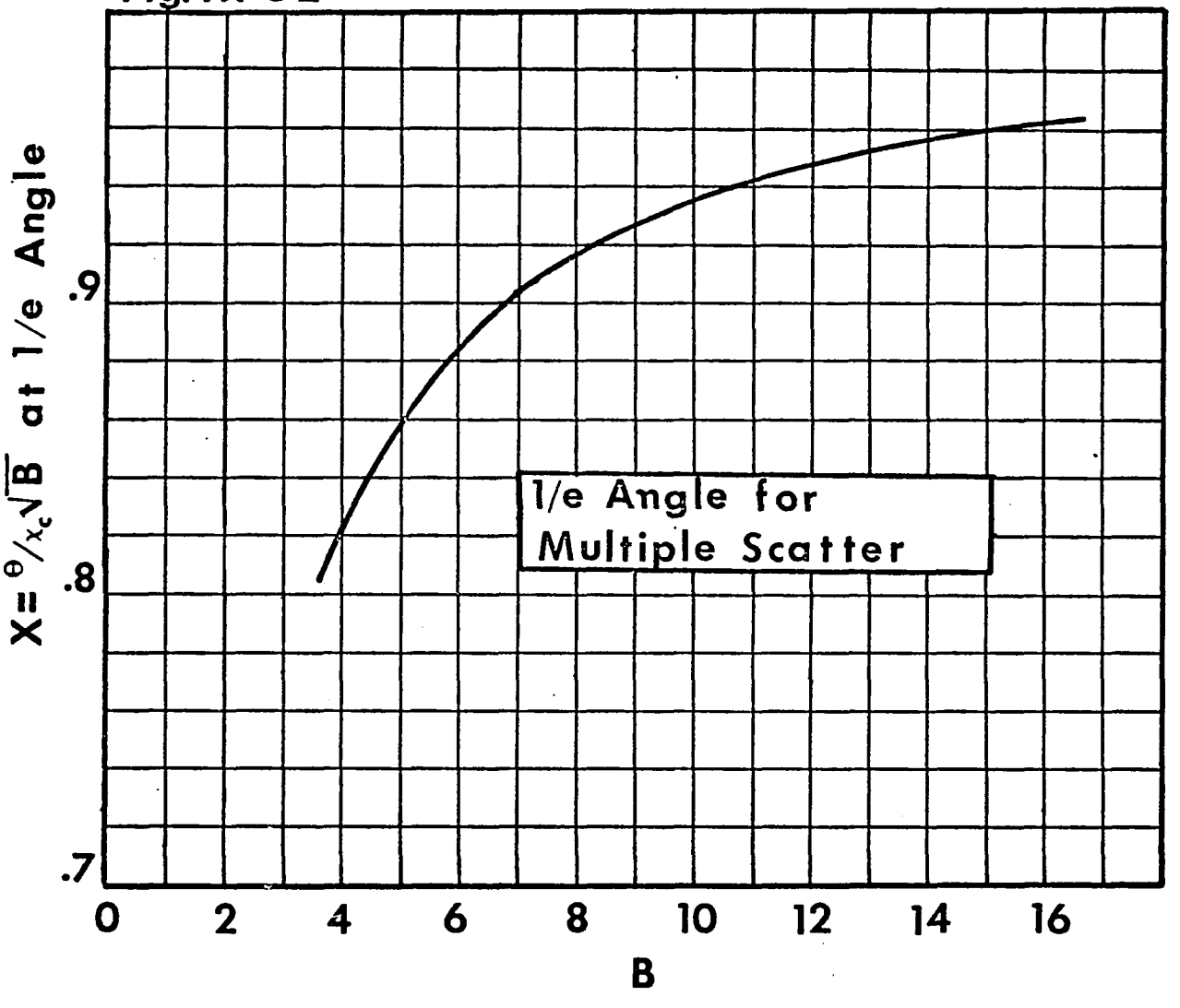
$X = \theta/\chi_c\sqrt{B}$ at 1/e Angle
.9
.8
.7
0
2
4
6
8
10
12
14
16
B
1/e Angle for
Multiple Scatter

Fig III-C-2 Radially Directed Distribution of Scattered Protons

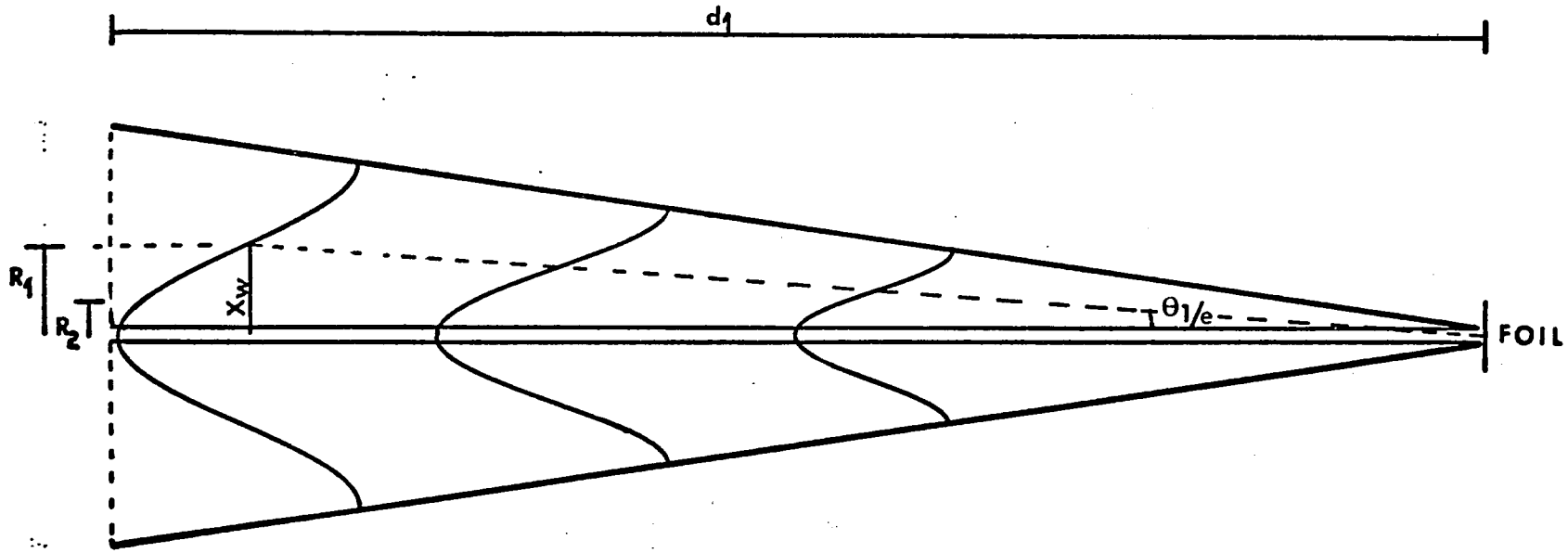

$$F\{X\} = \left\{\frac{1}{2\pi X_w^2}\right\}^{1/2} \exp - \frac{1}{2}\left\{\frac{X}{X_w}\right\}^2$$

$$d_1 = X_w / \tan \theta_{1/e}$$

x_w = angle at which F(x) has fallen to 1/e of its original value at x=0.

z= atomic # of incident particle

Z= atomic # of scatterer

t= scatterer thickness(g/cm^2)

(pv)= momentum-velocity product of incident Particle (MeV)

$$(pv)^2=(E^2+2EMc^2)\beta^2$$

$$\beta^2=1-(1+\frac{E}{Mc^2})^{-2}$$

E = average energy of incident particle in scatterer(MeV)

Mc^2= rest mass energy of incident particle(MeV).

One of the limitations of the theory is in the allowable values of B. The quantity e^b roughly approximates the number of collisions suffered by the particle in trasversing the foil. In order to use the approximation the number of collisions must exceed 10-20. If $e^b=15$, then b=2.7 and B=4. At the other extreme, too many collisions (i.e. target too thick), energy loss in the foil becomes excessive and the theory is no longer valid. As a reasonable criterion the particle must lose < 20% of its initial energy in the foil. This generally means $4\leq B\leq 15$. If one wishes to know the angular distribution, F(x), or the width, x_w, of the curve at the 1/e point, z, Z, A, t and β must be known. Next b is computed and B found from table III-C-1. The value of x_w and the angular distribution function can next be determined

by reading the value x from the graph (fig. III-C-2) and multiplying by $x_c B^{1/2}$ to obtain $\theta_{\frac{1}{e}}$ (in radians). The fraction of particles scattered into a cone corresponding to x_w (called $\theta_{\frac{1}{e}}$) can be computed from

$$\text{fraction} = \frac{\int_0^{\theta_{\frac{1}{e}}} F(\theta)\sin\theta d\theta}{\int_0^{\theta_{max}} F(\theta)\sin\theta d\theta} \qquad \text{(III-C-2)}$$

As an example, the case of a 0.1 mil gold foil and a 3.0 MeV proton will be considered. The number of collisions experienced by the average proton will be e^b;

$$e^b = \exp\left[\ln 2730\ (Z+1)Z_{\frac{1}{3}} z^2 \frac{t}{A\beta^2}\right] - 0.1544 \qquad \text{(III-C-3)}$$

where

$t = 4.83\ mg/cm^2$

$Z = 79$

$A = 197$ amu

$\beta^2 = 6.107 \times 10^{-3}$

$z = 1$

and therefore

$$e^b = \exp\left[\ln 3.757 \times 10^3\right] - 0.1544 \qquad \text{(III-C-3)}$$

$$e^b = \exp 8.077 = 3.22 \times 10^3 \text{ collisions} \qquad \text{(III-C-4)}$$

Table III-C-1 Values of B and $B^{1/2}$ Calculated from B-lnB=b

b	B	$B^{1/2}$	b	B	$B^{1/2}$
2.6	3.982	1.995	8.4	10.777	3.283
2.8	4.246	2.061	8.6	10.998	3.316
3.0	4.505	2.123	8.8	11.217	3.349
3.2	4.760	2.182	9.0	11.437	3.382
3.4	5.012	2.239	9.2	11.656	3.414
3.6	5.260	2.294	9.4	11.874	3.446
3.8	5.506	2.346	9.6	12.093	3.477
4.0	5.749	2.398	9.8	12.310	3.509
4.2	5.990	2.447	10.0	12.528	3.539
4.4	6.229	2.496	10.2	12.745	3.570
4.6	6.467	2.543	10.4	12.962	3.600
4.8	6.702	2.589	10.6	13.179	3.630
5.0	6.937	2.634	10.8	13.395	3.660
5.2	7.170	2.678	11.0	13.611	3.689
5.4	7.402	2.721	11.2	13.827	3.718
5.6	7.632	2.763	11.4	14.042	3.747
5.8	7.682	2.804	11.6	14.257	3.776
6.0	8.091	2.844	11.8	14.472	3.804
6.2	8.318	2.884	12.0	14.687	3.832
6.4	8.545	2.923	12.2	14.901	3.860
6.6	8.772	2.962	12.4	15.116	3.888
6.8	8.997	2.999	12.6	15.330	3.915
7.0	9.222	3.037	12.8	15.544	3.943
7.2	9.446	3.073	13.0	15.757	3.970
7.4	9.669	3.109	13.2	15.971	3.996
7.6	9.892	3.145	13.4	16.184	4.023
7.8	10.114	3.180	13.6	16.397	4.049
8.0	10.336	3.215	13.8	16.610	4.076
8.2	10.557	3.249	14.0	16.823	4.102

using table III-C-1, B=10.336 and $B^{1/2}$=3.215. Next x_c is calculated using

$$x_c^2 = 0.1569 \left[Z(Z+1) z^2 \frac{t}{Apv^2} \right] \qquad \text{(III-C-5)}$$

where

$$(pv)^2 = 5.877 \times 10^3 \beta^2 = 3.589 \times 10^1$$

$$\beta^2 = 6.107 \times 10^{-3}$$

and

$$x_c = 1.184 \times 10^{-2}$$

using the expression

$$x = \frac{\theta}{c B^{1/2}}$$

we can determine x_w as

$$x_w = (x_c B^{1/2}) = 0.038 \text{ radians} = 2.17^\circ$$

Thus $\theta_{\frac{1}{e}}$ is the 1/2 angle which defines a cone containing 69.5% of the scattered particles following a gaussian distribution defined by $F(\theta)$ and whose width is x_w. This distribution will, upon emerging from the foil, be radially directed in the foward direction as shown in fig. III-C-2. If collimation is allowed at some distance, d_1, from the surface of the foil, then the collimated beam will contain a fraction of the original cone (fig. 2) and to ensure 0.1% homogeneity of the beam the ratio of $\frac{R_3^2}{R_2^2}$ should be 1×10^{-1}. If

R_3= 0.5 cm then R_2=1.56 cm. Referring again to fig.2 , d_1, the distance necessary to achieve a radius R_2, can be calculated using the relationship, $d_1 = R_2 / \tan \theta$, where $\theta = \theta_{\frac{1}{e}}$. For this example d_1 turns out to be ca. 41 cm. Therefore, to achieve a homogeneous beam of protons using a 0.1 mil gold foil, final collimation must take place at a distance ca. 41 cm from the point of scatter.

Table III-C-2 contains the thermal and physical characteristics for some of the elements considered for thin foil defocusing.

Because of their relatively high densities and high Z, gold and tungsten are the best choices for scattering foils (high Z materials will minimize energy losses per collision and high density materials will allow use of thinner foils to provide the same scattering angle, which means longer foil lifetimes.). Nickel, with a melting point almost 400 degrees higher than gold but much lower than tungsten is a frequent choice as a scattering foil. Marion and Young[4] indicate that currents between 2.25 and 3.00 microamps of 3.0 MeV protons on a 0.1 mil nickel foil will rapidly lead to rupture. At currents above 3 microamps the foil will puncture immediately. Tungsten on the other hand, has the same density as gold and by far the highest melting point. We have been very successful in our laboratory using a 0.1 mil tungsten foil for 3 or 4 days at a time using 3.5 μA

Table III-C-2 Physical and Thermal Characteristics of Thin Foils

Element	Density g/cm^3	Therm. Cond $watts/cm^2$	Spec. Heat. $cal/g\ ^oC$	dE/dX $KeV/mg/cm^2$	M.P. $^oC.$	Proton Range mg/cm^2
Copper	8.92	3.98	.092	60	1093	-
Silver	10.5	4.27	.056	48	960	42.9
Nickel	8.9	.899	.106	60	1453	32.9
Gold	19.3	3.15	.031	37	1063	61.8
Tungsten	19.3	1.78	.032	38	3410	58.5

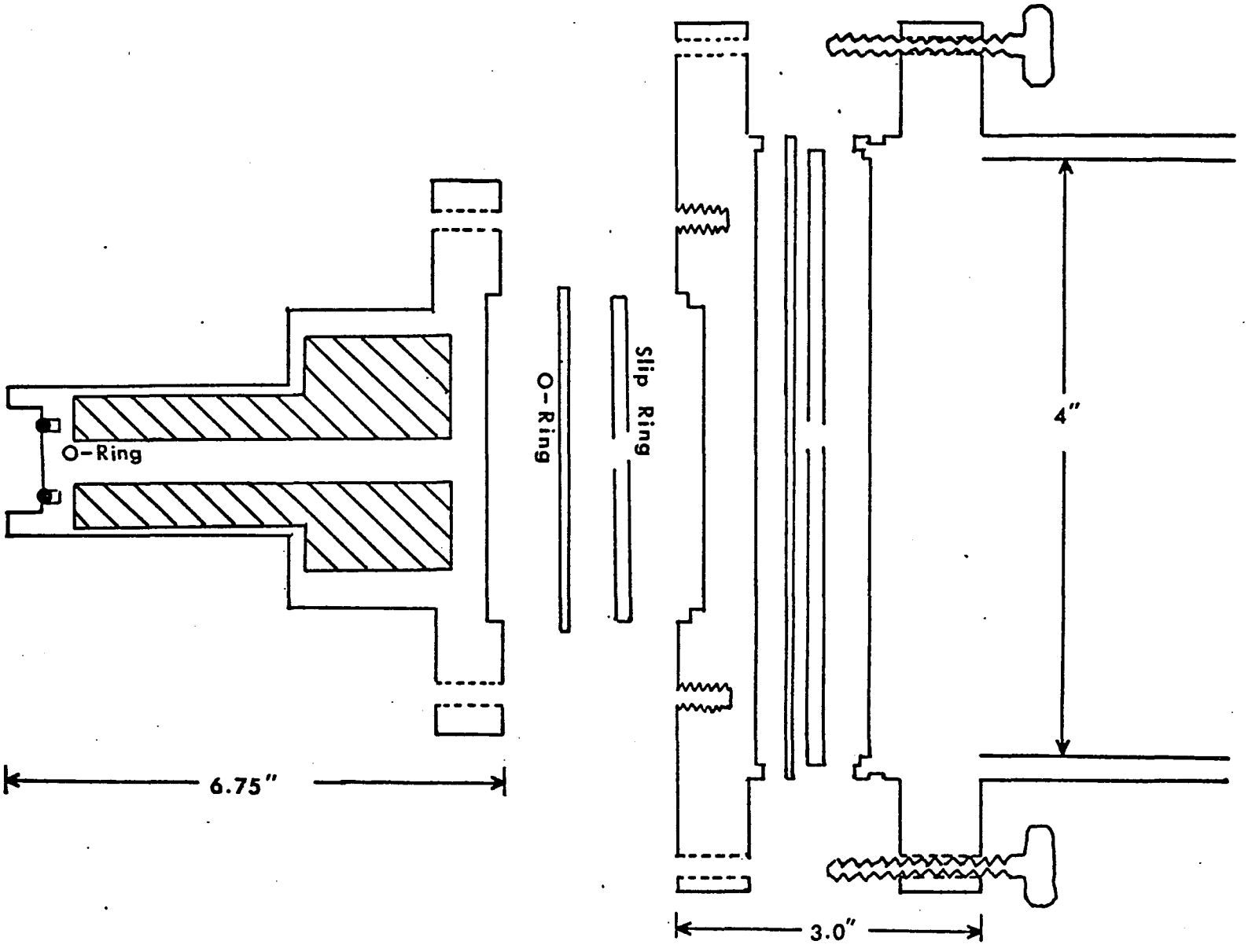

Fig. III-C-4. Final Collimator and Kapton Window Vacuum Port

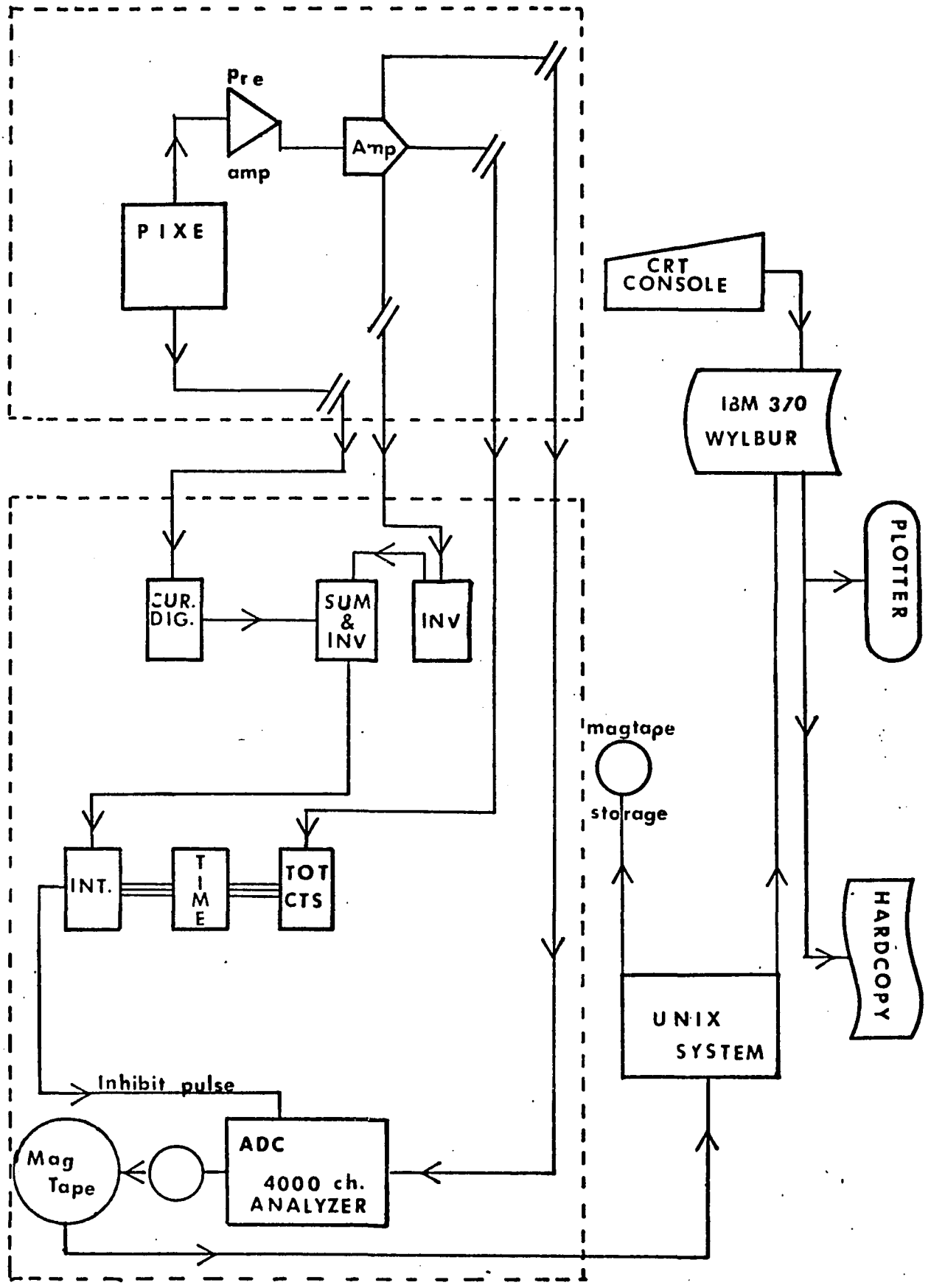

Fig III.C.5 PIXE Data Network

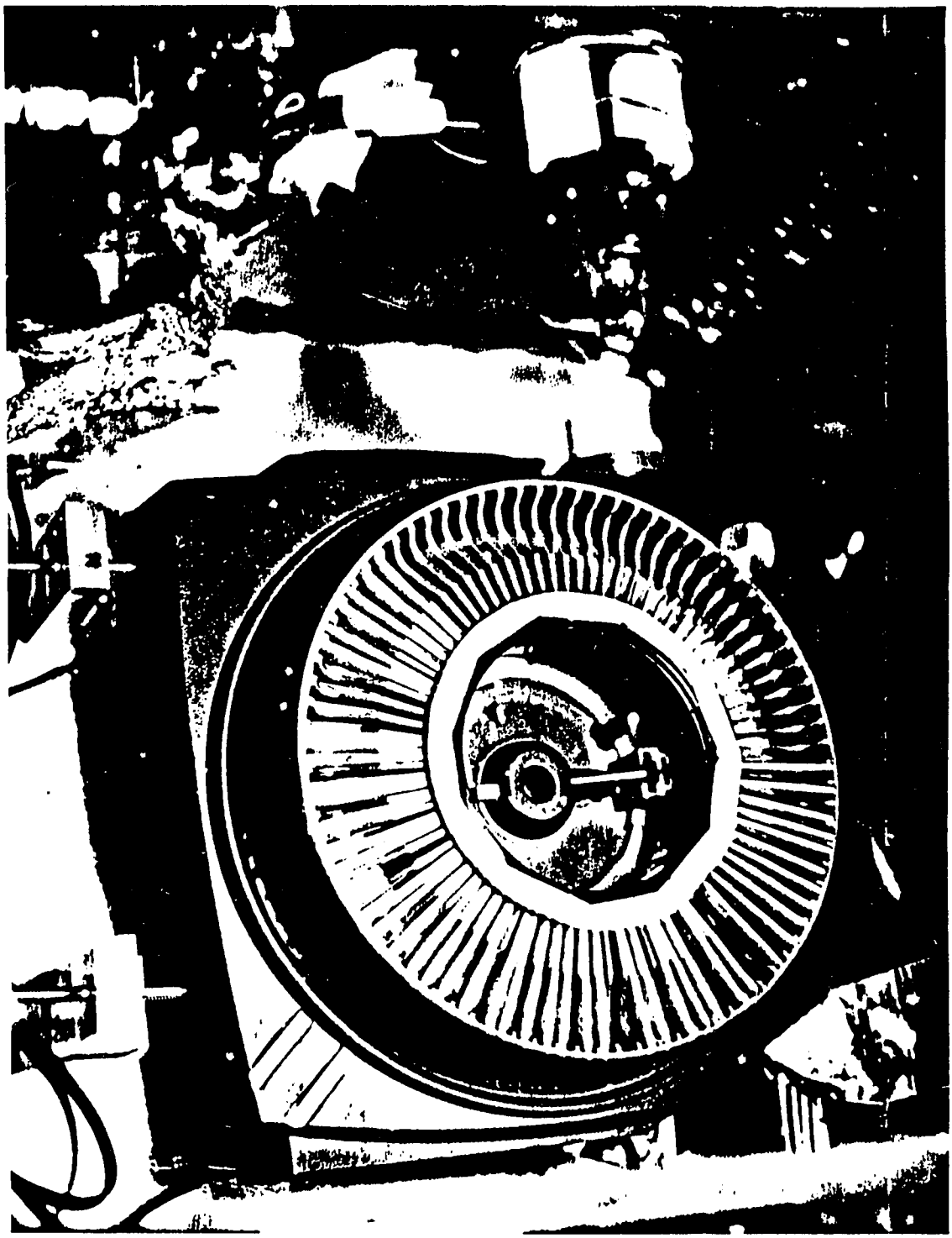

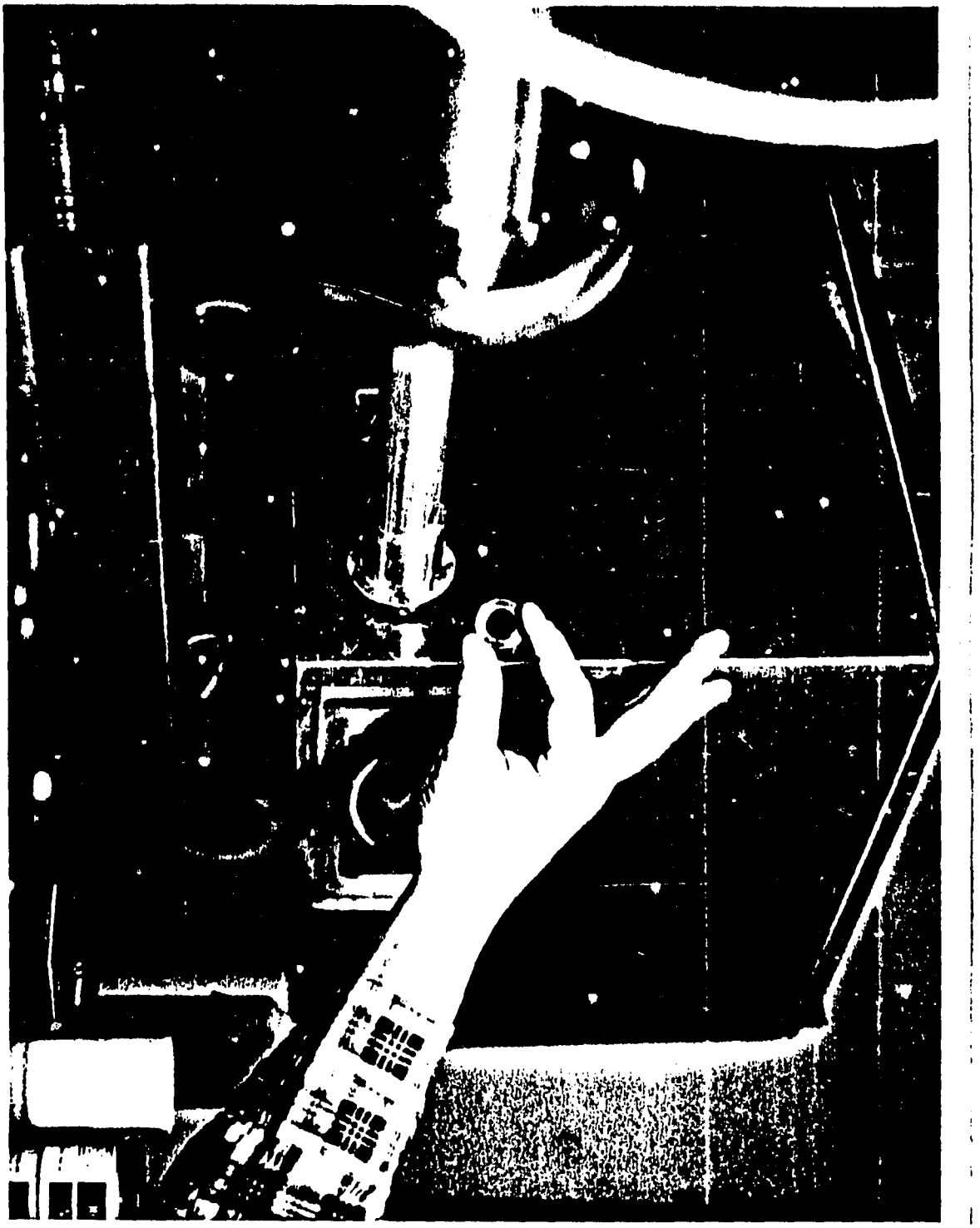

proton currents. This greatly surpasses the lifetime and current capabilities of Ni foils. In addition, its lifetimes are comparable with gold foils and much less expensive. One problem with the tungsten foils however, is that they may not be light tight at these thicknesses and so each foil has to be checked for pin holes. We have been fairly successful obtaining good foils from Goodfellow Metals Ltd.

The collimated beam enters the target chamber through a 1 mil Kapton window (fig III-C-4), epoxy sealed to a brass ring , which is located at the end of the beam tube. The brass ring is seated on an o-ring at the end of a graphite-lined port, which connects to the beam tube. The port is machined from aluminum and acts as a final collimator for the emerging proton beam. The energy loss in the Kapton is also about 400 kev. Kapton was chosen because of its excellent resistence to radiation damage. On the average each window will last from 2 to 3 days at 200 nA before radiation damage necessitates removal to prevent rupturing.

The helium-filled target chamber, an Al box, 18" on a side, contained the sample changer, a modified Carousel projector with lens, etc removed and so mounted that the emerging beam was 4 cm from the target. The Kapton window mounted on the end of the beam tube protrudes inside the chamber to a depth of about 30 cm. The entire chamber is maintained at a positive He pressure to decrease the proton scatter, eliminate charge build-up, provide target cooling

and to eliminate argon x-rays from the collected spectra. The energy loss in trasversing the He is about 125 kev. Thus the net energy loss for the entire system is about 1 MeV and the beam-current ratio from homogenizer to target is about 14:1. The advantages of using a helium atmosphere rather than the more usual vacuum in the target chamber are numerous:

a) the chamber requires no lengthy pump down times as do most conventional vacuum systems capable of handling such large numbers of samples. Most slide mounted targets require up to several days of outgassing before a tray of slides can be used in a vacuum system. For vacuum systems which have short pump down times (1/2 hour or more) the number of targets are very small (usually <10). In our helium system we can change a tray of 80 slides and be operational in less than 20 min.

b)the helium provides cooling for the target so that much larger currents are possible with little or no damage to the target and also, targets can be irradiated for longer periods of time. These two advantages compensate for the loss in signal intensity due to attenuation by the He in the x-ray path.

c) No special modifications had to be made to the Carousel projector to work under vacuum conditions.

d) construction costs were much lower than for a vacuum

system since no special precautions were needed for signal connectors, detector mounting, sample inlet, etc.

A disadvantage of the system is the loss of sensitivity for the lighter elements due to absorption and scatter of the long wavelength (low energy) x-rays by the beryllium window of the Si(Li) detector, by the (0.1 mil) Mylar window separating the detector from the helium atmosphere, and by the helium itself. In general, the lowest detectable element for our system is aluminum. The criterion we adopt here for detectability is that the net peak area (peak minus background) must be greater than 10 counts for a collected charge of 40 μcoulombs.

The Si(Li) detector is situated at 45 degrees from the front surface of the target in a fixed geometry (about 8 cm. from target to beryllium window). The targets are dropped into the beam path using the modified Kodak Carousel projector remotely activated from the control room area. The slide configuration is monitored using a remote television camera. Beam current is integrated using a graphite-lined Faraday cup, (this is also the beam dump) sealed at the open end with 0.1 mil Mylar and located ca. 6 cm behind the target. All spectra are recorded for a given amount of collected charge corrected for dead time. This procedure is preferred (rather than counting for a predetermined time) because of fluctuations in beam intensity. Figures III-C-4 and

III-C-6 show the experimental set-up.

The data handling network for the PIXE system is shown in fig. III-C-5. The current collected in the Faraday cup is sent via signal cable from the accelerator vault to the control room where a current digitizer (Ortec model 439) with a built in ammeter monitors instantaneous fluctuations in the proton current. The measured current is digitized, inverted and summed with the busy-out signal from the amplifier and then sent to a master scaler which acts as a beam integrator and controller for the 4000 channnel analyzer. When a busy-out pulse is summed with the digitized current pulse the resulting pulse causes an inhibit signal to be processed from the scaler to the analyzer stopping the spectrum accumulation until the amplifier recovers.

The x-rays are detected in a 30 mm^2 KeVex Si(li) detector which has a 1.0 mil Be window. The signals are shaped using the associated pre-amp-amplifier system in the accelerator vault. Some problems did arise originally, due to high levels of radiation which the pre-amp was exposed to, but adequate shielding has alleviated the problem. The amplifier signals are fed to the control room with some loss in pulse shape and characteristics (less than 10 eV loss in resolution) due to the 150' signal cables. Spectrum accumulation is normally for a given amount of collected charge, at which point the master scaler automatically terminates accumulation.

Once the run is complete, the spectra which have been recorded on magnetic tape are transported to a PDP-11/45 Unix system available on campus. The data are converted to card image format and all the associated run parameters (i.e. total collected charge, spectrum label, etc) are organized and submitted to the computer code for analysis. The computer code, Brutal, obtained from Brookhaven Laboratories was written at Livermore Laboratories for analysis of Ge(Li) spectra. Modifications to the code were made at Brooklyn College so that it could analyse x-ray spectra and be run on the IBM-370 instead of the CDC-6600 for which it was originally written. Output from the code can produce hardcopy plots on a Calcomp 30" plotter, while numerical results are sent to the printer. Turn-around time and the lack of direct interaction with spectra being analysed make this method of data reduction undesirable. The accelerator facility is in the process of modifying their existing data network to include on-line analysis capability.

D. Standards preparation

The following considerations were observed in establishing an experimental system from which quantitative determinations of unknowns could be made:

a) sample thickness must resemble the thickness of the standard

b) the concentration range must cover the range of analysis desired.

c) one must have a calibration curve from which unknown amounts of any detectable element can be determined.

Solutions of ca. 0.01 M concentration of a salt of the element in question were prepared and analyzed by standard analytical procedures. Table III-D-1 gives the method of analysis chosen for each solution and the error associated with that analysis. Appropriate dilutions of these stock solutions were made to obtain the desired concentrations of the element, in µgrams/ml, necessary to prepare the standard slides. A calibrated µliter pipette was used to apply ca. 0.05 ml of solution to a thin (0.1 mil) film of Mylar. The drop was then allowed to evaporate before being covered with a thin film (ca. 1 mg/cm^2) of Krylon (a clear acrylic plastic) to prevent flaking or loss through volatilization.

Table III-D-1. Description of Analytical Methods used for Preparing PIXE Standards.

Element	Compound	Analytical Method	Expt. Error
P	Na_3PO_4	Potentiometric Titration with HNO_3	±3ppt.
S	Na_{2SO_4}		
Cl	$BaCl_2$ + NaCl	gravimetric as AgCl + $AgNO_3$ potentiometric titration	±4ppt.
K	$K_2Cr_2O_7$	Primary Standard.	
Ca	$CaCl_2 H_{20}$	gravimetric as the oxalate	±5ppt.
Cr	$K_2Cr_2O_7$	Primary Standard.	
Ti	-	1000 ppm A.A.S. Standards	<5±
V	-	"	"
Mn	-	"	"
Fe	-	"	"
Co	-	"	"
Cu	$Cu(NO_3)_2 \cdot 2H_2O$	Idiometric Titration	±1.4ppt.
Br	$MgBr_2 6H_2O$	AgBr gravimetric	±5ppt.
Sr	-	1000 ppm A.A.S. Standards	
Pb	$Pb(NO_3)_2$	Chromate gravimetric	±ppt.
Ba	$BaCl_2 \cdot 2H_2O$	$BaCr_2O_4$ gravimetric	±ppt.
Lu	LuO	99.999% pure Na fusion to dissovle	
Ag	$AgNO_3$	Potentiometric titration vs. NaCl and Gravimetric as AgCl using NaCl (primary standard)	±1ppt.

E. System Calibration and Maintenance

The PIXE system is calibrated, as previously mentioned, with prepared standards (section III-D). Since the system is dynamic, and changes in the system will cause changes in the calibration, it is wise to calibrate the system periodically (fig III-C-5).

Our first successful use of the PIXE system was in August 1976, but due to inadequate detector shielding, the background radiation was severe and sensitivity was very limited. Proton and electron bremsstrahlung were very high as is shown in figs. III-E-1, III-E-2, and III-E-3. Fig. III-E-1 is a spectrum obtained from the PIXE chamber with beam, but no slide in place and so represents chamber background. Not only was the background high, but there were impurities due to argon, iron, and manganese. Fig. III-E-2 shows the spectrum obtained from 130 nanograms of Cu after being recorded for 40 μcoulombs, which represented our lower limit of detection. Fig. III-E-3 shows the spectrum of stage 6 in a preliminary air sample, and represents 0.5 μm particles, but only sulfur and copper peaks are evident above background.

Other problems which plagued us at this time were; non-reproducible proton beam integration, a leaky sampling chamber and a problem obtaining a constant configuration for the detector. We also experienced some signal transmission difficulties which we later found tracable to cross-talk in

PIXE ANALYSIS OF SAMPLE

TIME= 576·0 SECS.

SPECTRUM ID.= 21·

NO SLIDE-BKG

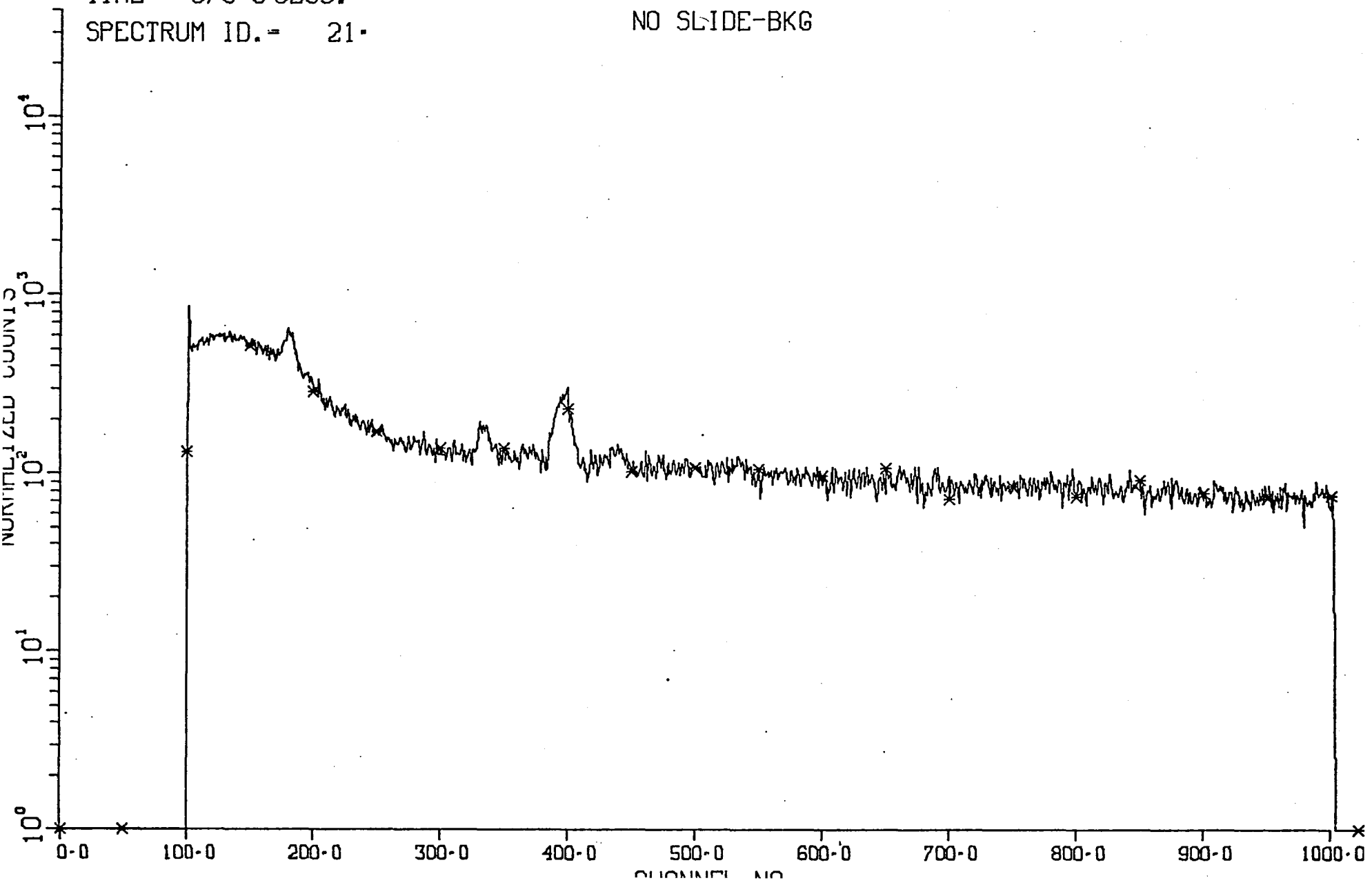

PIXE ANALYSIS OF SAMPLE

TIME= 703·0 SECS.

SPECTRUM ID.- 39·

6-3B STAGE 6

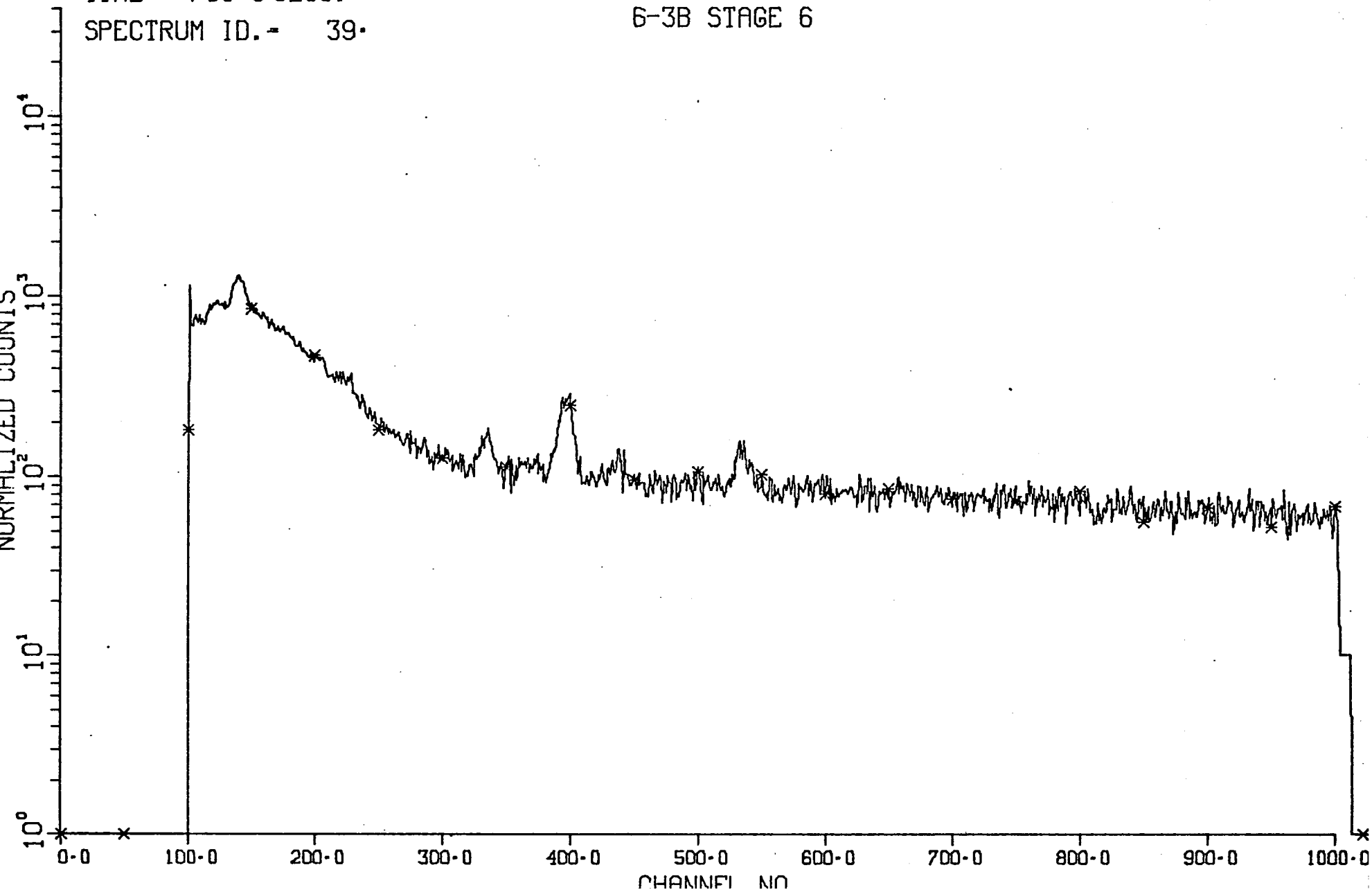

PIXE ANALYSIS OF SAMPLE

TIME= 569.0 SECS.

SPECTRUM ID.= 57.

.13UG CU

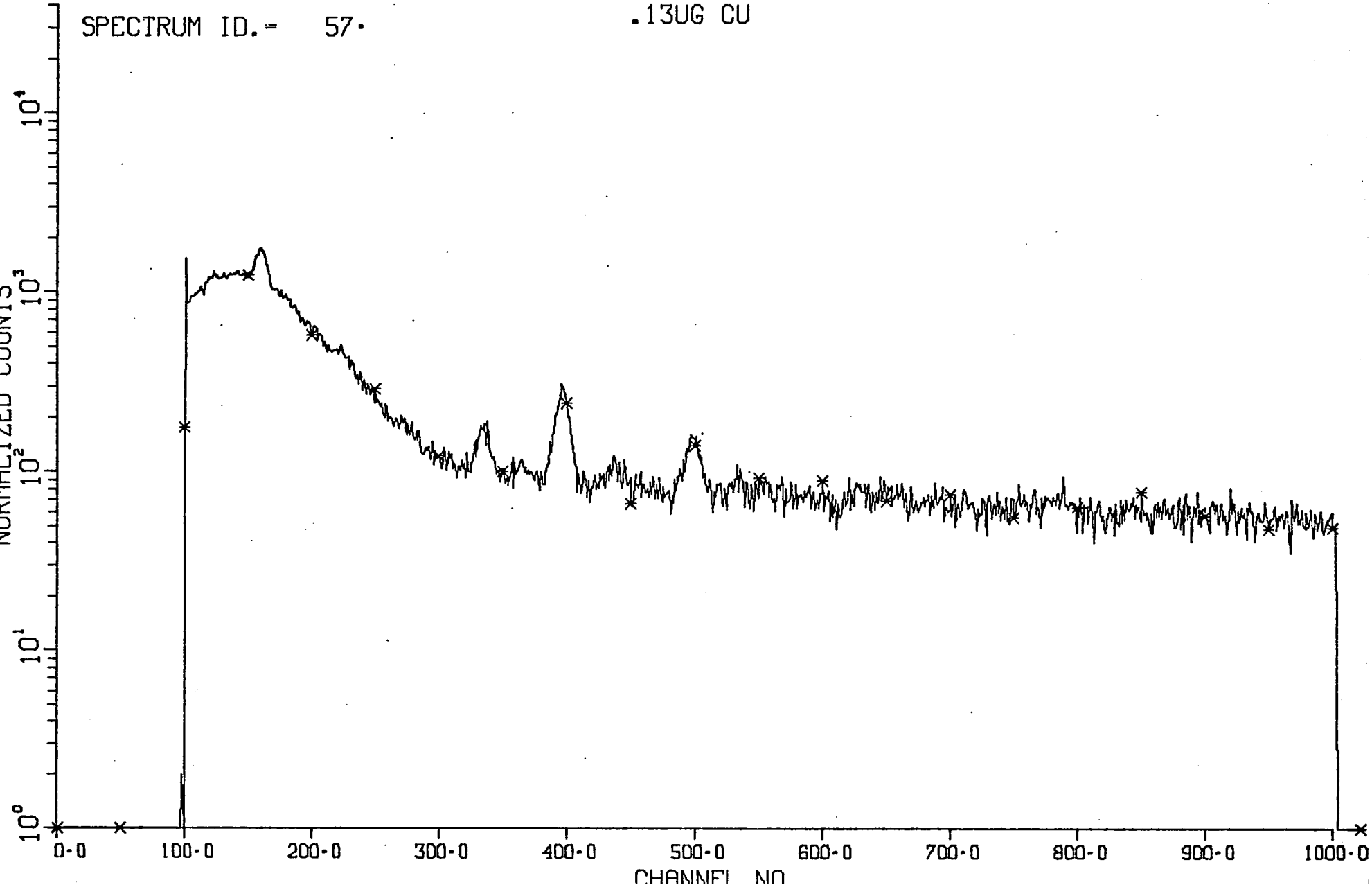

AIR SAMPLE 6-5C- 1ST FLOOR

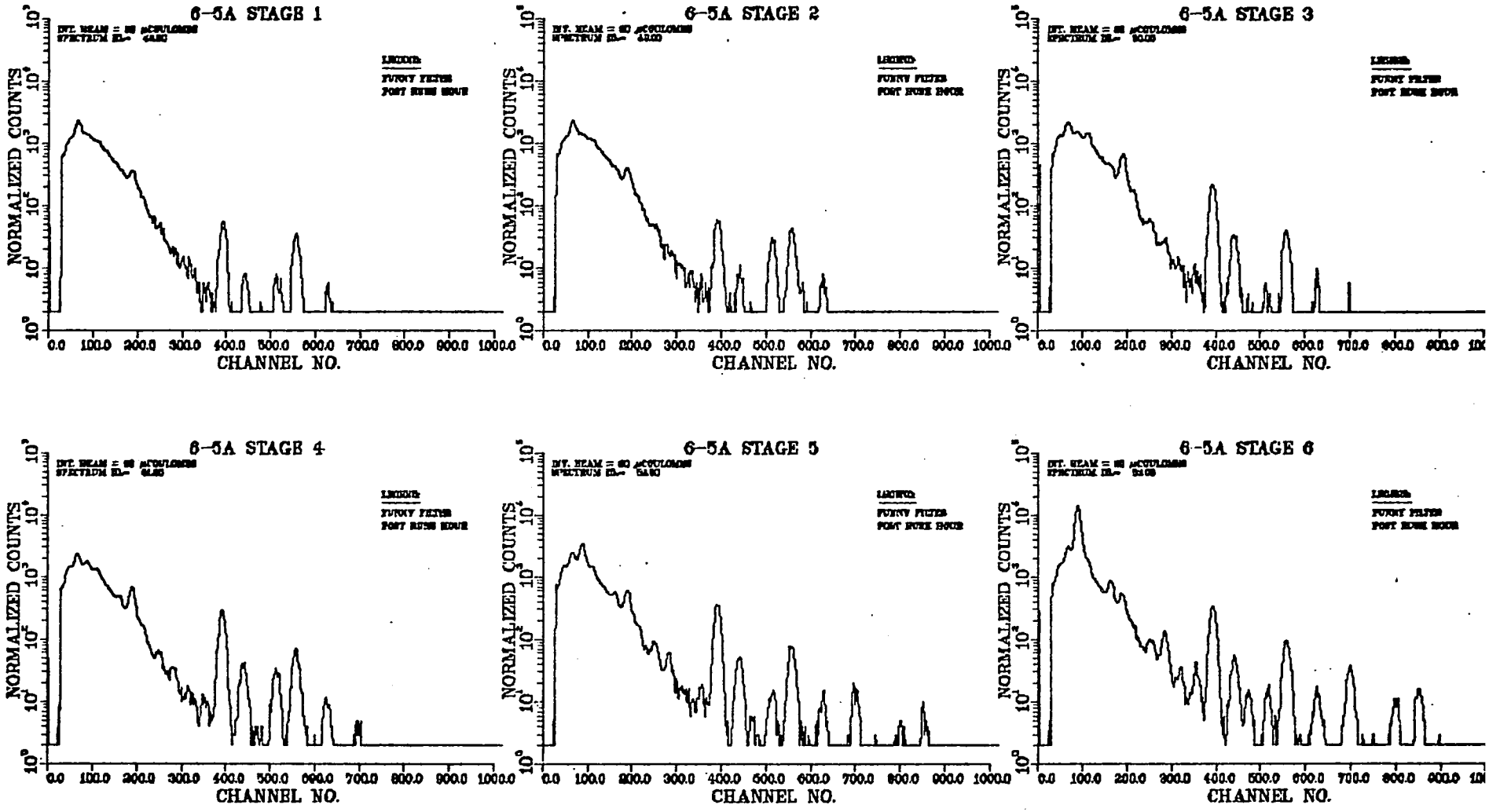

the cable bundles running from the accelerator vault to the control room.

Proper shielding, both inside the chamber and around the detector, minimized background radiation and allowed us to reduce our minimum detectable limits for Cu to 1 nanogram for 80 μcoulombs of collected charge. The problems associated with the non-reproducibility of the proton beam integration were alleviated by placing a piece of Mylar across the face of the Faraday cup. This eliminated charge build-up and escape of collected charge from the beam dump. Current integrations are now reproducible to better than 1%. A disadvantage to this technique, although not a serious one, is that the Mylar suffers from radiation damage and must be replaced at the end of each day. This takes no more than five minutes to accomplish.

The detector configuration was stabilized by affixing a Lucite adapter to the sample chamber which accepted the nose of the detector, with a tight fit, to a depth of about 3 inches. Fig III-E-4 shows the results of these modifications. This figure is a collection of spectra representing stages 1-6 of an air sample collected at Cooper Union. Fig III-E-5 shows the calibration curves for three PIXE runs during 1977. The change in sensitivity from run to run is most probably caused by changes in the detector positioning relative to the target, and variations in the scattering foil characteristics and thicknesses. These are major prob-

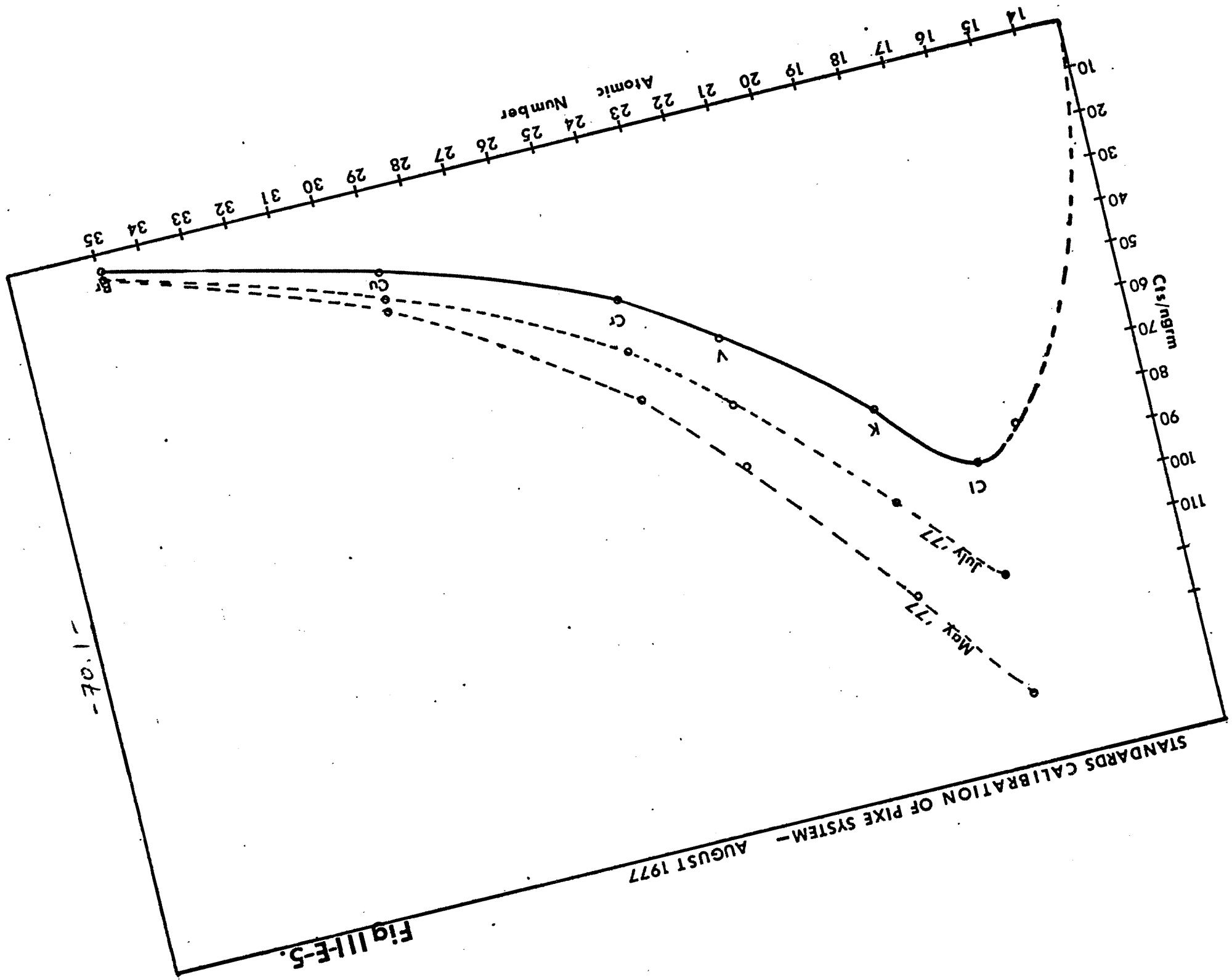

STANDARDS CALIBRATION OF PIXE SYSTEM— AUGUST 1977

Fig III-E-5.

-70.1-

lems with the system at present. The tolerance of the lucite holder necessary to remove and insert the detector allows for substantial detector movement and thus can change sensitivity. This does not, however, affect reproducibility, as once positioned, a constant configuration is maintained. Degradation of the scattering foil under the influence of high beam currents (< 3 μA) for long periods of time will change the ratio of beam current on Homogenizer to Faraday cup. The ratio (H./F.c) for a new tungsten foil is about 14:1. This ratio can degrade to about 9:1 within 48 to 72 hours of use at beam currents above 3 μA. The rate of foil deterioration is directly related to beam intensity and it has been observed that above 4.5 μA the foil will last only a few hours at best. The H/F.c. is an accurate monitor of the foil integrity and should be observed as normal procedure during the PIXE run.

It is recommended that, since changing the foil requires opening the beam tube to atmosphere, this operation be done at the completion of a day's run. Total time necessary to bring the beam tube vacuum down to operating conditions (> 5×10^{-6} torr) after foil replacement is usually around 2 hours. Experience has shown that a foil should be replaced every three days under normal running conditions or if the ratio drops below 8.5:1. Foil lifetime can probably be extended if the heat conduction from the foil could be increased.

Another portion of the beam transport section of the PIXE system which requires maintenance is the Kapton window. Kapton, a polyamide resin manufactured by Du Pont, was chosen for its excellent resistance to radiation damage. Rupture of the Kapton window is the single most significant system failure because it exposes the beam tube to the helium atmosphere of the target chamber. Foil fatigue could result in an implosion of the glass plate on top of the target chamber as a result of the sudden reduced pressure. To prevent major damage to the chamber, a safety valve, in the form of a 1/2" diameter hole covered with a thin glass plate, was installed. In the event of a rupture of the Kapton window, this plate should break, equalizing the pressure and preventing major damage.

In general, the Kapton, which is 1 mil thick, will last for three or four days of running under normal conditions. Considerations for changing the Kapton window are the same as for the scattering foil (i.e loss of beam tube vacuum) and so should be performed after a days run to allow for overnight pump-down. Usually it is good practice to change both the scattering foil and the Kapton window every third day. It is desirable to have many (8-10) windows prepared in advance of a run to ensure an adequate supply.

The high rate of helium consumption is also a minor problem which should be corrected. At present, consumption is approximately one 2500 lb/in^2 industrial grade tank per

12-14 hr. day, at a cost per tank of about 21 dollars. Reduction to 1/2 this rate should be possible by use of a more accurate flow-meter. It is also good practice to maintain a supply of helium in excesss of expected needs (a good rule of thumb is n+2 bottles where n is the number of anticipated days in the run).

Section IV.

A. Results and Conclusions

Before presenting the data obtained during the sampling periods described in section I., I would like to clarify some points and definitions which will be used to interpret the data. The meteorological information, including temperature, wind speed and direction (measured at Central Park), mixing height (measured at Ft. Totten), etc were obtained from the National Weather Service-New York Observatory. Although weather conditions at the sampling stations may have been different due to local situations discussed earlier (sec. I), it is felt that these local situations still reflect general atmospheric weather conditions and therefore data obtained from Central Park is valid.

Data, for other than frationated particulate material, were obtained from the D.E.P. Total Suspended Particulates (TSP) data are 24 hour samples measured at 41 locations throughout the city. Carbon monoxide and sulfur dioxide are measured continuously with hourly averages reported. The SO_2 readings were taken from all around the city and used to monitor SO_2 trends on a city wide basis. CO measurements were taken only from the three "Ecolyzer" samplers located at the temporary Rockefeller Center sampling sites and were used to monitor local emission sources. The particulate material data is presented in two forms, first, as nanograms/m^3 in tabular form and then, for selected ele-

ments, as mass distributions. I would like to stress that the particulate material collected via impactor does not represent the whole aerosol, but rather only that fraction contained in the size range 0.5 μm and above. Particles smaller than 0.5 μm, and therefore collected on the after-filter, were not routinely measured. Thus, any conclusions drawn from these data will be skewed slightly, in the large particle direction. For a description of the sampling locations please refer to sec. I.

Cooper Union

This preliminary investigation was undertaken to assess the magnitude of errors of sampling we could expect when doing a profile analysis of the aerosol. S. Mainwaring, et al.[1] observed 10-30% differences in the total amount of material collected and no difference in the size distributions when sampling in a non-canyon environment over a vertical height of 67m. Tables IV-A-1 through IV-A-12 show the data obtained at Cooper Union. Table IV-A-1 is the total concentration of each element for the sampling period, tables IV-A-2 through IV-A-7 are concentrations/stage and tables IV-A-8 through IV-A-12 are mass distributions calculated for PB, Br, S, Fe, and Zn.

Diurnal fluctuations in the mass concentration of material are evident in table IV-A-1. The elements, of the 13 examined, which had the highest concentrations were Pb, S, Fe, and Br. Sulfur showed instances of relatively high con-

Table IV-A-1 Total Elemental Concentrations for Aerosol Measured at Cooper Union-4/28--5/2/77 ng/m^3

Sample	S	Cl	K	Ca	Ti	V	Cr	Mn	Fe	Cu	Zn	Br	Pb
6-4A-1st	79	48	14	6	<1	<1	<1	<1	271	2	36	93	515
6-4B-1st	84	24	16	11	<1	<1	<1	32	124	2	18	147	670
6-4A-3rd	23	4	3	<1	<1	<1	<1	<1	48	<1	20	64	287
6-4B-3rd	32	8	7	5	<1	<1	<1	<1	98	8	6	101	425
6-4A-6th	48	27	9	4	<1	<1	<1	<1	147	1	28	62	335
6-4B-6th	65	20	15	11	<1	<1	<1	<1	108	3	25	109	419
6-5A-1st	377	7	12	38	<1	<1	<1	1	189	20	32	101	491
6-5B-1st	293	<1	3	46	<1	5	<1	9	261	6	18	71	340
6-5C-1st	554	<1	10	34	4	9	<1	3	144	10	19	72	416
6-5A-3rd	153	-	6	18	1	1	1	1	135	40	13	64	298
6-5B-3rd	130	-	2	48	1	2	1	1	199	17	4	63	257
6-5C-3rd	278	-	1	32	1	4	1	1	187	32	35	110	455
6-5A-6th	620	1050	23	22	<1	8	<1	2	157	21	38	97	496
6-5B-6th	207	2	10	29	<1	3	<1	5	198	10	5	78	301
6-5C-6th	395	-	6	37	<1	<1	<1	1	197	20	34	90	441

6-4A samples were from 6-8p.m. on 4/29/77
6-4B samples were from 8-10p.m on 4/29/77
6-5A samples were from 6-8p.m. on 5/2/77
6-5B samples were from 8-10p.m. on 5/2/77
6-5C samples were from 10-12p.m. on 5/2/77

Table IV-A-2 Element Concentrations for 1st Floor Cooper Union Stations Sampled 4/29-5/2/77 (ng/m^3).

Sample	S	Cl	K	Ca	Ti	V	Cr	Mn	Fe	Cu	Zn	Br	Pb
6-4a-1st													
16 μ.	-	-	-	<1	-	-	-	-	5	-	-	4	17
8 μ.	-	-	-	-	-	-	-	-	3	-	-	5	17
4 μ.	-	-	-	-	-	-	-	-	39	-	-	7	29
2 μ.	-	-	-	-	-	-	-	-	122	-	-	15	40
1 μ.	-	-	-	2	<1	<1	<1	<1	56	1	-	22	98
.5 μ.	78	48	14	4	<1	<1	<1	-	47	1	36	40	314
Total	78	48	14	6	<1	<1	<1	<1	271	2	36	93	515
6-4b-1st													
16 μ.	-	-	-	-	-	-	-	-	-	-	-	5	15
8 μ.	-	-	-	-	-	-	-	-	3	-	-	5	14
4 μ.	-	-	-	<1	<1	<1	<1	<1	19	<1	-	9	32
2 μ.	-	-	-	<1	<1	<1	<1	-	32	-	-	17	69
1 μ.	-	-	<1	4	<1	<1	<1	<1	38	<1	2	45	187
.5 μ.	84	24	16	7	<1	<1	<1	2	32	1	16	66	353
Total	84	24	16	11	<1	<1	<1	3	124	2	18	147	670

Table IV-A-3 Element Concentrations for 3rd Floor Cooper Union Stations Sampled 4/29-5/2/77 (ng/m^3).

Sample	S	Cl	K	Ca	Ti	V	Cr	Mn	Fe	Cu	Zn	Br	Pb
6-4a-3rd													
16 μ.	-	-	-	-	-	-	-	-	6	-	-	2	13
8 μ.	-	-	-	-	-	-	-	-	<1	-	-	3	15
4 μ.	-	-	-	-	-	-	-	<1	43	-	-	7	8
2 μ.	-	-	-	<1	-	-	-	-	50	<1	-	4	27
1 μ.	-	-	-	-	-	-	-	-	48	<1	20	18	57
.5 μ.	23	4	3	<1	<1	<1	<1	<1	49	<1	20	28	166
Total	23	4	3	1	<1	<1	<1	<1	192	<1	20	64	287
6-4b-3rd													
16 μ.	-	-	-	-	-	-	-	-	-	-	-	2	13
6 μ.	-	-	-	-	-	-	-	-	<1	-	-	4	14
3 μ.	-	-	-	-	-	-	-	-	7	8	-	5	18
2 μ.	-	-	-	-	-	-	-	-	32	-	-	17	52
1 μ.	-	-	-	-	-	-	-	-	33	-	-	25	108
.5 μ.	32	8	7	4	<1	<1	<1	<1	26	-	6	48	220
Total	32	8	7	5	<1	<1	<1	<1	98	8	6	101	425

Table IV-A-4 Element Concentrations for 6th Floor Cooper Union Stations Sampled 4/29-5/2/77 (ng/m^3).

Sample	S	Cl	K	Ca	Ti	V	Cr	Mn	Fe	Cu	Zn	Br	Pb
6-4a-6th													
16μ	-	-	-	-	-	-	-	-	-	-	-	6	12
8μ	-	-	-	-	-	-	-	-	-	-	-	4	14
4μ	-	-	-	-	-	-	-	-	10	1	-	5	11
2μ	-	-	-	1	<1	<1	-	-	47	-	-	9	31
1μ	-	-	-	1	<1	-	-	-	55	-	-	14	61
0.5μ	48	27	9	1	<1	<1	<1	<1	35	-	28	24	20
Total	48	27	9	3	2	2	<1	<1	147	1	28	62	335
6-4b-6th													
16 μ.	-	-	-	-	-	-	-	-	2	<1	-	5	12
8 μ.	-	-	-	-	-	-	-	-	2	-	-	5	12
4 μ.	-	-	-	<1	<1	-	-	-	10	-	-	19	18
2 μ.	-	-	-	2	<1	-	-	-	34	3	-	10	33
1 μ.	-	-	<1	3	<1	<1	<1	<1	40	<1	<1	26	116
.5 μ.	65	20	15	6	<1	<1	<1	<1	22	-	25	44	228
Total	65	20	15	11	<1	<1	<1	<1	108	2	25	109	419

Table IV-A-5 Element Concentrations for 1st Floor Cooper Union Stations Sampled 4/29-5/2/77 (ng/m^3).

Sample	S	Cl	K	Ca	Ti	V	Cr	Mn	Fe	Cu	Zn	Br	Pb
6-5a-1st													
16 μ.	-	-	-	1	<1	<1	<1	<1	4	7	1	6	22
8 μ.	-	7	6	6	<1	<1	<1	<1	7	-	-	7	21
4 μ.	-	<1	-	8	<1	<1	<1	<1	29	2	<1	9	32
2 μ.	-	-	-	11	<1	<1	<1	<1	61	2	1	20	57
1 μ.	11	-	-	6	<1	<1	<1	<1	54	4	6	25	130
.5 μ.	366	1	6	6	<1	<1	<1	1	34	5	23	34	229
Total	377	8	12	38	3	3	3	4	189	20	31	131	491
6-5b-1st													
16 μ.	-	-	-	-	-	-	-	-	3	<1	-	3	11
8 μ.	-	-	-	1	-	-	-	-	14	1	-	4	22
4 μ.	-	-	-	<1	-	-	-	-	9	<1	-	7	22
2 μ.	-	-	-	15	<1	<1	-	-	43	1	-	15	48
1 μ.	27	-	<1	12	<1	1	<1	41	73	<1	10	20	101
.5 μ.	266	-	3	2	<1	4	<1	<1	49	4	7	22	136
Total	293	-	3	30	2	5	<1	41	191	7	17	71	340
6-5c-1st													
16 μ.	-	-	-	-	-	-	-	-	4	<1	-	9	15
8 μ.	-	-	-	<1	-	-	-	-	3	3	-	4	16
4 μ.	-	-	-	10	<1	<1	<1	<1	24	-	-	7	27
2 μ.	-	-	-	10	<1	<1	<1	<1	32	3	5	13	30
1 μ.	45	-	-	8	2	2	<1	<1	42	2	-	18	88
.5 μ.	509	-	10	5	2	7	<1	3	39	2	14	27	125
Total	554	-	10	33	5	10	2	5	144	10	19	78	301

Table IV-A-6 Element Concentrations for 3rd Floor Cooper Union Stations Sampled 4/29-5/2/77 (ng/m^3).

Sample	S	Cl	K	Ca	Ti	V	Cr	Mn	Fe	Cu	Zn	Br	Pb
6-5a-3rd													
16 μ.	-	-	-	-	-	-	-	-	2	17	3	7	22
8 μ.	-	-	-	<1	<1	<1	-	-	3	-	-	6	21
4 μ.	-	-	-	2	-	-	-	-	13	5	2	6	16
2 μ.	-	-	-	5	-	-	-	-	38	<1	-	7	30
1 μ.	<1	-	3	5	<1	<1	<1	<1	49	12	4	13	81
.5 μ.	153	-	3	5	<1	<1	<1	<1	30	5	4	25	128
Total	153	-	6	17	3	3	1	<1	135	39	13	64	298
6-5b-3rd													
16 μ.	-	-	-	-	-	-	-	-	1	1	-	6	17
8 μ.	-	-	-	<1	<1	-	-	-	2	1	-	4	18
4 μ.	-	-	-	9	<1	-	-	-	22	8	1	7	28
2 μ.	-	-	-	22	1	<1	<1	<1	55	<1	-	9	32
1 μ.	-	-	-	12	<1	<1	<1	<1	66	6	3	19	61
.5 μ.	130	-	2	5	<1	<1	2	1	53	<1	-	18	101
Total	130	-	2	48	2	1	2	1	199	16	4	63	257
6-5c-3rd													
16 μ.	-	-	-	-	-	-	-	-	-	<1	<1		
8 μ.	-	-	-	-	-	-	-	-	-	4	-		
4 μ.	-	-	-	6	<1	<1	-	-	17	16	5		
2 μ.	-	-	-	13	<1	<1	<1	-	43	11	10		
1 μ.	6	-	-	9	<1	1	<1	1	78	2	8		
.5 μ.	278	-	1	4	<1	4	<1	<1	45	2	12		
Total	284	-	1	32	2	5	1	1	187	31	35		

Table IV-A-7 Element Concentrations for 6th Floor Cooper Union Stations Sampled 4/29-5/2/77 (ng/m^3).

Sample	S	Cl	K	Ca	Ti	V	Cr	Mn	Fe	Cu	Zn	Br	Pb
6-5a-6th													
16 μ.	-	-	-	-	<1	<1	<1	-	1	<1	-	6	16
8 μ.	-	-	-	-	<1	<1	<1	-	3	<1	-	7	27
4 μ.	-	-	-	-	<1	<1	<1	<1	9	3	-	5	15
2 μ.	-	-	-	5	<1	<1	<1	<1	36	<1	-	8	27
1 μ.	47	113	<1	8	<1	<1	<1	<1	65	10	8	26	119
.5 μ.	573	937	23	9	<1	8	<1	2	43	8	30	45	292
Total	620	1050	23	22	3	10	4	2	158	22	38	97	377
6-5b-6th													
16 μ.	-	-	-	-	-	-	-	-	<1	2	-	9	15
8 μ.	-	-	-	-	-	-	-	-	2	3	<1	4	16
4 μ.	-	-	-	4	<1	<1	<1	<1	18	1	<1	7	27
2 μ.	-	-	-	10	<1	<1	<1	<1	54	1	<1	13	30
1 μ.	1	-	-	11	<1	<1	<1	<1	7	1	1	18	88
.5 μ.	207	2	10	4	<1	3	-	1	51	2	4	27	125
Total	208	2	10	29	2	5	1	2	132	10	6	78	301
6-5c-6th													
16 μ.	-	-	-	-	-	-	-	-	-	-	-	5	16
8 μ.	-	-	-	-	-	-	-	-	1	2	-	5	14
4 μ.	-	-	-	7	<1	<1	-	-	19	6	-	8	18
2 μ.	-	-	-	14	<1	<1	<1	<1	52	4	6	13	53
1 μ.	29	-	-	12	<1	<1	<1	<1	72	7	20	25	134
.5 μ.	366	-	6	4	<1	<1	<1	1	53	1	8	34	206
Total	395	-	6	37	2	2	1	1	197	20	34	90	441

Table IV-A-8 Mass Distributions for Pb-1st, 3rd, and 6th Floor Cooper Union. (%)

Sample	Stage 1	Stage 2	Stage 3	Stage 4	Stage 5	Stage 6
6-4A-1st	3.30	3.30	5.63	7.77	19.03	60.97
6-4B-"	2.23	2.06	4.79	10.26	27.90	52.77
6-5A-"	4.51	4.18	6.58	11.69	26.50	46.54
6-5B-"	3.13	6.15	6.50	14.14	29.76	39.91
6-5C-"	4.75	3.12	5.53	9.70	24.97	51.93
6-4A-3rd	4.80	5.20	2.71	9.38	19.90	58.00
6-4B-"	3.08	3.35	4.19	12.15	25.36	51.87
6-5A-"	7.34	7.17	5.22	10.11	27.34	42.83
6-5B-"	6.43	6.94	11.03	12.61	23.58	39.41
6-5C-"	-	-	-	-	-	-
6-4A-6th	3.59	4.07	3.20	9.26	18.23	61.64
6-4B-"	2.85	2.93	4.35	7.93	27.64	54.31
6-5A-"	3.21	5.37	3.08	5.43	23.99	58.93
6-5B-"	4.91	5.28	8.64	10.08	29.16	41.73
6-5C-"	3.67	3.15	4.11	12.06	30.36	46.64
avg 1st	3.58±1.04	3.76±1.53	5.81±0.75	10.71±2.38	25.63 ±4.09	50.42±7.82
avg 3rd	5.41±1.88	5.67±1.78	5.79±3.64	11.06±1.56	24.05±3.16	48.03±8.48
avg 6th	3.65±0.78	4.16±1.15	4.72±2.37	8.95±2.47	25.88±4.90	52.65±8.34
Total avg	4.21±1.23	4.53±1.49	5.44±2.25	10.24±2.14	25.19±4.05	50.37±8.21

Table IV-A-9 Mass Distributions for Br-1st, 3rd, and 6th Floor Cooper Union. (%)

Sample	Stage 1	Stage 2	Stage 3	Stage 4	Stage 5	Stage 6
6-4A-1st	4.30	5.38	7.53	16.13	23.66	43.01
6-4B-"	3.33	3.47	5.93	11.71	30.51	45.05
6-5A-"	6.26	6.81	9.12	19.47	24.51	33.83
6-5B-"	4.51	5.66	9.68	20.61	28.09	31.45
6-5C-"	8.00	8.67	8.57	11.08	23.41	40.27
6-4A-3rd	6.81	5.24	11.31	5.76	27.75	43.14
6-4B-"	1.77	3.95	4.49	17.15	25.05	47.58
6-5A-"	10.63	9.88	8.93	11.26	19.77	39.53
6-5B-"	9.96	6.06	11.26	13.64	29.87	29.22
6-5C-"	-	-	-	-	-	-
6-4A-6th	9.65	7.13	7.24	14.47	22.48	39.04
6-4B-"	4.48	4.48	17.67	9.52	23.52	40.32
6-5A-"	5.87	7.43	5.23	8.13	26.80	46.53
6-5B-"	10.93	5.59	9.53	16.52	23.16	34.27
6-5C-"	5.90	5.75	8.93	13.92	27.46	38.05
avg 1st	5.28±1.85	6.00±1.92	8.17±1.48	15.80±4.35	26.06 ±3.11	38.72±5.87
avg 3rd	7.79±4.04	6.28±2.55	9.00±3.20	11.95±4.78	25.61±4.36	39.87±7.82
avg 6th	7.37±2.77	6.08±1.21	9.72±4.75	12.51±3.54	24.68±2.28	39.64±4.46
Total avg	6.81±2.89	6.12±1.89	8.96±3.14	13.42±4.22	25.45±3.25	39.41±6.05

Table IV-A-10 Mass Distributions for Fe-1st, 3rd, and 6th Floor Cooper Union. (%)

Sample	Stage 1	Stage 2	Stage 3	Stage 4	Stage 5	Stage 6
6-4A-1st	2.63	2.22	10.33	45.39	21.44	17.80
6-4B-"	2.13	3.89	15.42	24.50	28.97	25.09
6-5A-"	3.32	4.90	15.51	31.16	27.55	17.57
6-5B-"	2.22	4.62	17.27	27.56	28.88	19.45
6-5C-"	4.12	4.58	16.61	21.51	27.56	25.63
6-4A-3rd	5.20	2.06	6.99	26.44	30.07	29.23
6-4B-"	2.33	3.14	8.32	30.85	30.41	24.95
6-5A-"	3.29	3.72	10.47	26.89	34.10	21.53
6-5B-"	1.81	2.59	11.40	26.80	31.93	25.58
6-5C-"	-	-	-	-	-	-
6-4A-6th	1.87	1.57	8.10	30.17	35.31	22.98
6-4B-"	4.09	4.15	10.18	28.99	33.28	19.31
6-5A-"	2.44	3.06	6.95	22.40	39.17	25.99
6-5B-"	1.21	2.11	9.39	26.70	35.47	25.12
6-5C-"	1.33	1.92	10.03	25.87	34.74	26.10
avg 1st	2.88±0.84	4.04±1.08	15.03±2.74	30.02 ±9.31	26.88±3.12	21.11±3.95
avg 3rd	3.16±1.49	2.88±0.71	9.30±2.01	27.72±2.10	31.63±1.84	25.32±3.15
avg 6th	2.19±1.17	2.56±1.05	8.93±1.38	26.83±3.02	35.59±2.18	23.90±2.86
Total avg	2.74±1.17	3.14±0.95	11.09±2.04	28.19±4.81	31.37±2.38	23.44±3.32

Table IV-A-11 Mass Distributions for Zn-1st Cooper Union. (%)

Sample	Stage 1	Stage 2	Stage 3	Stage 4	Stage 5	Stage 6
6-4A-1st	8.95	8.22	8.51	8.51	13.55	52.27
6-4B-"	8.43	10.39	10.10	10.59	17.55	42.95
6-5A-"	14.00	9.11	11.42	12.61	20.07	32.80
6-5B-"	10.70	11.17	12.15	16.24	24.74	25.00
6-5C-"	9.50	11.86	10.80	19.44	22.31	26.10
6-4A-3rd	11.39	11.78	11.49	11.27	14.00	40.06
6-4B-"	9.99	10.23	18.13	10.98	12.84	37.83
6-5A-"	17.32	9.09	15.77	10.66	24.33	22.84
6-5B-"	9.91	11.99	19.63	13.37	23.05	22.06
6-5C-"	-	-	-	-	-	-
6-4A-6th	8.76	8.86	12.79	9.20	13.23	47.16
6-4B-"	9.92	9.74	10.53	12.33	15.46	42.03
6-5A-"	9.77	9.09	9.58	8.05	21.61	41.90
6-5B-"	12.34	13.20	12.49	16.18	17.39	28.39
6-5C-"	7.60	9.26	13.30	16.37	29.39	24.09
avg 1st	10.32±2.23	10.15±1.49	10.60±1.39	13.48±4.39	19.64±4.32	35.82±11.64
avg 3rd	12.15±3.51	10.77±1.37	16.26±3.55	11.57±1.23	18.56±5.97	30.70±9.57
avg 6th	9.68±1.75	10.03±1.80	11.74±1.60	12.43±3.85	19.42±6.37	36.71±9.91
Total avg	10.72±2.50	10.32±1.55	12.87±2.18	12.49±3.16	19.21±5.54	34.41±10.37

centration but did not show a pattern as regular as that for Pb and Br. The S concentrations were very low on Friday, 4/29, samples (6-4 set) averaging well below 100 ng/m^3, while the Monday, 5/2, samples showed higher concentrations (between ca. 150-600 ng/m^3). This pattern of high variability in S concentrations was also observed at the Rockefeller Center sites and further discussion of this will be delayed till these data are presented.

The Pb and Br concentrations, on the other hand, showed more consistency in their trends. The average value for Pb was 410 $\pm$110 ng/m^3, while for Br it was 88 $\pm$24 ng/m^3 for a Pb/Br ratio of 4.72 $\pm$0.6 for all samples at Cooper Union. Iron values ranged from ca. 50 to 275 ng/m^3 with no apparent pattern observable. In general, the fluctuations in mass concentrations observed with height range as high as $\pm$50% of the average. The apparent dip in concentration observed at the 3rd floor occurred for all samples. No explanation has yet been found for this behavior, but it is not considered due to a malfunction of the impactors, which all functioned normally during the sampling.

The mass distributions for some selected elements are shown in fig. IV-A-1 through IV-A-2. Although the mass concentrations do show patterns of fluctuation, the mass distributions are very nearly constant. This observation is in agreement with the results obtained by Mainwaring, et al,(1) and our results at Rockefeller Center.

The conclusions drawn from the preliminary sampling data taken at Cooper Union were:

a) Over a height of ca. 19 meters (6 stories), differences were observed in the concentrations of elements examined, but these differences could not be attributed to height. Lead and bromine, considered good tracers for automotive sources, showed reasonable agreement at all heights sampled, indicating good vertical mixing from street-level to roof-top (6 stories).

b) Mass distributions for elements showed good agreement at all sampling heights indicating that turblence, over 19 meters, is sufficient to prevent fractionation, by virute of differencial settling velocities, of the aerosol in this type of local environment.

c) most of the elements of interest are contained on particles less than 4 μm.

d) Concentration of elements examined at Cooper Union seemed to be lower than reported previously[2], indicating a light input from local sources (i.e local traffic) and different meteorological and seasonal conditions affecting transport from other sources.

Unfortunately, this preliminary investigation was not sufficient to answer many of the questions posed about representative sampling. It was anticipated that further sampling at Rockefeller Center would satify some of the remaining queries, e.g., a) what does the vertical profile

Mass Distributions for Pb and Br

Fig IV-A-1 Cooper Union April 1977

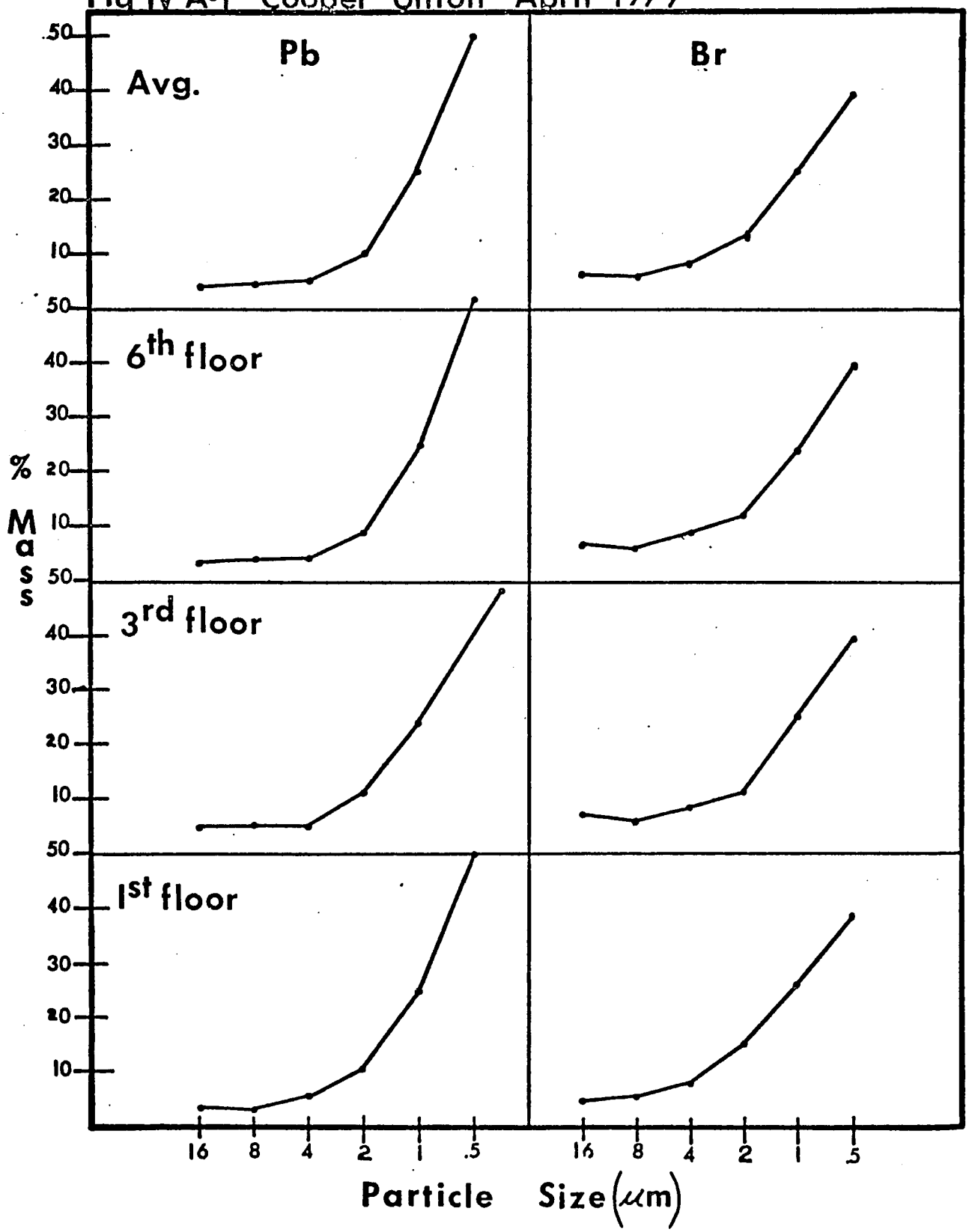

Mass Distributions for Selected Elements

Fig IV-A-2 – Cooper Union – April 1977

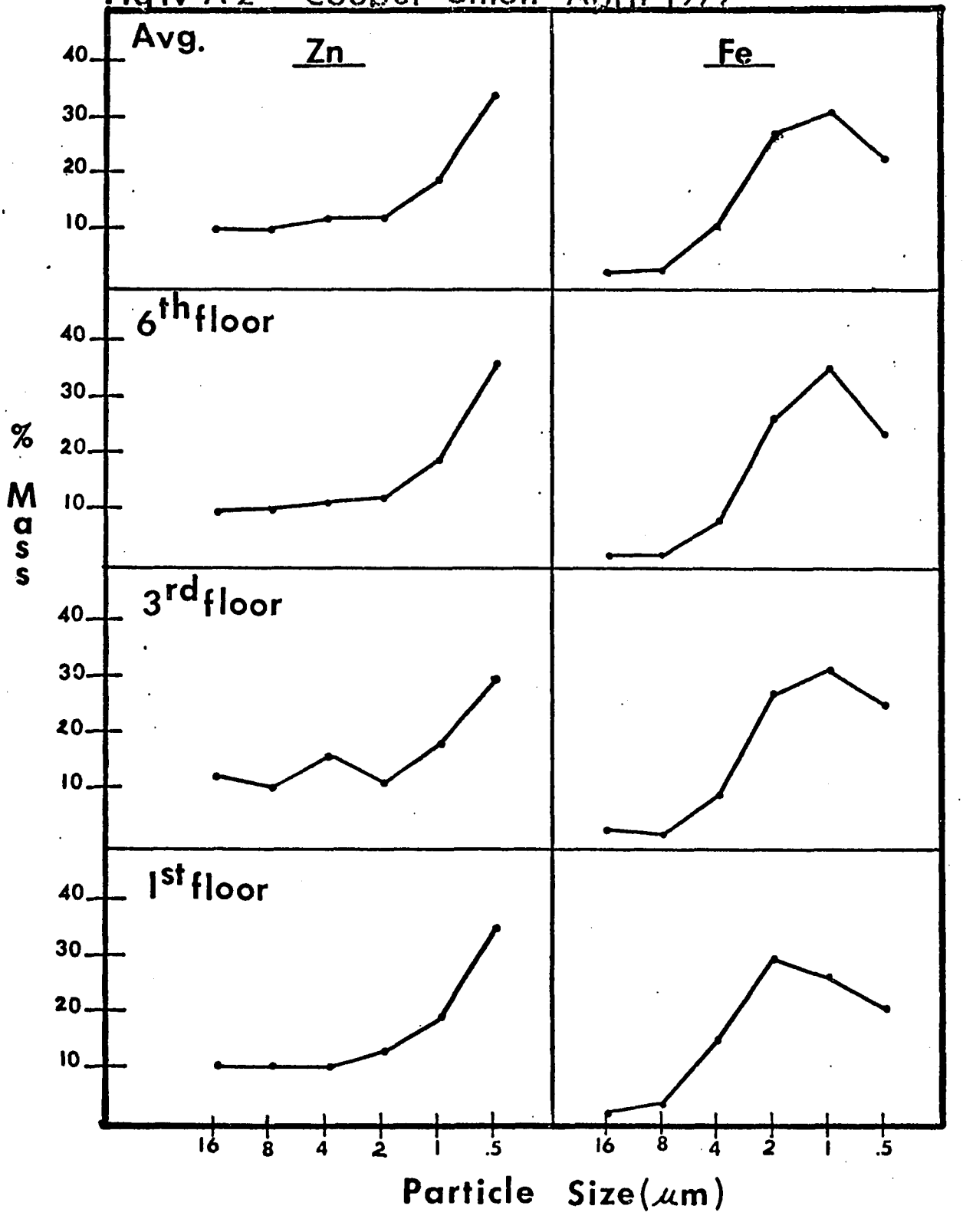

of the aersol look like in canyon environments, b) are samples collected around the corner from each other comparable and, c) can local input sources be used to monitor differences in horizontal and vertical profiles of the aerosol?

All samples taken at Rockefeller Center were collected for ca. 2 hours, sampling ca. 1.5 m^3. The 3 impactors were simultaneously run for a total of 6 hours a day, for 8 weekdays during the period from July 19^{th} to 30^{th}, 1977. This represents about 216 m^3 of air sampled over a period of 144 total hrs. The sampling generated 432 total stages to be analysed for particulate material, which, while modest compared to some programs, still respresents a problem in data reduction. I have tried to organize the data in what appears to be the most convenient format, although I'm sure many others can be found. Tables IV-A-13 through IV-A-30 show the data in various formats. Where possible, figures have been used to clarify the data.

The monthly hourly average concentrations of CO as recorded by the D.E.P. at each of the three locations is shown in fig. IV-A-3. The CO concentration at the 6^{th} Ave. site continuously climbs from early morning (4-5 a.m.) until it reaches a maximum between 5-6 p.m., after which, the CO level seems to fall rather quickly, so that by 1 a.m. the next day the level has returned to baseline. In general, the 6^{th} Ave. pattern seems to be a 14 hour period of accumulation followed by a 4-5 hour period of cleansing. Since CO

is usually considered a tracer for vehicular traffic, it can be used to monitor the affect that this source has on the air mass. The meaning of the data for 6th Ave. seems to be that the rate of input of pollutant material from vehicular traffic is greater, during the working day, than the rate at which the air mass, at street level can disperse it. Since the rate of traffic is fairly constant over the working day and does not ease till early evening, then ventilation on 6th Ave. must be poor. On the other hand, 51st seems to ventilate soon after its morning rush-hour peak. There is a slight afternoon rush-hour increase but with concentrations which are only 66% of the morning levels and 60% of the afternoon rush-hour levels on 6th Ave. The decrease in CO levels on 51st may be related, in part, to an easing of traffic flow towards the inner city during the day. A CO analyser located on 50th St., a one-way street leaving mid-town, could verify this hypothesis by showing an afternoon rush-hour peak. In any event, one point is very clear from the data. The horizontal mixing between streets and avenues in canynon environments is poor. The CO concentration during morning rush-hour was 1.3 times more on 51st than on 6th Ave., while 6th Ave. showed a 1.6 times more severe afternoon rush-hour condition. The federal standard of 8 ppm was exceeded 16 straight hours and 100% of the working day on 6th Ave. On 51st St., there were 9 consecutive hours which exceeded the federal limit, about 75% of the working day (7

a.m. to 7 p.m.). The 16th floor also showed a slight morning and afternoon rush-hour increase but, in general, showed a three-fold dilution effect as compared to street-level. If reliable patterns, as have been tried here, can be obtained, then roof-top samplers could be corrected to read street-level concentrations. Since CO is a street-level tracer, the vertical mixing pattern on 51st shown by CO measurements on the 16th floor and at street-level, should be a good indication of the air-mass flow patterns on this street. Rush-hour CO peaks are almost simultaneous in the morning, leading to the conclusion that the air mass probably circulates rather quickly (an hour or less) on 51st. Presumably the same could be established for 6th Ave. by placing a sampler at roof-top level but no data are available from which to draw any conclusions.

SO_2 readings for some representative stations are plotted along with wind speed and direction in fig IV-A-4. These locations are shown in fig. I-C-1 for reference. The range of values is from 0-70 ppb except for Staten Island, where the values tend to be lower. The SO_2 must be produced mainly by local sources, since even on days when prevailing winds are from the SW, inner-city levels are higher than S.I. I will return to this point again when particulate sulfate is discussed.

The data on particulate material are presented first in tabular form by location and week sampled, and then as mass

Fig IV-A-3.

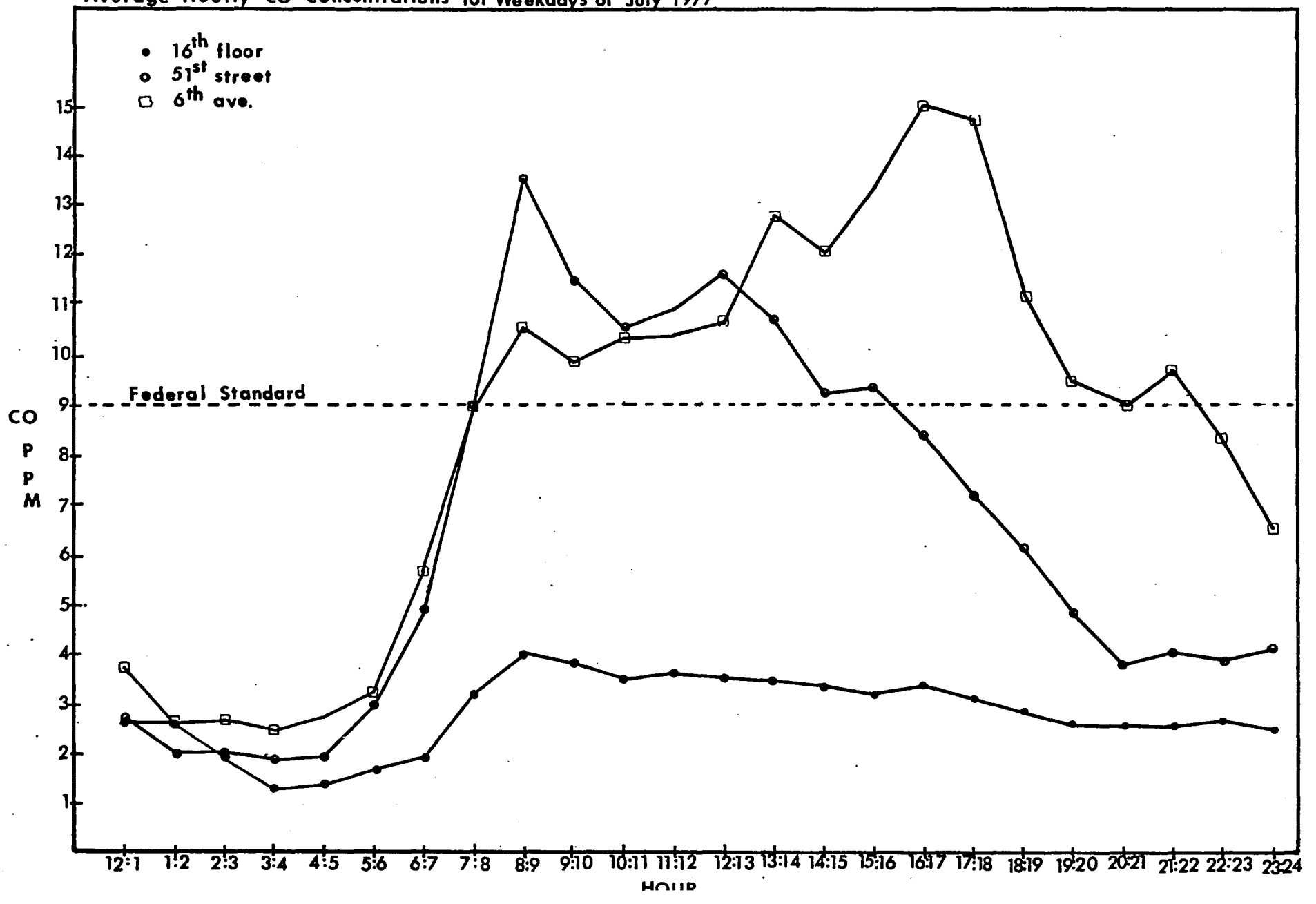
Average Hourly CO Concentrations for Weekdays of July 1977
16th floor
51st street
6th ave.
Federal Standard
CO PPM
15
14
13
12
11
10
9
8
7
6
5
4
3
2
1
12:1 1:2 2:3 3:4 4:5 5:6 6:7 7:8 8:9 9:10 10:11 11:12 12:13 13:14 14:15 15:16 16:17 17:18 18:19 19:20 20:21 21:22 22:23 23:24
HOUR

Fig IV A 4. Hourly SO_2 Conc. and Wind Correlation

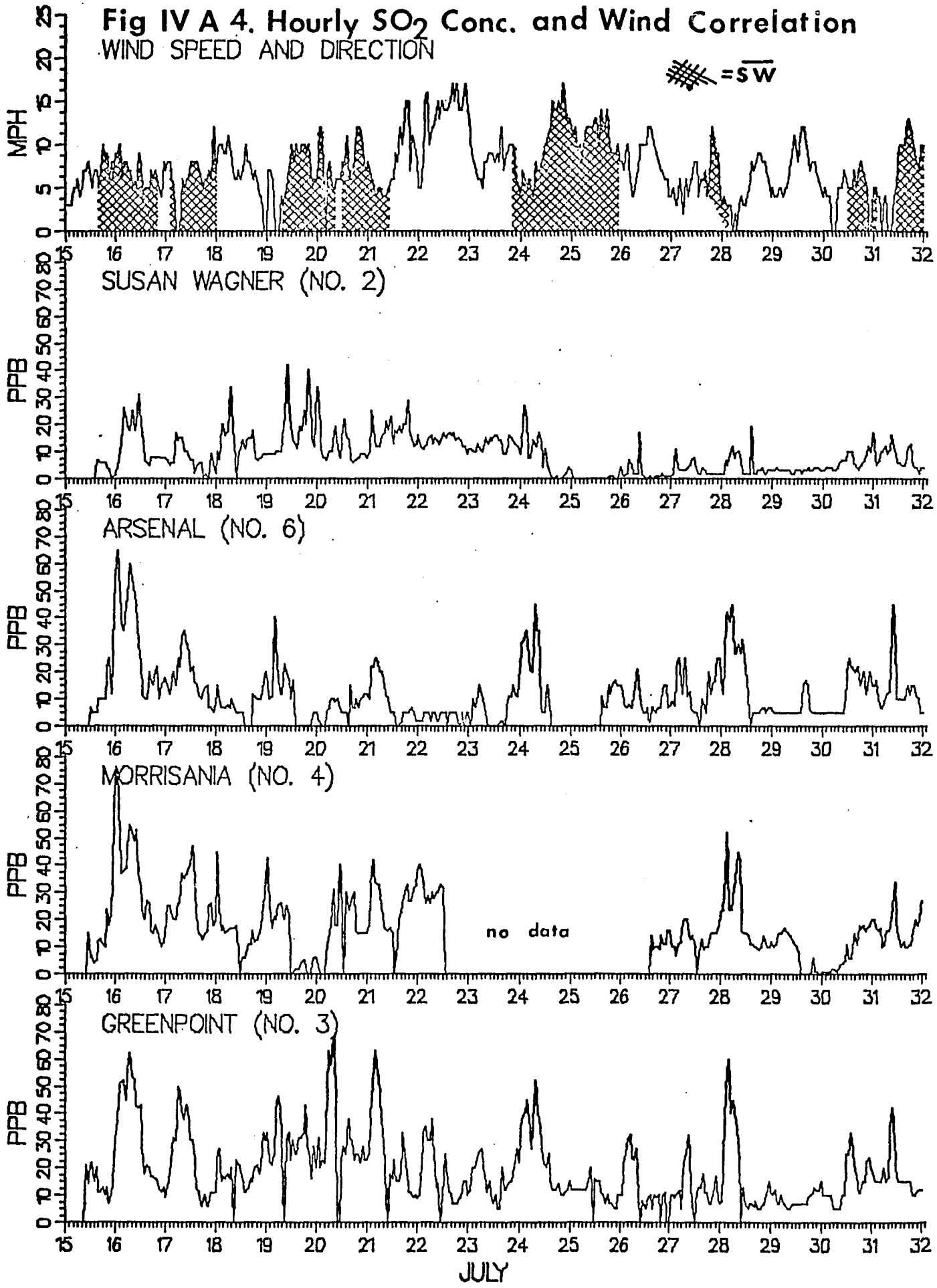

distributions, which are similarly subdivided. Table IV-A-13 is a compilation from samples, collected during the week of July 17th, and organized according to sampling location. The samples were taken from 1500-1700, 1700-1900, and 1900-2100 hrs. Table IV-A-14 is a compilation from samples, collected during the week of July 24th, and similarly organized according to sampling location. These samples were taken from 500-700, 700-900, and 900-1100 hrs.

It should be noted, before examining the data, that the average CO concentration from 5-11 A.M. during the week of morning samples was 8.53 ± 2.80, while the monthly average was 8.10 ± 2.98. Thus, there was good agreement and this sampling period was probably a good representation for the month. However, the average CO concentration from 3-9 P.M. during the week of afternoon sampling was only 6.63 ± 4.61, while the monthly average was 12.15 ± 4.61. These lower values in the afternoon, for the week sampled, were probably due to better ventilating conditions in the canyons. No attempt has been made to correct the data.

The major elemental constituents of the aerosol that we were able to analyse were: S, Cl, K, Ca, Fe, Zn, Cu, Pb, and Br. Minor constituents include Ti, V, Cr, Mn, and Ni with concentrations generally less than 100 ng/m^3 on the average, although higher values did occur. Chlorine concentrations, although sometimes very high when winds were from the east (off the ocean), generally ranged from 125-450 ng/m^3. Po-

Table IV-A-13 Element Concentrations for Rockefeller Center Stations Sampled 7/19-7/30/77 (ng/m^3).

Sample	S	Cl	K	Ca	Fe	Cu	Zn	Pb	Br
Afternoon:									
6th Ave.									
6-07-A	1626	-	-	296	2140	-	-	524	170
" " -B	6697	104	361	704	5526	-	282	1366	410
" " -C	11632	485	754	1689	5162	96	462	3043	742
6-08-A	6508	132	143	3220	2178	16	81	1531	407
" " -B	10145	-	1518	3848	4002	11	102	1971	505
" " -C	4244	142	173	2210	1199	98	58	871	244
6-09-A	563	408	227	1061	747	-	40	847	227
" " -B	414	332	374	1557	1286	-	19	939	264
" " -C	167	129	93	484	582	143	76	659	183
51st St.									
6-07-A	1380	-	-	425	580	-	3	448	129
" " -B	4704	121	291	1253	1609	34	104	1076	271
" " -C	6382	95	379	779	2414	322	569	1400	342
6-08-A	8540	309	533	1888	3726	65	98	1383	370
" " -B	10618	181	401	1389	4418	101	161	1218	319
" " -C	6120	119	263	1536	849	46	50	871	244
6-09-A	694	220	379	1648	1571	21	86	915	264
" " -B	579	182	189	1450	1716	40	60	994	302
" " -C	376	113	116	812	849	18	41	863	305
16th Floor									
6-07-A	2567	-	6	207	687	56	30	497	146
" " -B	6101	68	264	220	599	182	222	746	220
" " -C	7605	76	370	555	1130	81	243	1043	312
6-08-A	5146	60	506	1204	631	55	53	557	200
" " -B	8520	137	182	960	1230	6	53	659	176
" " -C	5964	102	225	1787	1447	25	74	534	159
6-09-A	265	118	164	1627	1234	27	69	471	132
" " -B	281	47	223	1369	1431	107	97	448	129
6-09-C	269	282	280	1434	970	19	112	539	136

Table IV-A-14 Element Concentrations for Rockefeller Center Stations Sampled 7/19-7/30/77 (ng/m^3).

Sample	S	Cl	K	Ca	Fe	Cu	Zn	Pb	Br
Morning:									
6th Ave.									
6-10-A	654	2121	218	548	3829	19	44	495	189
" " -B	1395	2252	256	1918	9964	92	138	1363	498
" " -C	2047	1647	489	2157	8758	23	173	1874	566
6-11-A	1665	320	133	956	4651	7	203	1561	383
" " -B	1707	463	598	2523	10667	39	229	2650	712
" " -C	1637	573	468	2286	3788	63	165	2003	447
6-12-A	1468	253	226	852	11179	9	112	1380	437
" " -B	-	494	255	2461	14051	79	293	-	-*
" " -C	1475	1015	348	1614	6738	66	579	2513	570
6-13-A	1095	5746	159	901	5687	144	347	1631	417
" " -B	1541	4361	123	1480	8220	125	287	2014	597
" " -C	977	3060	324	1715	3788	21	132	1658	502
51st St.									
6-10-A	1097	1554	201	343	1289	12	60	422	149
" " -B	817	1452	108	327	470	14	51	501	146
" " -C	1440	1033	185	1416	1534	30	72	602	166
6-11-A	1106	242	171	686	748	10	104	900	247
" " -B	939	336	48	834	613	45	70	1117	293
" " -C	1468	261	382	3558	1270	27	88	2288	732
6-12-A	1356	217	422	1084	1988	20	243	1380	437
" " -B	1382	191	233	1534	1747	51	188	2182	475
" " -C	2040	376	336	1240	1298	23	331	2290	515
6-13-A	924	3423	97	344	335	244	437	1354	298
" " -B	925	1613	70	709	825	59	147	844	220
" " -C	921	2605	28	2450	1683	12	122	1059	302

Table IV-A-14 Element Concentrations for Rockefeller Center Stations Sampled 7/19-7/30/77- Con't. (ng/m^3).

Sample	S	Cl	K	Ca	Fe	Cu	Zn	Pb	Br
Morning: 16th Floor									
6-10-A	82	1795	197	494	380	25	11	252	88
" " -B	483	1948	173	783	680	22	35	362	132
" " -C	1089	1034	232	1104	1521	129	183	717	220
6-11-A	1127	48	88	737	334	5	69	622	156
" " -B	638	96	127	1094	704	14	45	543	156
" " -C	722	82	197	1213	464	23	58	418	125
6-12-A	1126	99	437	993	1845	4	214	1438	285
" " -B	1401	268	287	1602	2131	31	246	2083	424
" " -C	1340	867	296	1826	2031	11	281	1859	420
6-13-A	755	5780	122	797	362	156	586	751	122
" " -B	765	4027	131	1426	540	27	142	453	163
" " -C	844	2520	77	998	871	37	77	366	112

* stage 6 of this set was lost. Results are based on 5 stages.

Table IV-A-15 Mass Distributions for Pb-6th Ave.-Afternoon Samples
Rockefeller Center-July 1977 (%)

Sample	Stage 1	Stage 2	Stage 3	Stage 4	Stage 5	Stage 6
7/20-A	5.22	8.20	22.18	24.42	16.03	23.95
7/21"	10.63	10.76	15.82	19.67	20.92	22.20
7/22"	8.30	7.48	13.14	25.04	22.13	23.91
7/20-B	1.78	1.63	3.13	2.63	9.03	81.80*
7/21"	24.83	12.62	14.95	14.81	15.77	17.02
7/22"	10.47	7.34	16.79	20.65	23.66	21.08
7/20-C	5.05	8.29	17.00	22.50	18.57	28.60
7/21"	17.64	11.95	16.63	18.67	18.07	17.04
7/22"	6..47	9.56	12.66	25.47	21.16	24.68
Avg A	8.05±2.71	8.81±1.72	17.05±4.64	23.04±2.94	19.69±3.23	23.35±1.00
Avg B	17.65±10.15	9.98±3.73	15.87±1.30	17.73±4.13	19.72±5.58	19.05±2.87
Avg C	9.72±6.90	9.93±1.86	15.43±2.41	22.21±3.41	19.27±1.66	23.44±5.88
Total Avg	11.81±6.59	9.57±2.44	16.13±2.78	20.99±3.50	19.56±3.49	21.95±3.25

* result considered erroneous-rejected.

Table IV-A-16 Mass Distributions for Pb-6th Ave.-Morning Samples
Rockefeller Center-July 1977 (%)

Sample	Stage 1	Stage 2	Stage 3	Stage 4	Stage 5	Stage 6
7/26-A	10.97	12.59	21.32	22.13	11.30	21.69
7/27"	3.98	4.12	8.72	19.35	17.99	45.84
7/28"	3.97	6.19	14.40	27.17	14.58	33.69
7/29"	2.82	6.48	16.64	25.35	18.90	29.82
7/26-B	9.44	10.37	16.27	25.01	16.84	22.06
7/27"	4.69	5.61	14.83	20.57	16.36	37.94
7/28"	7.16	11.21	25.08	27.92	28.63	-
7/29"	4.10	10.27	16.55	29.04	19.23	20.80
7/26-C	7.00	10.69	17.81	23.06	15.19	26.24
7/27"	6.34	6.11	9.98	15.73	16.94	41.92
7/28"	3.43	6.98	11.65	21.93	15.91	40.10
7/29"	5.92	8.34	17.23	27.37	19.07	22.07
Avg A	5.44±3.73	7.35±3.65	15.27±5.23	23.50±3.46	15.69±3.47	32.76±10.05
Avg B	6.35±2.45	9.37±2.54	18.15±4.66	25.64±3.78	20.27±5.72	26.93±9.55
Avg C	4.49±1.96	8.03±2.00	14.17±3.94	22.77±3.57	16.78±1.69	32.58 ±9.91
Total avg	5.43±2.71	8.85±2.73	15.87±4.61	23.97±3.60	17.58±3.00	30.76±9.84

A:pre rush-hour sample
B:rush-hour sample
C:post rush-hour sample

Table IV-A-17 Mass Distributions for Br-6th Ave.-Afternoon Samples
Rockefeller Center-July 1977 (%)

Sample	Stage 1	Stage 2	Stage 3	Stage 4	Stage 5	Stage 6
7/20-A	6.12	10.10	180.7	27.56	17.91	20.23
7/21"	10.84	12.07	15.51	20.95	22.35	18.98
7/22"	6.37	5.77	15.71	27.84	22.55	21.76
7/20-B	3.05	1.91	3.31	3.05	10.27	78.41*
7/21"	14.68	10.73	20.93	24.60	15.39	13.67
7/22"	23.02	10.44	18.57	21.28	14.31	12.38
7/20-C	6.61	9.83	19.05	27.84	18.71	17.95
7/21"	13.86	15.33	16.23	21.20	19.33	14.04
7/22"	5.67	7.55	9.98	32.64	19.85	24.30
Avg A	7.78±2.66	9.31±3.22	16.43±1.42	25.44±3.89	20.94±2.62	20.09±1.74
Avg B	18.85±5.90	10.59±0.21	19.75±1.67	22.94±2.35	14.85±0.76	13.03±0.91
Avg C	8.71±4.48	10.90±4.00	15.09±4.64	27.23±5.74	19.30±0.57	18.76±5.18
Total avg	11.78±4.34	10.27±2.48	17.16±1.55	25.20±3.99	18.36±1.18	17.29±2.61

*: sample data point was rejected.
A: pre rush-hour sample
B: rush-hour sample
C: post rush-hour sample

Table IV-A-18 Mass Distributions for Br-6th Ave.-Morning Samples
Rockefeller Center-July 1977 (%)

Sample	Stage 1	Stage 2	Stage 3	Stage 4	Stage 5	Stage 6
7/25-A	9.49	10.99	22.27	27.02	12.36	17.86
7/27"	3.46	6.52	13.00	21.19	15.15	40.67
7/28"	6.75	7.66	26.08	31.93	12.03	15.55
7/29"	3.97	7.20	19.56	28.58	16.99	23.70
7/25-B	8.07	12.90	22.30	24.58	16.05	16.10
7/27"	5.46	9.01	19.85	25.42	13.24	27.02
7/28"	-	-	-	-	-	-
7/29"	3.34	7.94	20.85	27.91	20.53	19.44
7/25-C	6.21	10.17	17.12	29.32	16.23	20.95
7/27"	8.23	7.39	16.16	22.21	14.64	30.86
7/28"	4.26	7.43	18.51	27.16	11.35	31.29
7/29"	6.38	7.37	18.58	28.71	20.64	18.31
Avg A	5.92±2.779	8.09±1.99	20.23±5.51	27.18±4.49	14.13±2.36	24.45±11.35
Avg B	5.62±2.37	9.95±2.61	21.00±1.23	25.97±1.73	16.61±3.68	20.85±5.60
Avg C	6.40±1.83	8.09±1.39	17.61±1.16	26.85±3.22	13.63±7.53	25.35±6.70
Total avg	5.98±2.33	8.71±2.00	19.61±2.63	26.67±3.15	14.79±4.52	23.55±7.88

A: pre rush-hour sample
B: rush-hour sample
C: post rush-hour sample

Table IV-A-19 Mass Distributions for Pb-51st St.-Afternoon Samples Rockefeller Center-July 1977 (%)

Sample	Stage 1	Stage 2	Stage 3	Stage 4	Stage 5	Stage 6
7/20-A	6.49	8.87	13.20	17.53	19.48	34.42
7/21"	7.88	12.94	18.79	21.36	12.80	26.23
7/22"	8.82	11.42	19.27	20.13	17.59	22.77
7/20-B	2.80	11.21	14.99	18.51	25.18	27.32
7/21"	6.23	8.73	17.99	23.39	16.15	27.51
7/22"	11.43	13.18	18.45	24.18	16.15	16.60
7/20-C	5.29	5.44	11.13	17.88	16.19	44.07
7/21"	11.05	10.79	13.23	23.05	19.05	22.83
7/22"	5.67	8.84	11.90	17.80	20.52	35.27
Avg A	7.73±1.17	11.08±2.06	17.09±3.37	19.67±1.96	16.62±3.44	27.81±5.98
Avg B	6.82±4.35	11.04±2.23	17.14±1.88	22.03±3.07	19.16±5.21	23.81±6.24
Avg C	7.34±3.22	8.36±2.71	12.09±1.06	19.58±3.01	18.59±2.20	34.06±10.67
Total avg	7.30±2.91	10.16±2.34	15.44±2.10	20.43±2.68	18.12±3.62	28.5±7.63

A: pre rush-hour sample
B: rush-hour sample
C: rush-hour sample

Table IV-A-20 Mass Distributions for Pb-51st St.-Morning Samples
Rockefeller Center-July 1977 (%)

Sample	Stage 1	Stage 2	Stage 3	Stage 4	Stage 5	Stage 6
7/25-A	6.09	5.87	10.43	11.08	41.08	25.45
7/27"	8.14	6.32	10.64	12.81	19.99	42.10
7/28"	4.26	5.21	6.17	22.55	22.32	39.49
7/29"	2.07	11.50	8.61	26.10	17.47	34.25
7/25-B	14.50	8.06	15.04	19.16	21.13	22.11
7/27"	1.84	3.59	9.64	14.63	28.36	41.93
7/28"	3.30	2.99	6.95	15.51	19.89	51.35
7/29"	5.09	7.99	10.42	20.61	21.71	34.18
7/25-C	14.76	10.02	13.69	18.22	17.11	26.20
7/27"	4.90	4.91	7.26	23.67	31.25	28.01
7/28"	2.05	2.09	5.10	15.59	20.13	55.04
7/29"	9.29	8.88	15.89	19.12	21.10	25.71
Avg A	5.14±2.59	7.23±2.89	8.96±2.07	18.14±7.33	25.22±10.73	35.32±7.35
Avg B	6.18±5.70	5.66±2.74	10.51±3.36	17.48±2.86	22.77±3.80	37.74±12.37
Avg C	7.75±5.54	6.48±3.65	10.49±5.13	19.15±3.37	22.40±6.14	33.74±14.23
Total Avg	6.36±4.51	6.46±2.90	9.99±3.46	18.26±4.53	23.46±6.89	35.48±10.69

A: pre rush-hour sample
B: rush-hour sample
C: rush-hour sample

Table IV-A-21 Mass Distributions for Br-51st St.-Afternoon Samples
Rockefeller Center-July 1977 (%)

Sample	Stage 1	Stage 2	Stage 3	Stage 4	Stage 5	Stage 6
7/21-A	8.49	12.54	13.35	23.46	20.46	21.71
7/22"	9.25	11.92	16.44	30.70	12.77	18.93
7/23"	11.47	13.22	16.75	22.19	18.77	17.61
7/21-B	4.50	10.17	17.60	28.79	21.53	17.41
7/22"	5.83	11.08	22.66	27.21	15.12	18.10
7/23"	11.13	10.95	23.14	23.73	15.93	15.12
7/21-C	8.82	9.46	14.02	21.83	17.18	28.69
7/22"	10.50	14.60	16.65	22.54	15.56	20.13
7/23"	5.64	8.88	12.64	18.11	19.49	35.24
Avg A	9.74±1.55	13.46± 1.67	15.51±1.88	25.45±4.59	17.33±4.04	19.42±2.09
Avg B	7.15±3.51	10.73±0.49	16.32±9.95	26.58±2.59	17.53±3.49	16.88±1.56
Avg C	8.34±2.47	10.98±3.15	14.44±2.04	20.83±2.38	17.41±1.98	28.02±7.58
Total avg	8.40±2.51	11.72±1.77	15.42±4.62	24.29±3.19	17.43±3.17	21.44±3.74

A: pre rush-hour sample
B: rush-hour sample
C: rush-hour sample

Table IV-A-22 Mass Distributions for Br-51st St.-Morning Samples
Rockefeller Center-July 1977 (%)

Sample	Stage 1	Stage 2	Stage 3	Stage 4	Stage 5	Stage 6
7/25-A	6.01	8.68	13.69	13.69	33.84	24.07
7/27"	10.16	9.08	12.10	15.13	17.53	36.01
7/28"	3.32	6.34	9.09	21.62	23.29	36.33
7/29"	4.25	13.26	10.37	28.27	15.14	28.72
7/25-B	9.80	8.49	16.66	22.86	22.86	19.32
7/27"	3.23	4.85	11.67	17.27	30.22	32.75
7/28"	3.40	3.84	8.48	19.38	17.75	47.14
7/29"	4.85	7.76	9.70	18.18	21.23	38.28
7/25-C	14.67	14.67	11.74	20.54	13.40	24.97
7/27"	7.96	3.37	6.90	23.45	34.21	24.12
7/28"	2.74	3.04	8.01	21.14	18.52	46.55
7/29"	8.32	11.27	14.57	21.68	22.20	21.97
Avg A	5.94±3.03	9.34±2.88	11.31±2.01	19.68±6.69	22.60±8.35	31.28±5.96
Avg B	5.32±3.07	6.24±2.24	11.63±3.60	19.42±2.45	23.02±5.25	34.37±11.65
Avg C	8.42±4.88	8.09±5.81	10.31±3.52	21.70±1.25	22.08±8.85	29.40±11.50
Total avg	6.56±3.66	7.89±3.64	11.08±3.04	20.27±3.46	22.57±7.48	31.68±9.70

A: pre rush-hour sample
B: rush-hour sample
C: rush-hour sample

Table IV-A-23 Mass Distributions for Pb-16th Floor-Afternoon Samples
Rockefeller Center-July 1977 (%)

Sample	Stage 1	Stage 2	Stage 3	Stage 4	Stage 5	Stage 6
7/21-A	7.27	8.04	20.86	19.33	17.70	26.79
7/22"	11.72	9.22	15.20	22.76	18.64	22.46
7/23"	30.34	11.60	18.64	16.81	11.10	11.50
7/21-B	5.22	8.58	16.16	20.63	16.84	32.57
7/22"	7.23	9.40	14.60	20.14	18.72	29.92
7/23"	31.75	8.47	21.98	12.90	13.61	11.29
7/21-C	3.46	8.57	14.40	22.70	17.80	33.08
7/22"	21.79	8.21	15.90	16.95	15.29	21.85
7/23"	25.65	11.79	8.91	17.94	13.15	22.56
Avg A	16.44±12.24	9.62±1.81	18.23±2.85	19.63±2.99	15.81±4.11	20.25±7.88
Avg B	14.73±14.77	8.82±0.51	17.58±3.89	17.89±4.33	16.39±2.58	24.59±11.60
Avg C	16.97±11.86	9.52±1.97	13.07±3.68	19.20±3.07	15.41±2.33	25.83±6.29
Total avg	16.05±12.96	9.32±1.43	16.29±3.47	18.91±3.46	15.87±3.01	23.56±8.59

A: pre rush-hour sample
B: rush-hour sample
C: rush-hour sample

Table IV-A-24 Mass Distributions for Pb-16th Floor.-Morning Samples
Rockefeller Center-July 1977 (%)

Sample	Stage 1	Stage 2	Stage 3	Stage 4	Stage 5	Stage 6
7/25-A	19.84	14.29	16.27	24.21	11.90	13.49
7/27"	6.76	7.66	11.41	17.87	17.97	38.34
7/28"	2.78	3.04	10.20	14.77	23.10	46.11
7/29"	3.10	7.64	7.88	15.88	28.61	36.90
7/25-B	12.43	11.82	18.58	18.02	22.10	17.05
7/27"	7.25	7.58	15.33	20.61	20.04	29.18
7/28"	2.85	3.50	11.09	16.47	22.48	43.60
7/29"	11.24	8.86	22.70	10.38	19.68	27.14
7/25-C	29.67	15.24	14.36	12.64	12.97	15.12
7/27"	13.22	8.59	14.32	15.86	19.83	28.19
7/28"	2.87	5.98	11.52	18.50	20.90	40.23
7/29"	17.17	13.65	19.00	165.59	17.40	16.19
Avg A	8.12±8.02	8.16±4.63	11.44±3.54	18.18±4.22	20.40±7.14	33.71±14.07
Avg B	8.44±4.34	7.94±3.45	16.93±4.92	16.37±4.34	21.08±1.42	29.24±10.94
Avg C	15.73±11.08	10.87±4.32	14.80±3.10	15.90±2.44	17.77±3.52	24.93±11.79
Total avg	10.76±7.81	8.99±4.13	14.39±2.77	16.82±3.67	19.75±4.03	29.29±12.27

A: pre rush-hour sample
B: rush-hour sample
C: rush-hour sample

Table IV-A-25 Mass Distributions for Br-16th Floor-Afternoon Samples
Rockefeller Center-July 1977 (%)

Sample	Stage 1	Stage 2	Stage 3	Stage 4	Stage 5	Stage 6
7/21-A	5.16	12.04	24.77	23.74	12.90	21.39
7/22"	14.33	13.37	18.38	23.40	17.33	13.19
7/23"	19.69	8.22	23.08	17.67	16.63	14.70
7/21-B	12.01	10.20	19.49	21.76	14.41	22.13
7/22"	8.22	10.21	20.98	24.99	16.87	18.73
7/23"	23.02	10.44	18.57	21.28	14.31	12.38
7/21-C	4.21	8.89	18.75	22.50	21.00	24.64
7/22"	28.36	9.97	14.07	21.50	12.83	13.27
7/23"	19.24	12.37	14.62	20.24	15.93	17.61
Avg A	13.06±7.35	11.21±2.67	22.08±3.31	21.60±3.41	15.62±2.38	16.43±4.36
Avg B	14.42±7.69	10.28±0.14	19.68±1.22	22.68±2.02	15.20±1.45	17.75±4.95
Avg C	17.27±12.19	10.41±1.78	15.81±2.56	21.41±1.13	16.59±4.12	18.51±5.74
Total avg	14.92±9.08	10.63±1.53	19.19±3.16	21.90±2.19	15.80±2.65	17.56±5.02

A: pre rush-hour sample
B: rush-hour sample
C: rush-hour sample

Table IV-A-26 Mass Distributions for Br-16th Floor.-Morning Samples
Rockefeller Center-July 1977 (%)

Sample	Stage 1	Stage 2	Stage 3	Stage 4	Stage 5	Stage 6
7/25-A	15.40	9.43	18.24	18.24	18.87	19.81
7/27"	10.12	16.32	15.34	20.24	16.89	21.08
7/28"	3.93	7.17	13.39	15.71	17.60	42.24
7/29"	6.44	15.46	15.89	23.61	16.85	21.75
7/25-B	9.62	10.88	20.50	20.92	20.08	17.99
7/27"	7.29	7.90	19.14	24.30	19.47	21.90
7/28"	3.30	6.36	12.50	18.74	17.60	41.48
7/29"	7.45	8.10	23.33	10.69	19.15	31.27
7/25-C	21.00	15.94	16.70	18.22	12.55	15.58
7/27"	10.87	10.49	21.36	23.69	14.37	19.22
7/28"	4.50	3.27	16.40	19.50	19.29	37.04
7/29"	14.98	14.01	18.84	17.39	21.01	13.77
Avg A	9.97±4.98	12.09±4.50	15.72±2.00	19.45±3.34	17.55±0.94	26.22±10.71
Avg B	6.92±2.63	8.31±1.88	18.87±4.59	18.66±5.79	19.08±1.06	28.16±10.48
Avg C	12.84±6.94	10.93±5.58	18.33±2.30	19.70±2.80	16.81±4.00	21.40±10.67
Total avg	9.58±4.85	10.44±3.99	17.64±2.96	19.27±3.98	17.81±2.00	25.26±10.62

A: pre rush-hour sample
B: rush-hour sample
C: rush-hour sample

Table IV-A-27 Average Concentrations for Pb, Br and S for Rockefeller Center Sampling Locations- Morning and Afternoon- July 1977

	Pb	Br	S
Morning:			
6th Ave.			
A	1267±525	357±114	1221±445
B	2009±644	602±107	1548±156
C	2012±363	521±58	1534±443
51st St.			
A	1082±538	260±84	1120±178
B	1161±726	283±141	1015±250
C	1560±862	429±248	1467±457
16th Floor			
A	766±496	163±86	772±493
B	860±819	218±137	819±406
C	840±697	219±142	998±274
Afternoon:			
6th Ave.			
A	967±514	268±123	2899±3170
B	1425±518	393±121	4564±4677
C	1524±1319	390±307	5347±5812
51st St.			
A	915±468	254±120	3538±4345
B	1096±113	297±24	5300±5046
C	987±369	279±79	4293±3394
16th Floor			
A	529±30	159±36	2659±2441
B	618±153	175±46	4967±4235
C	705±292	202±96	4612±3850

TABLE IV-A-28

CORRELATION OF PARTICULATE SULFUR WITH WIND DIRECTION

(ng/m^3)

A) WINDS FROM S to SW

SITE	JULY 19th AFTERNOON			JULY 20th AFTERNOON			JULY 21st AFTERNOON			JULY 25th MORNING		
	PRE	MID	POST	PRE	MID	POST	PRE	MID	POST	PRE	MID	POST
16th	2140	5249	6875	2567	6101	7605	5146	8520	5964	< 50	473	764
51st	2217	3116	5987	1380	4704	6382	8540	10618	6120	1097	817	1440
6th	1819	5771	9624	1626	6697	11632	6508	10145	4244	654	1395	2337

B) WINDS FROM NW to SE

	JULY 22nd AFTERNOON			JULY 27th MORNING			JULY 28th MORNING			JULY 29th MORNING		
	PRE	MID	POST	PRE	MID	POST	PRE	MID	POST	PRE	MID	POST
16th	72	61	111	1127	638	722	1126	1401	1340	755	765	844
51st	477	340	249	1106	939	1468	1356	1386	2040	924	925	921
6th	350	252	98	1665	1707	1637	1468	.....	1475	1095	1541	1977

tassium and calcium concentrations also underwent wide fluctuations in their range of values, although they did not always correlate well with each other. Copper and zinc concentrations, which also showed no correlation with each other, also exhibited a wide range of values. With the single exception of iron, no elements showed a consistent rush-hour pattern. Fig IV-A-5 demonstrates the consistent rush-hour trend for iron observed on 6th Ave., which is not observed on either 51st or the 16th floor. Lead and Br, both street-level emissions, showed no consistent rush-hour peaks. This is further support, along with the CO data, for constant traffic patterns on avenues in the mid-town area, i.e., they do not change significantly from initial morning rush-hour levels, except for the express busses that run on 6th Ave. during the rush-hour. Fig. IV-A-6 shows the variations in the Pb and Br concentrations with time of day. As expected, 6th Ave. suffered the most severe rush-hour conditions while the 16th floor was a factor of 2.5 times less than 6th Ave. and about 1.6 times less 51st St. in Pb and Br. This was a somewhat less drastic change than occurred for the CO levels.

Iron presents an interesting case for discussion. As pointed out, only 6th Ave. showed a distinct rush-hour peak with Fe concentrations a factor of ten higher than on 51st St. or 16th floor, which besides confirming the poor lateral mixing at street-level, also indicates a possible street-

Diurnal Variations in Fe Concentrations

Fig. IV-A-5 Rockefeller Center–July 1977

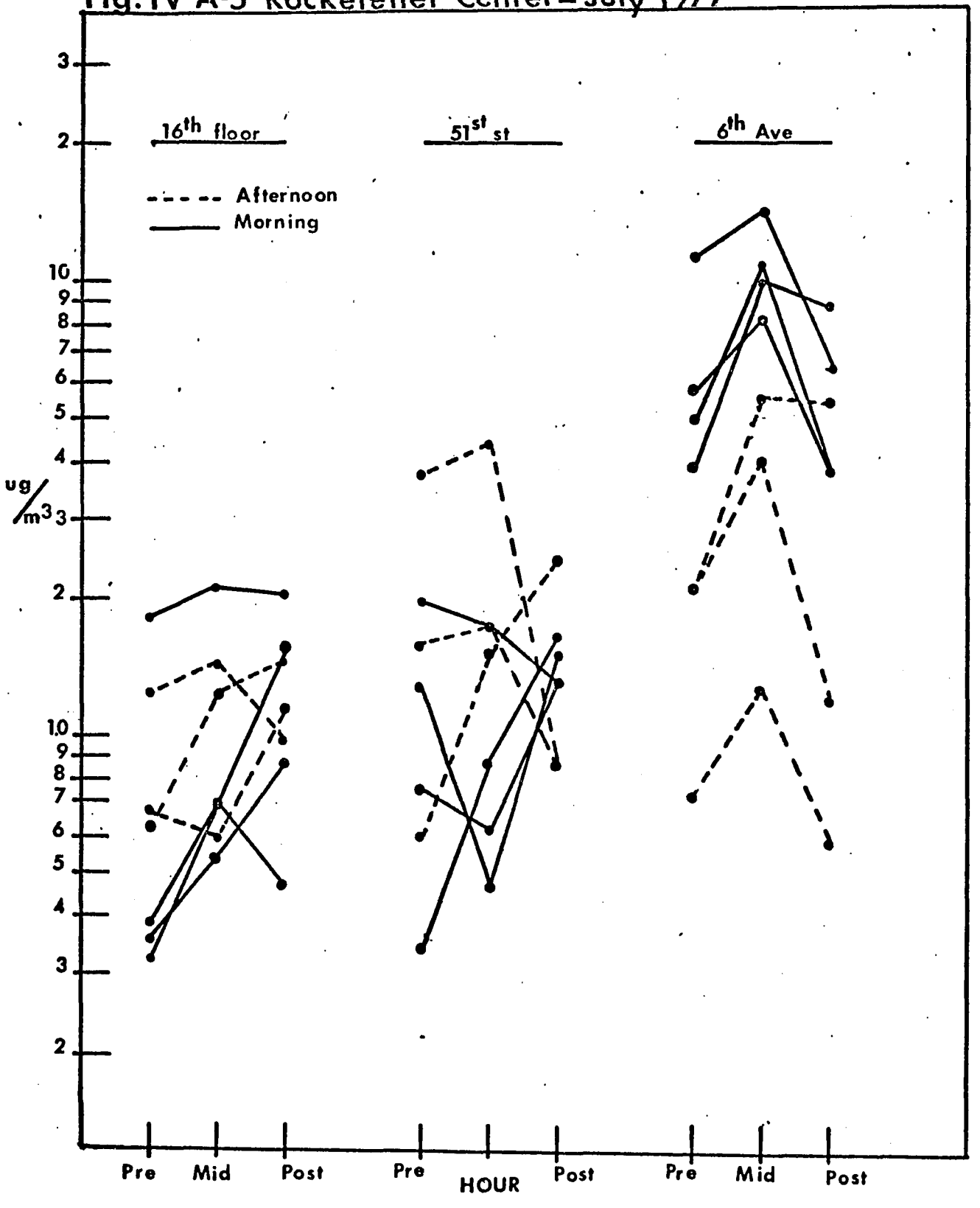

Diurnal Variations in Pb and Br Conc.

Fig IV-A-6 Rockefeller Center 1977

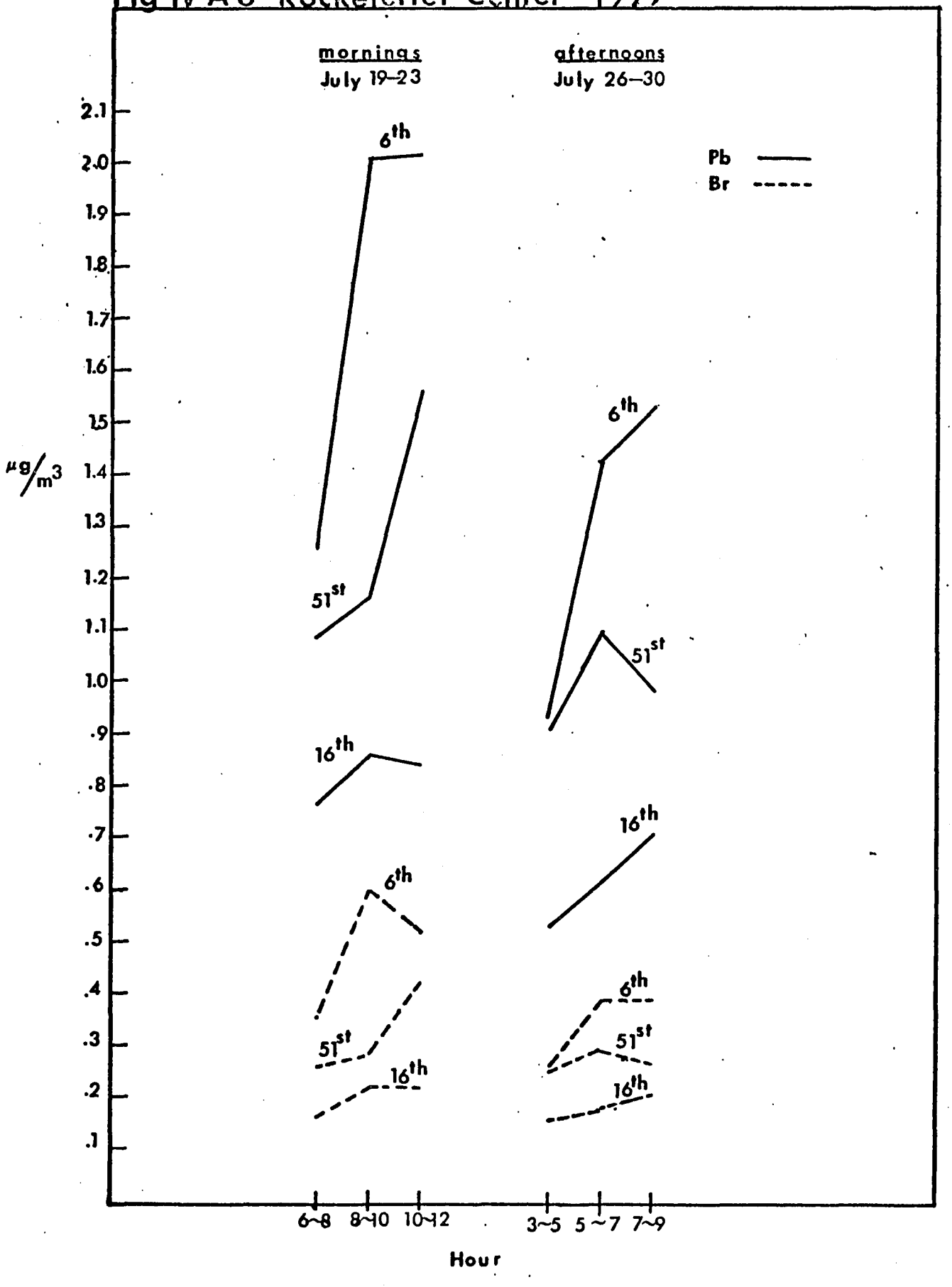

Mass Distributions for Calcium

Fig.IV-A-8 -Rockefeller Center- July 1977

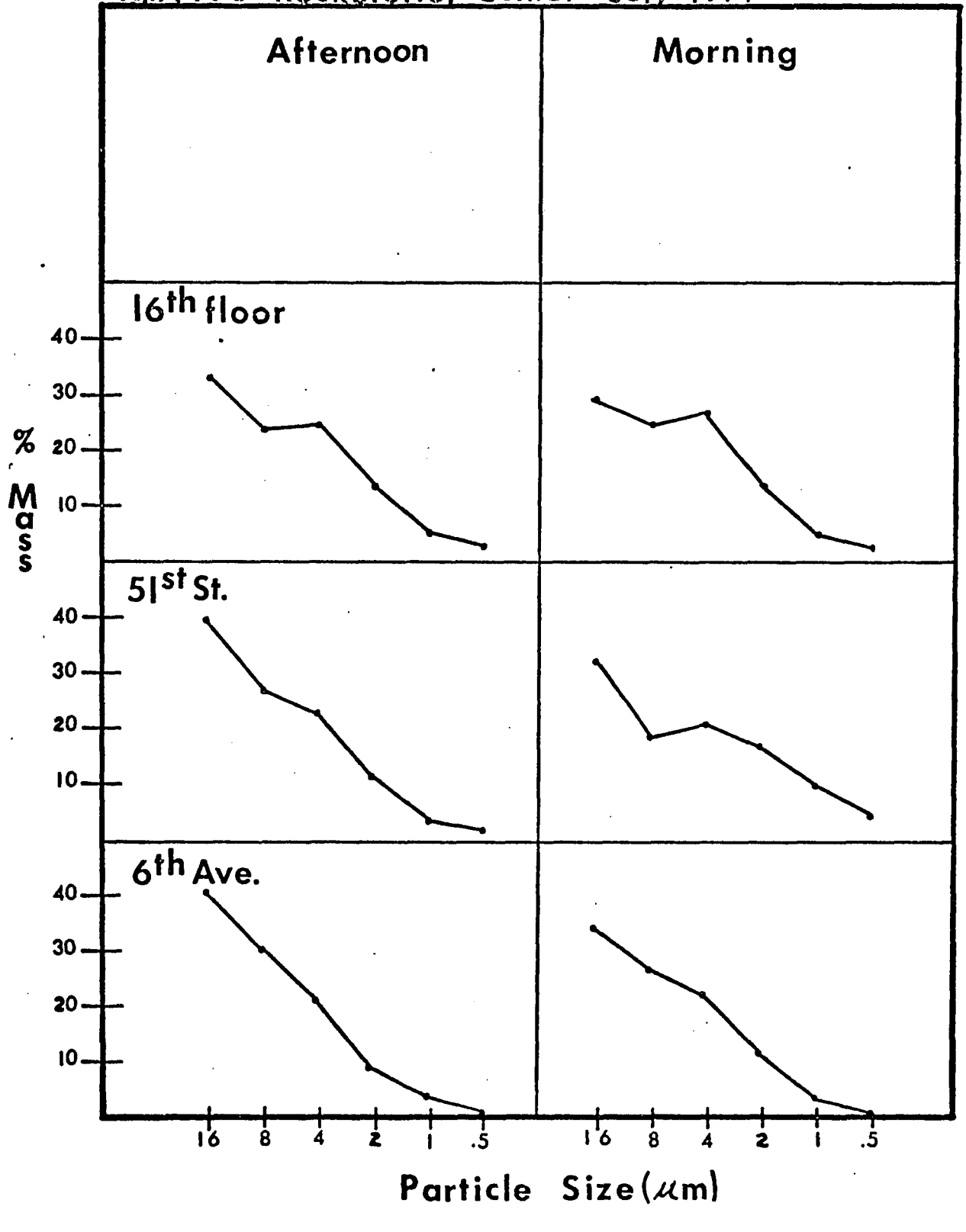

Mass Distributions for Fe, Pb, and Br

Fig. IV-A-9 Rockefeller Center – July 1977

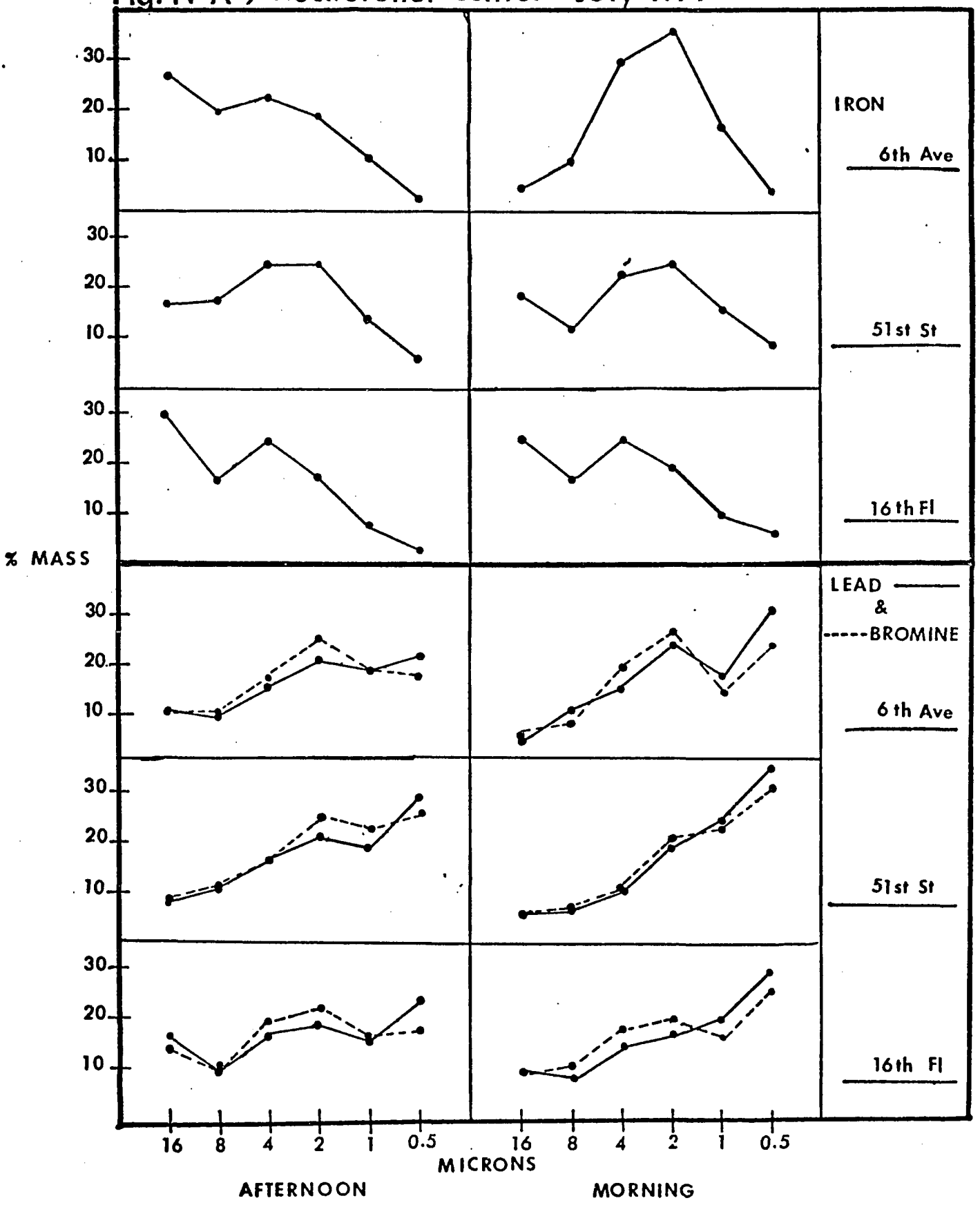

level source of iron on 6th Ave. Previous studies of urban aerosols generally attribute the presence of iron to automobiles in areas where steel plants or other heavy industry are absent. In the case where iron is being produced exclusively from vehicle exhaust systems, the Fe levels tend to be lower than the Pb levels and we see this on 51st St. and the 16th floor. This is not to imply that there were no other sources of Fe. On the contrary, the impactor on the 16th floor was located near a water cooling tower which probably injected corrosion products into the air, suspended in the evaporating spray. Sixth Ave, however, with concentration levels an order of magnitude higher, in some cases, indicates a completely independent source of iron. One possible answer is the 6th Ave subway system. There were numerous entrances and ventilation gratings in the immediate vicinity of the sampling location. The levels of iron measured on 6th Ave. correlated well with actual subway traffic as shown in fig. IV-A-7. It is of note in fig. IV-A-7 that a sharp emission peak may be obscured if the sampling period either doesn't coincide with the peak emission period or is long compared to it. Also, the fact that ventilation during the week of afternoon samples was better than the monthly average for this time period, could explain why differences in the morning Fe levels were greater than the differences in the afternoon levels. Under normal conditions (i.e. average) of ventilation, it is probably valid to assume that

Fig-IV-A-7 D-Train Schedule for 6th Ave. Subway

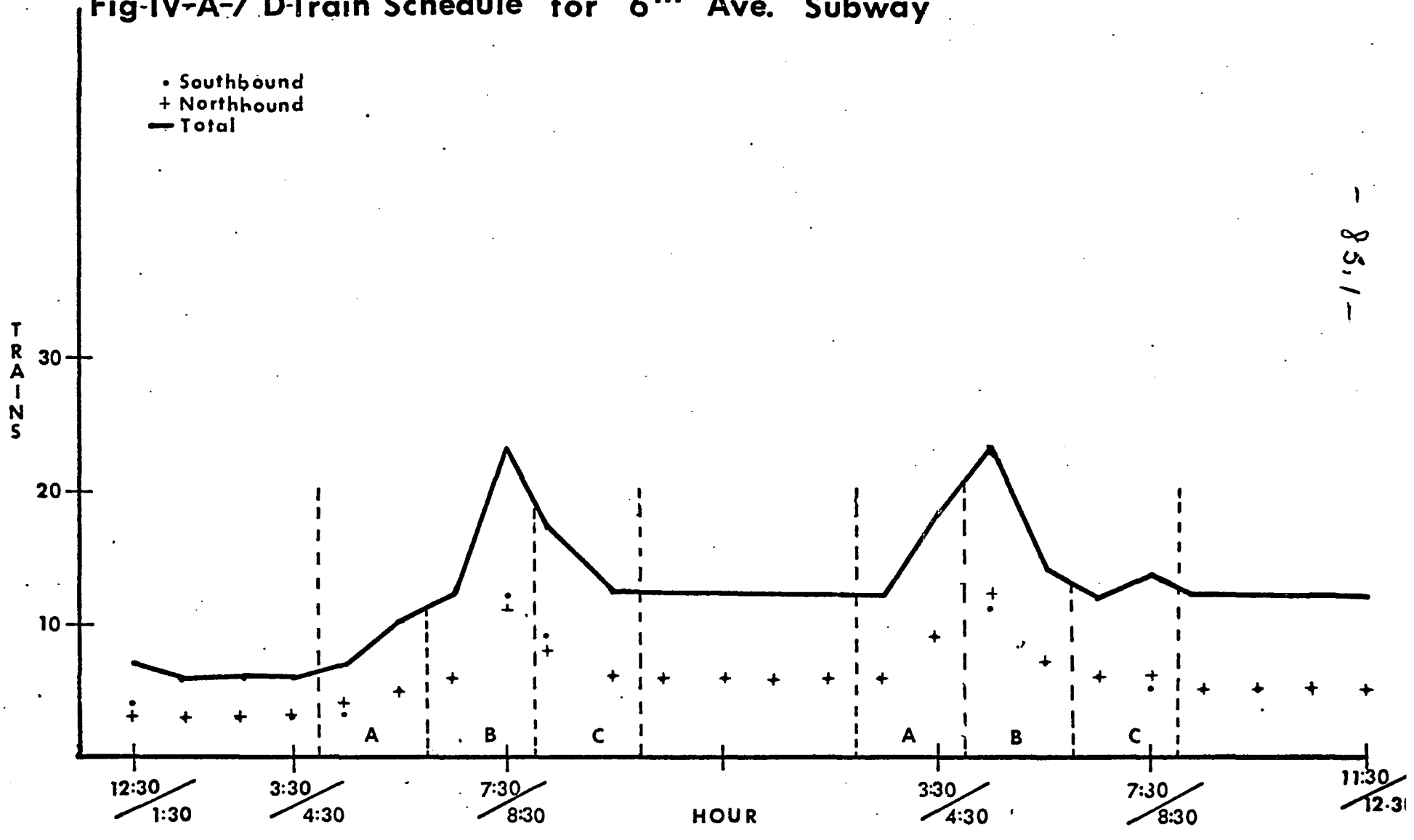

afternoon Fe concentrations on 6th Ave. would be greater than would morning rush-hour concentrations. A verification of this source could be obtained by taking a sample below street-level in the subway itself, but such a test has not yet been possible. Although not considered a harmful constituent of the aerosol, iron, in concentrations as high as 12-15 $\mu g/m^3$, represents as much as 15% of the TSP. It is evident from the mass distribution data (fig IV-A-8), that almost all of this iron is respirable, thus representing a considerable burden on the respiratory system. In addition, there is some speculation that Fe may provide a catalytic surface for the conversion of SO_2 to $SO_4^=$. Such mechanisms are of great concern because of the danger associated with sulfuric acid mist aerosols which are quickly becoming a major pollution problem.

Particulate sulfur also represents an unusual situation for the New York aeorosl. As was previously mentioned, particulate sulfate results from the photochemical conversion of SO_2, for which numerous possible mechanisms have been proposed. A more recent development has been the observation that, as a consequence of this conversion, large amounts of sulfuric acid mist aerosol have been reported in urban atmospheres(3). In additon to photochemical conversion, SO_2 is also being converted to sulfuric acid in catalytic converters presently installed in late model automobiles(4). A point of interest for many urban areas is to

know what fraction of the sulfate burden can be ascribed to street-level sources, i.e. catalytic converters on automobiles, and what fraction is contributed from space heating and power producing sources.

The N.Y.C.D.E.P continuously measures SO_2 and reports hourly averages at stations throughout the city. We have examined the readings for several of these stations (fig IV-A-4) and compared the trends with levels of sulfur on particulate matter. The major local sources of SO_2 during the summer are generally acknowledged to be the power generating plants located within the metropolitan area and oil-fired hot-water heaters. The levels of SO_2 ranged anywhere from 1 to 75 ppb during the sampling period. Fig IV-A-4 shows the concentration of SO_2 on an hourly basis for the month of July at the representative stations chosen. In addition, the wind speed and direction for the corresponding hours of sampling is also plotted.

Examining the levels of particulate sulfur experienced during the sampling periods (tables IV-A-13, IV-A-27, and IV-A-28), the following observations were made:

a) The morning sample averages were consistently lower than the afternoon samples for every sampling period (A,B,C). In addition, the variance of the afternoon samples were a order of magnitude higher than were the morning samples.

b) No consistent rush-hour pattern was observed during

either of the sampling periods.

c) When the values are low (i.e. mornings in the week of July 24th to July 29th) there is a pattern of 6th Ave.>51st St.>16th floor, similar to that observed for CO, Pb and Br, which might indicate a local street-level source, however, there is no such pattern when S is high indicating that the particles have already been mixed into the air mass before entering the sampling location. Furthermore, the absence of a rush-hour trend when S is low is consistent with vehicular patterns observed during the same period.

d) The high readings of SO_2 occurred during a period when CO data indicated a better than average ventilating condition at street-level.

e) The afternoon concentrations of particulate S were anywhere from 2-6 times those of the morning samples but so was the variability. The amount of S ranged from 167 ng/m^3 to 11,632 ng/m^3 with 11 of the 27 samples being over 6,000 ng/m^3, a concentration of sulfur 4 times higher than the highest value reported for all the morning samples.

This evidence, interpreted as follows, indicates a source of particulate S external to the local area. Table IV-A-28 shows that every occurence of high particulate S was accompanied by winds from the S to SW. The same cannot be said for SO_2 concentrations indicating that the particulate S is

not related SO_2. The SO_2 concentrations were fairly insensitive to changes in wind direction. Staten Island had a generally lower SO_2 concentration than the mid-metropolitan area as measured at Morrisania, Greenpoint and Arsenal, indicating that nearly all SO_2 originated in the metropolitan area. Since the 1/e time constant for conversion of SO_2 to $SO_4^=$ is from 3 to 30 hours(5) depending on weather conditions, it is therefore probable that most of the particulate S experienced in New York City during the week of July 24th was the result of transport from sources over one hundred miles. Recent investigations by Winchester, et al.(6) suggest transport of particulate S can occur over hundreds of miles and possibly as far as the mid-west (St. Louis). Thus we conclude that the high levels of particulate sulfur represent sulfate transported from the west.

Other elements examined showed no unusual patterns or abnormal concentrations. Ambient levels are about what one would expect from urban areas. Concentration ranges for elements are generally large, extending over a factor of ten in normal cases, and the patterns for these elements seem to indicate that locally high relative concentrations can appear for many hours probably due to shifting of the wind direction.

B. Discussion and Recommendations

The results of the sampling program at both sampling locations are that mass distributions do not change with

elevation. 16th floor mass distributions agree quite well with street-level mass distributions, even for sources emitted at street level. There is, however, a definite dilution effect observed for aerosol components emitted at street level and measured at the 16th floor. Furthermore, variations in street-level concentrations are observed for sampling sites located on intersecting streets and avenues whose proximity would reasonably suggest a common aerosol. This implies that local mixing of the atmosphere is retarded by conditions exisiting in the mid-town area.

A dilution factor of from 3 to 4 was observed for street-level emissions when measured at the 16th floor, and the absence of this factor can be used to determine the presence of transported aerosol. The poor vertical and lateral mixing patterns observed at Rockefeller Center indicate that studies are needed to determine where to best place a sampler for maximum information. I do not think a 24-hr. sampling period, or weekly sampling periods, can accurately assess the impact of work-day pollutant levels. There are very dramatic differences observed during work-day situations that are masked by 24-hr. sample averaging. Roof-top sampling can lead to erroneous conclusions about concentrations at street-level, if care is not exercised and a knowledge of mixing patterns is not known.

A new contributor to the local aerosol is being reported. Unusually high levels of iron on 6th, exhibiting defin-

ite rush-hour patterns and correlating well with subway traffic, indicates that ablation of subway wheels and tracks are responsible for large quantities of Fe being introduced into the aerosol on 6th Ave. I also recommend a further investigation of this new source, possibly even sampling in the subway itself, to ascertain the levels to which subway riders and workers are exposed.

It is also being reported that multiple sources of particulate sulfur might exist. Our evidence shows that transported sulfur seems responsible for much larger quantities of sulfur than local sources. The transported material seems to originate from the west, possibly hundreds of miles away. The lower levels of sulfur seen on some days in the absence of transported sulfur suggests the automobile as a possible source for, as of now, low amounts of particulate sulfur. However, the absence of data on the particulate sulfate entering the city prevents a firm interpretation of these results. Attention should be paid to this new source of sulfur since it has the potential, due to greater percentages of new model cars containing catalytic converters, of becoming a much larger source.

Bibliography

1. S. Mainwaring, "Size Distributions of Aerosols in Melbourne", loc. cit. , see ref. 6, Sec IC.
2. T.J. Kneip, "Trace Metals in Urban Aerosols", loc. cit , see ref. 2 sec IB.
3. C.M. Sheih, "Application of a Statistical Trajectory Model to the Simulation of Sulfur Pollution Over Northeastern U.S.", Atmospheric Environ., 11 , p 173-178, 1977.
4. C.M. Sheih, ibid., p 173.
5. C.M. Sheih, ibid., p 173.
6. J.W. Winchester, "Atmospheric Aerosol Chemistry of Sulfur:...", loc. cit. , see ref. 11 sec IA.

Autobiographical Note

I was born Sene Ellis on October 21, 1948 to my parents Mildred and Arthur Bauman. The eldest of three sons, I spent most of my childhood in the Sheepshead Bay area of Brooklyn, New York, where I attended the N.Y.C. public school system. Graduating Sheepshead Bay Highschool in 1966, I immediately entered Brooklyn College in the fall of the same year.

Initially starting as a pre-engineering major, I soon changed to Chemistry when I was in my sophomore year. As a freshman I joined Sigma Alpha Mu fraternity and remained active for almost three years until my interests and the fraternities popularity waned. It was in the spring term of my sophomore year that I first met my future advisor(s) Evan T. Williams and Harmon L. Finston. Since then these men helped through some very trying moments and our friendships have grown continuously. I graduated B.S. in chemistry in the spring of 1971 and immediately sought my fortune in the business world.

After many fruitless months, I finally obtained a job with Olin Water Service Laboratories, located at 125th St. and Broadway in Manhattan, where I analysed boiler waters, and other aqueous samples. Finally, nearly drowning in boredom I applied and was accepted to graduate school at CUNY in the spring of 1972. My initial teaching responsibility as a graduate student was to teach Integrated Sci-

ence, a course for non-science majors, which eventually Evan and I taught together as an environmental chemistry course.

It was during this period of my life that I first met my lovely wife, Susan, who at the time was a student in my class. We married two years later on May 26, 1974 and have remained happily so since. The only other member of our family is our beloved Chelsea, a grey tiger-striped cat who eats us out of house and home and sleeps all day.